Gö-VIP-9: Prof. Dr. Ralf Dressel

Institut für Zelluläre und Molekulare Immunologie

***Originalpublikation**: "The MICA-129 dimorphism affects NKG2D signaling and outcome of hematopoietic stem cell transplantation" In: EMBO Mol Med, Oktober, 2015, (E-Pub)*

Autoren Antje Isernhagen (1), Dörthe Malzahn (2), Elena Viktorova (2), Leslie Elsner (1), Sebastian Monecke (1), Frederike von Bonin (3), Markus Kilisch (4), Janne Marieke Wermuth (3), Neele Walther (3), Yesilda Balavarca (2,7), Christiane Stahl-Hennig (5), Michael Engelke (1), Lutz Walter (6), Heike Bickeböller(2,†), Dieter Kube (3,†), Gerald Wulf (3,†), Ralf Dressel (1,*)

(1) Institut für Zelluläre und Molekulare Immunologie, Universitätsmedizin Göttingen
(2) Institut für Genetische Epidemiologie, Universitätsmedizin Göttingen
(3) Klinik für Hämatologie und Medizinische Onkologie, Universitätsmedizin Göttingen
(4) Institut für Molekularbiologie, Universitätsmedizin Göttingen
(5) Abteilung Infektionsmodelle, Deutsches Primatenzentrum Göttingen
(6) Abteilung Primatengenetik, Deutsches Primatenzentrum Göttingen
(7) gegenwärtige Adresse: Abteilung Präventive Onkologie, DKFZ Heidelberg
(†) geteilte Position des vorletzten Autors
(*) korrespondierender Autor

Dr. Sebastian Monecke, Leslie Elsner, Prof. Dr. Ralf Dressel, Dr. Antje Isernhagen

Zusammenfassung des wissenschaftlichen Inhalts

(Prof. Dr. Ralf Dressel)

Durch eine Transplantation allogener hämatopoietischer Stammzellen können zahlreiche maligne Erkrankungen des blutbildenden Systems erfolgreich behandelt werden, die auf andere Therapien nicht ansprechen. Es besteht allerdings in vielen Fällen ein erhebliches Risiko, dass Immunzellen aus dem Transplantat gegen den Empfänger reagieren. In dieser Arbeit wurde der Einfluss des Austausches einer Aminosäure an Position 129 im MICA-Protein von Valin (Val) zu Methionin (Met) auf diese als „graft versus host disease“ (GVHD) bezeichnete Komplikation untersucht. MICA ist ein Ligand des Rezeptors NKG2D, der auf NK-Zellen und zytotoxischen T-Lymphozyten exprimiert wird und die Aktivierung dieser Zellen steuert. In einer Kohorte von 452 Patienten, die an der Universitätsmedizin Göttingen transplantiert wurden, war das Vorhandensein einer MICA-129Met-Variante mit einer erhöhten Wahrscheinlichkeit des Überlebens und einer geringeren Wahrscheinlichkeit an einer akuten GVHD zu versterben assoziiert, obwohl Träger dieser Variante ein erhöhtes Risiko aufwiesen, überhaupt eine akute GVHD zu entwickeln. Das Überleben von Trägern des Genotyps *MICA-129Val/Val* wurde durch eine Behandlung mit Anti-Thymozytenglobulin (ATG), das die Zahl der T-Lymphozyten vermindert, signifikant verbessert. Funktionell löste die MICA-129Met-Isoform eine stärkere zytotoxische Aktivität und eine vermehrte Produktion von Interferon-γ durch NK-Zellen aus. Zytotoxische T-Zellen wurden durch ein MICA- vermitteltes co-stimulatorisches Signal schneller aktiviert. Die MICA-129Met-Isoform löste aber auch eine starke und schnelle Gegenregulation aus, die zu einer verminderten Expression des NKG2D-Rezeptors führte. Diese reduzierte Expression von NKG2D auf alloreaktiven zytotoxischen T-Lymphozyten scheint das Risiko einer schweren und unter Umständen tödlich verlaufenden GVHD zu vermindern. Homozygote Träger der MICA-129Val-Isoform profitierten daher besonders von einer Behandlung mit ATG zur Reduktion des Risikos einer GVHD. Die Resultate zeigen wie der MICA-129Met/Val-Dimorphismus die Funktion von NK-Zellen und zytotoxischen T-Lymphozyten beeinflusst. Dieser Dimorphismus wurde auch mit Risiken für verschiedene Autoimmun-, Herz- und Tumorerkrankungen assoziiert. Die Aufklärung der Funktion der MICA-129Met/Val-Proteinvarianten verbessert nun das Verständnis auch dieser Krankheitsassoziationen und kann neue therapeutische Optionen mit anti-NKG2D-Antikörpern oder hochaffinen NKG2D-Liganden eröffnen.

WEITERE INFORMATIONEN:

Prof. Dr. Ralf Dressel
Einrichtung: Institut für Zelluläre und Molekulare Immunologie
Telefon: 0551/39-5884
Humboldtallee 34, 37073 Göttingen
Ralf.Dressel@med.uni-goettingen.de

Research Article

TRANSPARENT PROCESS OPEN ACCESS

EMBO Molecular Medicine

The MICA-129 dimorphism affects NKG2D signaling and outcome of hematopoietic stem cell transplantation

Antje Isernhagen[1], Dörthe Malzahn[2], Elena Viktorova[2], Leslie Elsner[1], Sebastian Monecke[1], Frederike von Bonin[3], Markus Kilisch[4], Janne Marieke Wermuth[3], Neele Walther[3], Yesilda Balavarca[2,‡], Christiane Stahl-Hennig[5], Michael Engelke[1], Lutz Walter[6], Heike Bickeböller[2,†], Dieter Kube[3,†], Gerald Wulf[3,†] & Ralf Dressel[1,*]

Abstract

The MHC class I chain-related molecule A (MICA) is a highly polymorphic ligand for the activating natural killer (NK)-cell receptor NKG2D. A single nucleotide polymorphism causes a valine to methionine exchange at position 129. Presence of a *MICA-129Met* allele in patients (n = 452) undergoing hematopoietic stem cell transplantation (HSCT) increased the chance of overall survival (hazard ratio [HR] = 0.77, P = 0.0445) and reduced the risk to die due to acute graft-versus-host disease (aGVHD) (odds ratio [OR] = 0.57, P = 0.0400) although homozygous carriers had an increased risk to experience this complication (OR = 1.92, P = 0.0371). Overall survival of *MICA-129Val/Val* genotype carriers was improved when treated with anti-thymocyte globulin (HR = 0.54, P = 0.0166). Functionally, the MICA-129Met isoform was characterized by stronger NKG2D signaling, triggering more NK-cell cytotoxicity and interferon-γ release, and faster co-stimulation of $CD8^+$ T cells. The MICA-129Met variant also induced a faster and stronger down-regulation of NKG2D on NK and $CD8^+$ T cells than the MICA-129Val isoform. The reduced cell surface expression of NKG2D in response to engagement by MICA-129Met variants appeared to reduce the severity of aGVHD.

Keywords cytotoxic T cells; graft-versus-host disease; NK-cell receptors; NK cells; single nucleotide polymorphism

Subject Categories Stem Cells; Immunology; Haematology

DOI 10.15252/emmm.201505246 | Received 14 March 2015 | Revised 15 September 2015 | Accepted 17 September 2015

Introduction

Allogeneic hematopoietic stem cell transplantation (HSCT) offers an option to cure for several hematological diseases. Depending on the disease entity, 5-year survival rates vary, with limitations imposed by post-transplant complications, such as graft-versus-host disease (GVHD), relapse of malignancy, and infection (Dickinson, 2008). Human leukocyte antigen (HLA) matching is mandatory to reduce the risk of graft rejection and GVHD, but minor histocompatibility antigens also affect transplant outcome (Warren *et al*, 2012). Moreover, single nucleotide polymorphisms (SNPs) can influence the success of transplantations. SNPs in the tumor necrosis factor (TNF)-α or interleukin (IL)-6 genes, for example, have been associated with an increased risk of GVHD (Dickinson, 2008; Harris *et al*, 2013).

A candidate gene that could affect the outcome of HSCT is the major histocompatibility complex (MHC) class I chain-related A (*MICA*). It is the most polymorphic non-classical MHC class I gene in humans (Bahram *et al*, 1994; Leelayuwat *et al*, 1994; Choy & Phipps, 2010), and currently, 100 alleles are known encoding for 79 protein variants (http://www.ebi.ac.uk/imgt/hla/, release 3.17.0). The structure of MICA is similar to classical MHC class I molecules, but it is not associated with β2-microglobulin and does not present peptides. It is constitutively expressed on a few cell types, such as gastrointestinal epithelium (Groh *et al*, 1996) but becomes induced by cellular and genotoxic stress (Groh *et al*, 1996; Gasser *et al*, 2005) in malignant or virus-infected cells (Champsaur & Lanier, 2010; Raulet *et al*, 2013). MICA functions as ligand for the activating NK receptor NKG2D (NK group 2, member D; Bauer *et al*, 1999), which is present on NK cells, $CD8^+$ αβT cells, subsets of $CD4^+$ αβT cells, γδT cells, and NKT cells (Champsaur & Lanier, 2010; Raulet

1 Institute of Cellular and Molecular Immunology, University Medical Center Göttingen, Göttingen, Germany
2 Institute of Genetic Epidemiology, University Medical Center Göttingen, Göttingen, Germany
3 Department of Hematology and Medical Oncology, University Medical Center Göttingen, Göttingen, Germany
4 Institute of Molecular Biology, University Medical Center Göttingen, Göttingen, Germany
5 Unit of Infection Models, German Primate Center, Göttingen, Germany
6 Primate Genetics Laboratory, German Primate Center, Göttingen, Germany
*Corresponding author. Tel: +49 551 395884; Fax: +49 551 395843; E-mail: rdresse@gwdg.de
†HB, DK and GW share the second to last author position
‡Present address: German Cancer Research Center, Division of Preventive Oncology, Heidelberg, Germany

et al, 2013). While NKG2D signaling triggers cytotoxicity (Billadeau *et al*, 2003) and cytokine secretion in NK cells (Andre *et al*, 2004) and Vγ9Vδ2T cells (Rincon-Orozco *et al*, 2005), it is a co-stimulator for activation of $CD8^+$ αβT cells (Groh *et al*, 2001). NKG2D is important for elimination of malignant cells (Guerra *et al*, 2008), contributes to rejection of mouse bone marrow grafts (Ogasawara *et al*, 2005), and is critical in defense against some pathogens (Fang *et al*, 2008; Wesselkamper *et al*, 2008; Champsaur & Lanier, 2010; Choy & Phipps, 2010).

MICA genotype matching and *MICB* genotype matching were associated with improved survival after HSCT (Kitcharoen *et al*, 2006), whereas mismatching was associated with increased incidence of acute GVHD (aGVHD; Parmar *et al*, 2009; Askar *et al*, 2014) although not in all studies (Anderson *et al*, 2009). The SNP at nucleotide position 454 (G/A) causing a valine (Val) to methionine (Met) exchange at amino acid position 129 in the α2 domain of the MICA protein was found to be associated with the incidence of chronic GVHD (cGVHD) and relapse (Boukouaci *et al*, 2009). This SNP has also been associated with the risks for nasopharyngeal carcinoma (Douik *et al*, 2009), hepatitis B virus-induced hepatocellular carcinoma (Tong *et al*, 2013), the severity of chronic Chagas heart disease (Ayo *et al*, 2015), and autoimmune diseases, including ankylosing spondylitis (Amroun *et al*, 2005), rheumatoid arthritis (Kirsten *et al*, 2009), inflammatory bowel disease (Lopez-Hernandez *et al*, 2010; Zhao *et al*, 2011), lupus erythematosus (Yoshida *et al*, 2011), type I diabetes (Raache *et al*, 2012), and psoriatic disease (Pollock *et al*, 2013). Moreover, the MICA-129 dimorphism is functionally relevant and the *MICA* alleles can be separated into two groups with respect to this polymorphism. MICA isoforms containing a methionine at position 129 have been characterized to bind NKG2D with high avidity, whereas those with a valine bind NKG2D with low avidity (Steinle *et al*, 2001). However, the finding that high-avidity MICA-129Met isoforms were associated with an increased incidence of relapse whereas the low-avidity isoforms were associated with an increased incidence of cGVHD (Boukouaci *et al*, 2009) appeared to be counterintuitive in view of the known functions of NKG2D. Therefore, we analyzed the MICA-129 dimorphism in an independent cohort of HSCT patients and investigated its functional effects beyond NKG2D binding to understand the mechanism how the SNP might impact the outcome of HSCT.

Results

Association of the MICA-129Val/Met dimorphism with the outcome of HSCT

The characteristics of 452 consecutive patients (P), who underwent allogeneic HSCT in the Department of Hematology and Medical Oncology of the University Medical Center Göttingen (UMG) between October 2002 and July 2013, and their donors (D) are shown in Table 1. Recipients and donors were typed at high resolution for *HLA*-loci *A*, *B*, *C*, *DR*, and *DQ*, and a match of at least 7/8 loci at *HLA-A*, *B*, *DRB1*, and *DQB1* was considered eligible for transplantation. We analyzed these 452 P/D pairs for the SNP rs1051792, responsible for the MICA-129Val/Met dimorphism. Most P/D pairs (90.7%) had the same *MICA-129* genotype. About 54.4% of the patients experienced aGVHD (any grade) and 30.5% cGVHD (any

Table 1. HSCT pairs, diseases, transplantation characteristics, and outcome.

Characteristics	Values
Recipients (*n* = 452)	
Median age, years (y)	52
Younger than 20 y, *n* (%)	7 (1.5)
20 to 40 y, *n* (%)	72 (15.9)
Older than 40 y, *n* (%)	373 (82.5)
Male, *n* (%)	275 (60.8)
MICA-129 genotype frequencies	
Val/Val, *n* (%)	232 (51.3)
Met/Val, *n* (%)	161 (35.6)
Met/Met, *n* (%)	59 (13.1)
MICA-129 allele frequencies	
Val, *n* (%)	625 (69.1)
Met, *n* (%)	279 (30.9)
Underlying diagnosis	
Acute leukemia, *n* (%)	180 (39.8)
Hodgkin lymphoma, non-Hodgkin lymphoma, *n* (%)	165 (36.5)
Multiple myeloma, *n* (%)	49 (10.8)
Myelodysplastic syndrome, *n* (%)	28 (6.2)
Myeloproliferative diseases, chronic myeloid leukemia, *n* (%)	15 (3.3)
Other diagnoses, *n* (%)	15 (3.3)
Disease status for malignant disorders	
Early, *n* (%)	94 (20.8)
Intermediate, *n* (%)	97 (21.5)
Advanced, *n* (%)	120 (26.5)
ND[a], *n* (%)	141 (31.2)
Donors (*n* = 452)	
Median age, y	40
Younger than 20 y, *n* (%)	2 (0.4)
20 to 40 y, *n* (%)	209 (46.2)
Older than 40 y, *n* (%)	189 (41.8)
ND, *n* (%)	52 (11.5)
Male, *n* (%)	283 (62.6)
Female, *n* (%)	134 (29.6)
ND, *n* (%)	35 (7.7)
Female donor to male recipient, *n* (%)	77 (17.0)
HLA-matched unrelated donor, *n* (%)	307 (67.9)
Less than 8/8-matched unrelated donor, *n* (%)	68 (15.0)
Matched-related donor, *n* (%)	143 (31.6)
MICA-129 genotype frequencies	
Val/Val, *n* (%)	224 (49.6)
Met/Val, *n* (%)	156 (34.5)
Met/Met, *n* (%)	63 (13.9)
ND, *n* (%)	9 (2.0)

Table 1 (continued)

Characteristics	Values
MICA-129 allele frequencies	
Val, *n* (%)	604 (68.2)
Met, *n* (%)	282 (31.8)
Transplantation	
Source of stem cells	
Peripheral blood, *n* (%)	441 (97.6)
Bone marrow, *n* (%)	11 (2.4)
Busulfan-based conditioning, *n* (%)	402 (88.9)
Total body irradiation-based conditioning, *n* (%)	47 (10.4)
Reduced intensity conditioning, *n* (%)	170 (37.6)
T-cell depletion, *n* (%)	252 (55.8)
Outcome	
Occurrence of acute GVHD, *n* (%)	246 (54.4)
Grade I to II, *n* (%)	159 (35.2)
Grade III to IV, *n* (%)	87 (19.2)
Occurrence of chronic GVHD, *n* (%)	138 (30.5)
Occurrence of relapse, *n* (%)	86 (19.0)
Mortality, *n* (%)	178 (39.4)
Treatment-related mortality (TRM), *n* (%)	109 (24.1)
Mortality due to acute GVHD, *n* (%)	52 (11.5)
Infection and other TRM, *n* (%)	57 (12.6)
Mortality due to relapse, *n* (%)	57 (12.6)
Unknown reason of mortality, *n* (%)	12 (2.7)

[a]ND, missing data or not determined parameters.

grade), and in 19.0%, a relapse occurred. The overall mortality was 39.4%, and the treatment-related mortality (TRM) amounted to 24.1%. One reason for TRM was aGVHD, and 11.5% of the patients succumbed to aGVHD complications (Table 1).

Patients carrying a *MICA-129Met* allele had an increased probability of overall survival (hazard ratio [HR] = 0.77 per allele, $P = 0.0445$), and *MICA-129Met* homozygote patients had a trend toward a lower TRM (odds ratio [OR] = 0.51, $P = 0.0907$; Table 2). Specifically, the mortality due to aGVHD was reduced (OR = 0.57 per allele, $P = 0.0400$) despite an increased risk for *MICA-129Met* homozygous carriers to experience this complication (OR = 1.92, $P = 0.0371$). These homozygous carriers showed also a trend toward a lower severity of aGVHD (OR = 0.55, $P = 0.1570$), which might explain this finding. Notably, having a < 8/8 HLA-matched unrelated donor ($n = 68$, 15.0%) did not significantly affect these outcomes, in contrast to the *MICA* genotype.

Kaplan–Meyer curves stratified for the *MICA-129* genotypes are shown in Fig 1A for the complete cohort. An improved overall survival was observed similarly in the subgroup transplanted with *MICA-129*-matched grafts (HR = 0.73 per allele, $P = 0.0226$), showing that the effects were associated with the *MICA-129* variants itself and not caused by a *MICA-129* mismatch (Fig 1B). The beneficial effect of the *MICA-129Met* allele on overall survival was present in patients experiencing aGVHD (HR = 0.61 per allele, $P = 0.0116$; Fig 1C) but not in patients without aGVHD (HR 1.37, $P = 0.4634$; Fig 1D), suggesting that the SNP modulates the risk of fatal aGVHD. The beneficial effect was also present in patients who did not receive a T-cell-depleting treatment (HR = 0.67 per allele, $P = 0.0382$; Fig 1E), in contrast to those receiving anti-thymocyte globulin (ATG; HR = 0.88, $P = 0.4821$; Fig 1F), suggesting an effect on T-cell function. Particularly patients carrying a *MICA-129Val/Val* genotype appeared to profit from T-cell depletion when overall survival was compared with *MICA-129Val/Val* carriers not treated with ATG (HR = 0.54, $P = 0.0166$; Fig 1G). No advantage of treatment with ATG was seen in patients carrying one or two *MICA-129Met* alleles (HR = 1.26, $P = 0.3960$; Fig 1H).

In patients not treated with ATG, the beneficial effect of carrying a *MICA-129Met* allele on overall survival (HR = 0.67 per allele, $P = 0.0382$) and mortality due to aGVHD (OR = 0.44 per allele, $P = 0.0420$) even canceled out the unfavorable effects of not giving ATG on overall survival (HR = 1.59, $P = 0.0165$; Table 2). In this patient subgroup, an even clearer trend toward a lower severity of aGVHD (OR = 0.30, $P = 0.0768$) was observed than in all patients. On the other side, *MICA-129Met* alleles might increase the risk of death due to relapse although not at a significant level in this patient subgroup (OR = 3.43 per allele, $P = 0.1450$). In patients receiving ATG, the association of the *MICA-129Met/Met* genotype with an increased risk of aGVHD (OR = 2.46, $P = 0.0271$) was more prominent than in all patients despite an overall lower risk of occurrence of aGVHD due to T-cell depletion (OR = 0.46, $P = 0.0011$; Table 2).

In summary, *MICA-129Met* alleles appeared to confer a higher risk of aGVHD albeit with beneficial effects on survival after HSCT. Specifically, the risk to die due to aGVHD was reduced in patients carrying a *MICA-129Met* allele, whereas patients carrying a *MICA-129Val/Val* genotype profited particularly from ATG treatment. To address the immunological mechanisms involved in these partially counterintuitive outcomes, we investigated whether the MICA-129 variants differ in their ability to trigger NKG2D signals after binding.

Experimental tools used to study functional effects of the MICA-129Val/Met dimorphism

We generated two sets of tools to analyze the functional effects of the MICA-129Val/Met dimorphism. First, we stably transfected L cells, which like all mouse cells do not possess a *MICA* gene, with expression constructs encoding a MICA-129Met or MICA-129Val variant. The MICA-129Met variant was the *MICA*00701* allele, which has a methionine at amino acid position 129. In the MICA-129Val construct, the amino acid position 129 was changed to valine. The resulting L-MICA-129Met and L-MICA-129Val cells, in contrast to vector-only transfected L-con cells, expressed MICA and bound a human NKG2D-Fc protein (Appendix Fig S1A). A broad range of MICA expression intensities was observed on different clones, but on average, these intensities were similar for both variants (Appendix Fig S1B). Analysis of the ratio of MICA expression and NKG2D binding revealed clearly a higher avidity of the MICA-129Met than MICA-129Val variant for NKG2D (Appendix Fig S1C and D) in accord with previous results (Steinle *et al*, 2001). Notably, binding of NKG2D to the MICA-129Met isoform was more dependent on the intensity of MICA expression on individual clones (coefficient of determination $R^2 = 0.62$) than to the MICA-129Val isoform ($R^2 = 0.39$). The slope (regression coefficient) of NKG2D binding with increasing MICA expression intensity was steeper for

Table 2. Association of the *MICA-129* genotype with the outcome of HSCT.

	Effect of *MICA-129Met*[a]				
Cohort *n* = 452	**HR/OR**	**95%-CI**	***P*-value**	**Risk model[b]**	**Adjusted covariates[c]**
Overall survival	**0.77**	[0.60, 0.99]	**0.0445**	additive	MUD, TCD, diagnosis
Treatment-related mortality	0.51	[0.22, 1.07]	0.0907	recessive	MUD, TCD, diagnosis
Mortality due to aGVHD	**0.57**	[0.32, 0.95]	**0.0400**	additive	MUD, TCD, diagnosis
Mortality due to relapse	1.64	[0.71, 4.01]	0.2607	additive	MUD, TCD, FtoM, diagnosis
Occurrence of aGVHD	**1.92**	[1.05, 3.63]	**0.0371**	recessive	MUD, TCD, diagnosis
Severity of aGVHD[d]	0.55	[0.23, 1.21]	0.1570	recessive	MUD, TCD, diagnosis
Occurrence of cGVHD	1.30	[0.96, 1.77]	0.0884	additive	MUD, TCD, TBI, diagnosis
Occurrence of relapse	0.87	[0.61, 1.23]	0.4313	additive	MUD, TBI, diagnosis

	Effect of *MICA-129Met*[a]				Effect of no T-cell depletion[f]	
w/o T-cell depletion *n* = 197[e]	**HR/OR**	**95%-CI**	***P*-value**	**Risk model[b]**	**HR/OR**	***P*-value**
Overall survival	**0.67**	[0.46, 0.98]	**0.0382**	additive	**1.59**	**0.0165**
Treatment-related mortality	0.35	[0.08,1.17]	0.1220	recessive	1.60	0.0991
Mortality due to aGVHD	**0.44**	[0.18, 0.92]	**0.0420**	additive	2.16	0.0559
Mortality due to relapse	3.43	[0.82, 26.1]	0.1450	additive	**4.92**	**0.0285**
Occurrence of aGVHD	1.54	[0.59, 4.53]	0.4037	recessive	**2.16**	**0.0011**
Severity of aGVHD[d]	0.30	[0.06, 1.02]	0.0768	recessive	1.57	0.1720
Occurrence of cGVHD	1.18	[0.76, 1.81]	0.4600	additive	**2.59**	**0.0001**
Occurrence of relapse	0.65	[0.37, 1.11]	0.1257	additive	1.01	0.9670

	Effect of *MICA-129Met*[a]				Effect of T-cell depletion[f]	
T-cell depletion *n* = 252[e]	**HR/OR**	**95%-CI**	***P*-value**	**Risk model[b]**	**HR/OR**	***P*-value**
Overall survival	0.88	[0.62, 1.25]	0.4821	additive	**0.63**	**0.0165**
Treatment-related mortality	0.65	[0.22, 1.61]	0.3799	recessive	0.62	0.0991
Mortality due to aGVHD	0.71	[0.31, 1.50]	0.3941	additive	0.46	0.0559
Mortality due to relapse	1.68	[0.45, 7.60]	0.4565	additive	**0.20**	**0.0285**
Occurrence of aGVHD	**2.46**	[1.13, 5.66]	**0.0271**	recessive	**0.46**	**0.0011**
Severity of aGVHD[d]	0.89	[0.29, 2.52]	0.8365	recessive	0.64	0.1720
Occurrence of cGVHD	1.44	[0.92, 2.25]	0.1039	additive	**0.39**	**0.0001**
Occurrence of relapse	1.14	[0.71, 1.81]	0.5720	additive	0.99	0.9670

[a]Significant effects (HR/OR) with *P*-values ≤ 0.05 are highlighted in bold.
[b]For each outcome, statistics are given for the most powerful genetic model. A recessive *MICA-129* effect was quantified for the *Met/Met* genotype compared to the pooled *Val/Met* and *Val/Val* genotypes. An additive *MICA-129* effect was quantified per *Met* allele.
[c]In addition, all analyses were adjusted for a binary indicator distinguishing whether patient and donor had the same *MICA-129* genotype or not. The following abbreviations for covariates are used: FtoM, female donor for male recipient; MUD, HLA-matched unrelated donor; TBI, total body irradiation; and TCD, T-cell-depleting treatment. Analyses for the strata not receiving (w/o T-cell depletion) and receiving ATG (T-cell depletion) were adjusted for the same covariates except for TCD.
[d]To analyze severity of aGVHD, grades I and II were compared versus grades III and IV.
[e]Three patients were omitted in the stratified analyses because of missing information on T-cell depletion.
[f]Effects of applying or not applying a T-cell-depleting treatment with ATG were analyzed irrespective of the MICA genotype with adjustment for the relevant covariates to confirm the expected effects of applying or omitting ATG treatment on outcome in the cohort. The HR/OR in these strata are reciprocal values having the same *P*-value.

the MICA-129Met (0.23; Fig 2A, left panel) than for the MICA-129Val variant (0.08; Fig 2A, right panel).

Second, we produced for further examination of the MICA-NKG2D interaction both MICA variants and, as control, ovalbumin (OVA) as mouse-IgG_{2a}-Fc fusion proteins (Appendix Fig S2A and B). Both MICA-Fc proteins, in contrast to the OVA-Fc protein, bound specifically and concentration-dependent ($P = 4.28 \times 10^{-9}$, analysis of variance (ANOVA)) to NK cells (Appendix Fig S2C and D). However, there was no significant difference between the MICA-129Met-Fc and MICA-129Val-Fc proteins when the mean fluorescence intensity (MFI; $P = 0.2833$) or the percentage of MICA-binding NK cells ($P = 0.2050$) was evaluated (two-way analysis of covariance (ANCOVA) adjusted for protein concentration). No significant difference was seen in binding of the two MICA-Fc fusion proteins

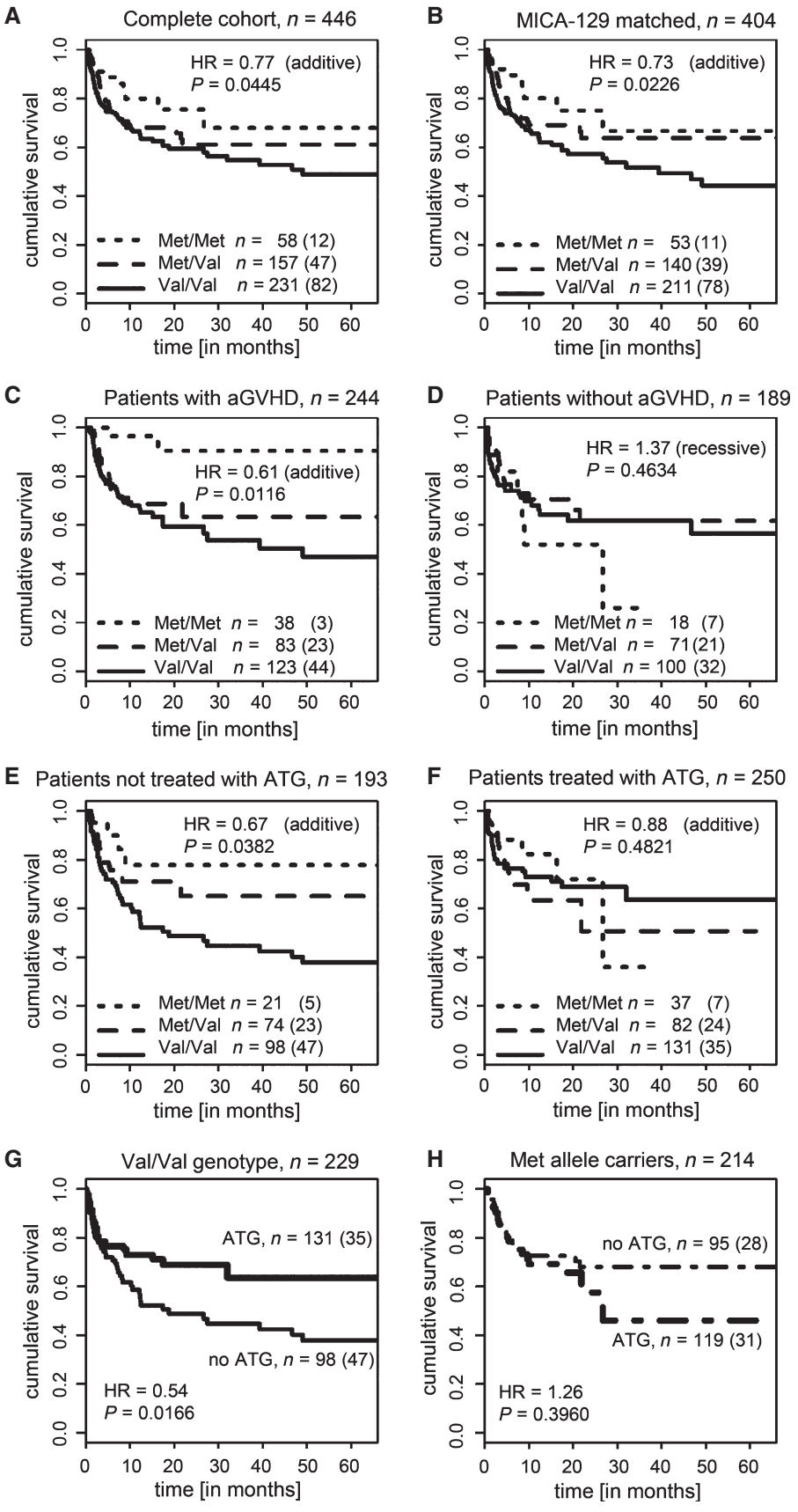

Figure 1.

Figure 1. Cumulative survival according to *MICA-129* genotype.

A Kaplan–Meier survival curves stratified by the patient *MICA-129* genotype for all patients (n = 446). The survival curve is displayed for the first 66 months; 7.6% of the patients were followed longer. Effects on overall survival were determined by Cox regression with covariate adjustment as indicated in Table 2. The HR indicates the risk per *MICA-129Met* allele carried by the patients (additive risk model). The numbers of patients carrying the three genotypes and the number of events (in brackets) are indicated.

B Kaplan–Meier survival curves for patients receiving a graft matched for the *MICA-129* genotype (n = 404).

C Kaplan–Meier survival curves for patients who experienced aGVDH (any grade, n = 244).

D Kaplan–Meier survival curves for patients not experiencing aGVHD (n = 189). The HR indicates the risk of patients carrying two *MICA-129Met* alleles (recessive risk model).

E Kaplan–Meier survival curves for patients who did not receive a T-cell-depleting treatment with ATG (n = 193).

F Kaplan–Meier survival curves for patients treated with ATG (n = 250).

G Kaplan–Meier survival curves for patients with the *MICA-129Val/Val* genotype (n = 229) stratified by treatment with ATG.

H Kaplan–Meier survival curves for patients carrying one or two *MICA-129Met* alleles (n = 214) stratified by treatment with ATG.

to NKG2D in surface plasmon resonance (SPR) analysis (Appendix Fig S3). Nonetheless, these proteins differed in their ability to elicit NKG2D signals (see below).

Engagement of NKG2D alone is not sufficient to induce the release of cytotoxic granules from resting NK cells (Bryceson *et al*, 2009), and freshly isolated NK cells indeed failed to kill the L-MICA-129Met or L-MICA-129Val cell lines in contrast to K562 target cells (Appendix Fig S4A and B). Moreover, no degranulation (CD107a expression) or interferon (IFN)-γ release was elicited (Appendix Fig S4C and D). Exposure to MICA-expressing targets also failed to induce the release of TNF-α, IL-10, and IL-13 from NK cells at least within the first 4 h of co-culture (Appendix Fig S4E). However, we have shown previously that IL-2-stimulated NK cells readily kill MICA-expressing L cells (Elsner *et al*, 2010). Therefore, we used IL-2-stimulated NK cells in subsequent experiments. A comparison of freshly isolated and IL-2-stimulated (100 U/ml for 4 days) NK cells is shown in Fig EV1. The NKG2D expression intensity was not significantly altered by IL-2 on the major NK-cell subpopulations ($CD56^{dim}CD16^{+}$ and $CD56^{bright}CD16^{-}$) and the intermediate population ($CD56^{bright}CD16^{+}$), but the frequency of $CD56^{dim}CD16^{+}$ cells was reduced in contrast to the other two populations.

The MICA-129Met variant triggers stronger phosphorylation of SRC kinases in NK cells than the MICA-129Val variant

NKG2D signaling has been characterized best in NK cells (Billadeau *et al*, 2003; Andre *et al*, 2004). Therefore, we stimulated human NK cells for 3, 10, and 30 min with immobilized MICA-129Met-Fc and MICA-129Val-Fc proteins to determine differences in NKG2D-mediated signaling. Western blot analysis using anti-phospho-tyrosine and anti-phospho-SRC family kinases (Tyr419) antibodies (Ab), respectively, showed a stronger phosphorylation of SRC kinases triggered by the MICA-129Met compared to the MICA-129Val variant (Fig 2B). The ratio of phosphorylated SRC kinase and β-actin signals was determined in three independent experiments and revealed a significant difference 10 min after stimulation (P = 0.0336, t-test; Fig 2C). Inhibition of SRC family kinases by PP2 completely abolished MICA-129Met-Fc- and MICA-129Val-Fc-triggered degranulation (Fig 2D and E), and lysis of L-MICA-129Met and L-MICA-129Val target cells (Appendix Fig S5A), as well as MICA-129Met-Fc- and MICA-129Val-Fc-triggered IFNγ and TNF-α release (Appendix Fig S5B). In these assays, the inhibitor PP2 did not induce apoptosis of NK cells (Appendix Fig S5C and D). The augmented SRC kinase phosphorylation induced by the MICA-129Met variant could therefore be relevant for the extent of NK-cell activation.

The MICA-129Met variant is overall a stronger trigger of NK-cell cytotoxicity than the MICA-129Val variant, but the MICA-129Val variant is outperforming at high MICA expression intensities on target cells

The MICA-129Met-Fc protein indeed elicited significantly more NK-cell degranulation than the MICA-129Val-Fc protein (Fig 3A) based on the MFI of the degranulation marker CD107a (P = 0.0011) and the percentage of $CD107a^{+}$ NK cells (P = 0.0003; two-way ANCOVA adjusted for MICA protein concentration). $CD56^{dim}CD16^{+}$ and, to a lesser extent, $CD16^{bright}CD16^{+}$ NK cells responded to NKG2D engagement by degranulation in contrast to $CD56^{bright}CD16^{-}$ NK cells (Fig EV2A). The MICA-129Met-Fc variant elicited in both $CD16^{+}$ NK-cell populations significantly more degranulation than the MICA-129Val-Fc protein as indicated by the proportion of $CD107a^{+}$ cells (P = 0.0108 and P = 0.0240, t-test) and the MFI of CD107a (P = 0.0250 and P = 0.0049, t-test; Fig EV2B).

Next, we measured the CD107a expression on NK cells exposed to L-con, L-MICA-129Met, or L-MICA-129Val clones (Appendix Fig S6). After adjustment for MICA expression intensity on different clones, the MFI of CD107a was 38.5 units lower on NK cells exposed to L-MICA-129Val targets compared to NK cells attacking MICA-129Met clones (P = 0.0174, ANCOVA) and 10.1%-points less NK cells were $CD107a^{+}$ (P = 0.0456, ANCOVA). Notably, for NK cells encountering the MICA-129Val variant, degranulation significantly increased with MICA expression intensity (MFI of CD107a regression coefficient 0.29), in contrast to NK cells exposed to the MICA-129Met variant (MFI of CD107a regression coefficient 0.05; Fig 3B).

To establish the relevance of the MICA-129 dimorphism for killing of target cells, we analyzed the susceptibility of L cells expressing the MICA-129 variants to killing by lymphokine-activated killer (LAK) cells as exemplified in Fig 3C. For statistical analysis, the killing of K562 cells at an effector to target (E:T) ratio of 200:1 was set to 100% in all individual experiments and used to calculate the relative lysis of the other targets. With adjustment to the MICA expression intensity on different clones, the relative lysis of the MICA-129Val variant expressing L cells was by 13.0%-points reduced compared to L cells expressing the Met variant (at an E:T ratio of 200:1, n = 84 clones, P = 0.0044, two-way ANCOVA). Notably, the MICA expression intensity had even a negative influence on killing for targets expressing the MICA-129Met variant (regression coefficient −0.0834, P = 0.0083, two-way ANCOVA). In contrast, killing increased with expression intensity of the MICA-129Val variant (regression coefficient 0.1257, P < 0.0001 for interaction between MICA-129 variant and MICA expression intensity, two-way ANCOVA).

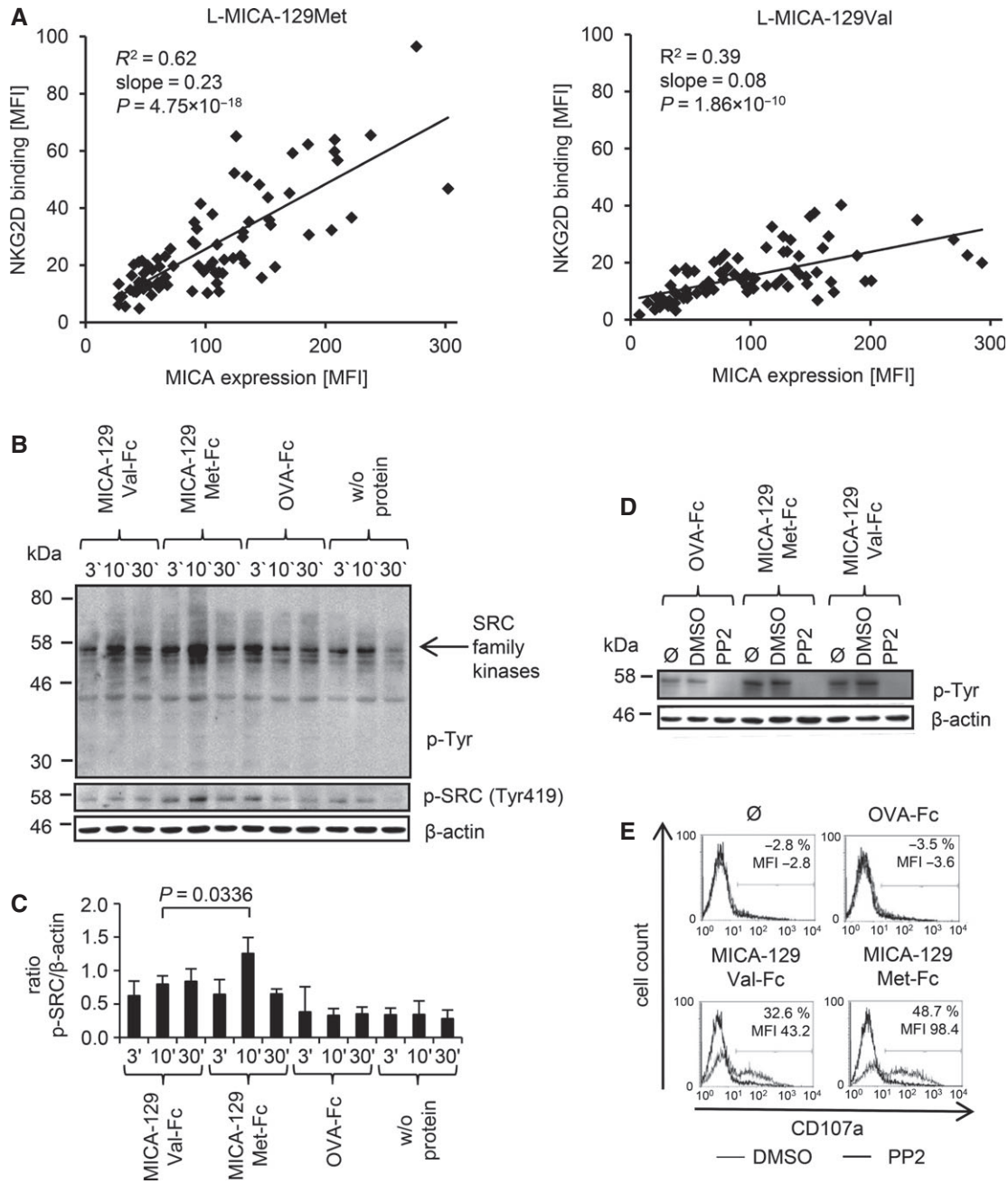

Figure 2. NKG2D binding to the MICA-129Met and MICA-129Val isoform and triggering of phosphorylation of SRC family kinases.

A The linear regression of MICA expression intensity and binding of a recombinant NKG2D-Fc fusion protein both determined as MFI by flow cytometry is displayed for L-MICA-129Met (n = 79, left panel) and L-MICA-129Val clones (n = 81, right panel). The coefficients of determination (R^2), the regression coefficients (reg. coeff.), and the P-values for Pearson correlation are indicated.

B Purified IL-2-stimulated (100 U/ml for 4 days) NK cells (10^6) were stimulated with immobilized MICA-129Met-mIgG_{2a}-Fc or MICA-129Val-mIgG_{2a}-Fc or OVA-mIgG_{2a}-Fc fusion proteins (10 μg/ml) for 3, 10, or 30 min. The protein lysates of these cells were separated by SDS–PAGE, and the blot was probed subsequently with an anti-phospho-Tyr mAb, an anti-phospho-SRC family (Tyr419) kinases Ab, and an anti-β-actin mAb as a loading control. The arrow points toward phosphorylated SRC family kinases.

C Blots obtained from three independent experiments were analyzed by densitometry, and the means plus SD of the ratio between phospho-SRC family kinase and β-actin signals is displayed. The difference between NK cells stimulated for 10 min by MICA-129Met-Fc or MICA-129Val-Fc proteins was assessed by t-test.

D Purified IL-2-stimulated NK cells (100 U/ml for 4 days, 10^6) were incubated with the SRC kinase inhibitor PP2 (25 μM), the vehicle DMSO, or medium only (Ø) for 30 min before being added to immobilized MICA-129Met-Fc, MICA-129Val-Fc, or OVA-Fc fusion proteins (10 μg/ml) for 10 min. The protein lysates of these cells were separated by SDS–PAGE, and the blot was probed subsequently with an anti-phospho-Tyr mAb and an anti-β-actin mAb as a loading control. The blot is representative for two independent experiments.

E In parallel, degranulation of the NK cells was measured by anti-CD107a staining in flow cytometry. The difference between DMSO- and PP2-treated cells with respect to $CD107a^+$ cells and the MFI of CD107a is indicated in the histograms. The results are representative for two independent experiments.

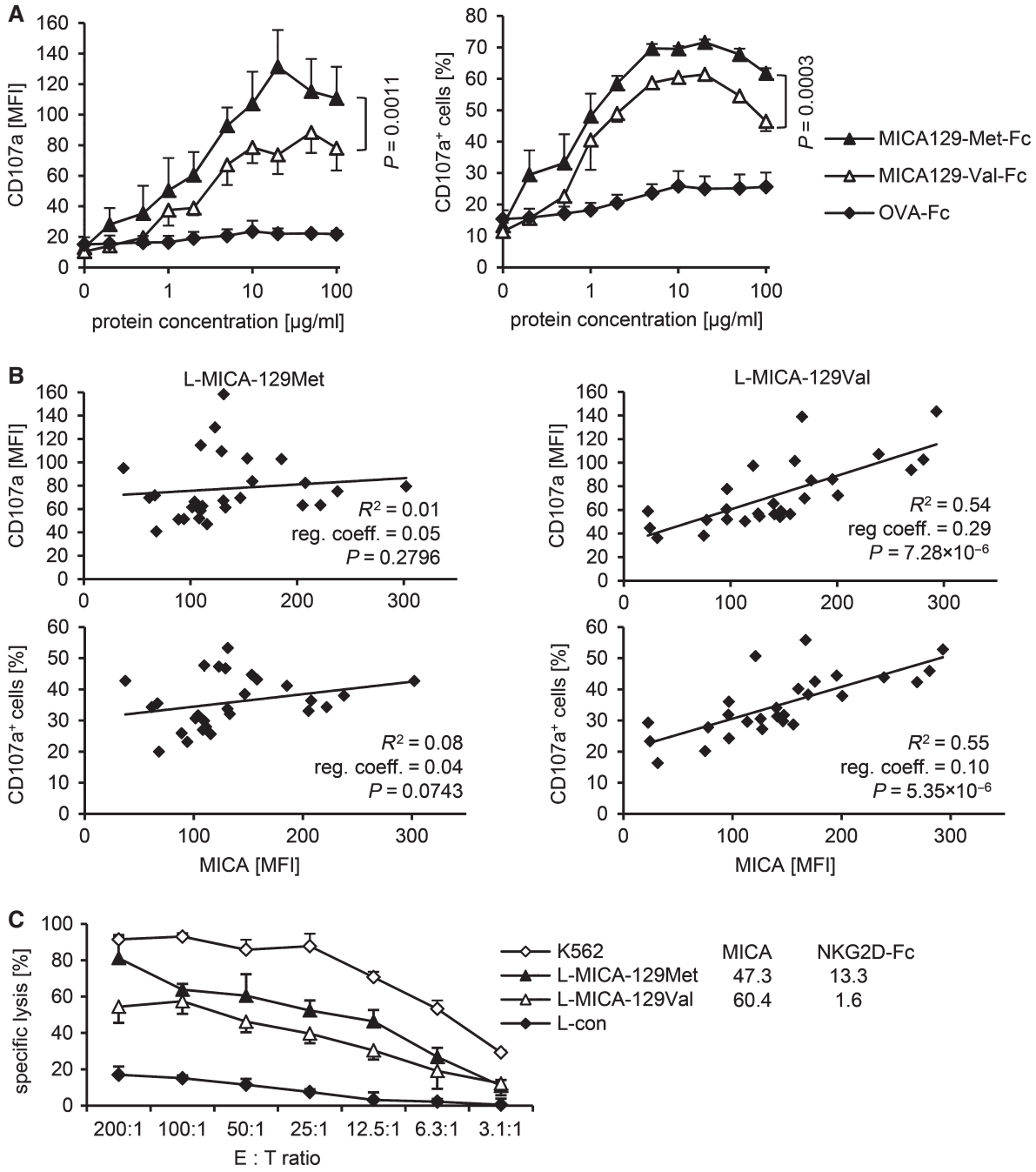

Figure 3. Cytotoxic activity of NK cells in response to the MICA-129Met and MICA-129Val isoforms.

A The degranulation (CD107a expression) of purified IL-2-stimulated (100 U/ml for 4 days) NK cells in response to immobilized MICA-129Met-Fc and MICA-129Val-Fc, and as negative control, OVA-Fc fusion proteins was determined by flow cytometry after 1 h (n = 3). Displayed are means and SD of the MFI (left panel) and the percentage of $CD107a^+$ cells (right panel). Differences between MICA-129Met-Fc- and MICA-129Val-Fc-induced NK-cell degranulation were analyzed by two-way ANCOVA adjusted for MICA protein concentration, and the respective P-values are indicated.

B The degranulation of IL-2-stimulated LAK cells (100 U/ml for 4 days) exposed to L-MICA-129Met (n = 27) or L-MICA-129Val clones (n = 27) for 1 h was determined by flow cytometry. CD107a cell surface expression was analyzed after gating on $CD56^+$ NK cells. In parallel, the MICA expression on target cells was determined. Displayed are the linear regressions of the MFI of CD107a on NK cells (upper panels) or the proportion of $CD107a^+$ NK cells (lower panels) and the MICA expression intensity on target cells (MFI) for the L-MICA-129Met (left panels) and L-MICA-129Val clones (right panels). The coefficients of determination (R^2), the regression coefficients (reg. coeff.), and the P-values for Pearson correlation are indicated.

C A representative of 21 experiments is shown demonstrating the specific cytotoxic activity of LAK cells against an L-MICA-129Met and an L-MICA-129Val clone. L-con cells served as a negative and K562 cells as a positive control. The means of specific lysis of triplicates plus SD at different E:T ratios (200:1 to 3:1) were measured in an ^{51}chromium-release assay. The MICA expression intensity and the binding of a recombinant NKG2D-Fc fusion protein to the target cells were determined in parallel by flow cytometry, and the MFIs are indicated.

Taken together, the MICA-129Met variant triggered stronger NK-cell cytotoxicity at lower MICA expression intensities compared to the MICA-129Val variant. Degranulation increased with expression intensity of the MICA-129Val variant, whereas high expression of the MICA-129Met variant even decreased target cell killing.

The MICA-129Met variant is overall a stronger trigger of IFNγ release by NK cells than the MICA-129Val variant, but IFNγ expression decreases at high MICA-129Met expression intensities

IFNγ release is a further effector function of NK cells triggered by NKG2D. $CD56^{bright}CD16^{-}$ and, to a lesser extent, $CD56^{bright}CD16^{+}$ NK cells responded to the MICA-129Met-Fc and MICA-129Val-Fc proteins with IFNγ expression in contrast to $CD56^{dim}CD16^{+}$ NK cells (Fig EV3A). The MICA-129Met-Fc protein induced more $IFN\gamma^{+}$ NK cells than the MICA-129Val-Fc variant ($P = 0.0026$ and $P = 0.0434$, ANCOVA adjusted for MICA protein concentration), and the MFI of IFNγ was higher ($P = 0.0306$ and $P = 0.0074$; Fig EV3B). The MICA-129Met-Fc protein elicited more IFNγ ($P = 0.0216$, ANCOVA adjusted to protein concentration) and also more TNF-α release from NK cells than the MICA-129Val-Fc variant ($P = 0.0363$) as determined by enzyme-linked immuno-sorbent assays (ELISA). Release of the Th_2 cytokines IL-10 and IL-13 was not induced at least not within the first 4 h of stimulation. Engagement of NKG2D appeared even to inhibit IL-13 production (Appendix Fig S8).

Next, we exposed NK cells to MICA-expressing L cells. After adjustment to MICA expression intensity on different clones, $CD56^{bright}CD16^{-}$ NK cells co-cultured with L-MICA-129Val targets expressed less IFNγ compared to cells exposed to MICA-129Met clones. The MFI of IFNγ was on average 12.5 units lower ($P = 0.0032$, ANCOVA), and 7.5%-points less $CD56^{bright}CD16^{-}$ NK cells were IFNγ positive ($P = 0.0061$, ANCOVA). For $CD56^{bright}CD16^{-}$ NK cells encountering the MICA-129Val variant, the proportion of $IFN\gamma^{+}$ cells and the MFI of IFNγ increased with MICA expression intensity (regression coefficients 0.14 and 0.09, respectively), whereas cells exposed to the MICA-129Met variant expressed less IFNγ when co-cultured with targets with higher MICA expression intensity (MFI, regression coefficient −1.11; Fig 4A). The results obtained for $CD56^{bright}CD16^{+}$ and $CD56^{dim}CD16^{+}$ NK cells in these experiments are shown in the Appendix Fig S7.

The effect of the MICA-129 dimorphism was further confirmed when IFNγ release was measured by ELISA in an independent set of experiments. Adjusted to MICA expression intensity on different clones, IFNγ production was by 176.5 pg/ml higher for NK cells exposed for 24 h to L-MICA-129Met compared to L-MICA-129Val clones ($P < 0.0001$, ANCOVA; Fig 4B). For NK cells exposed to the MICA-129Val variant, the MICA expression intensity had a strong effect on IFNγ release (1.103 pg/ml per MFI unit of MICA, $P < 0.0001$, ANCOVA), in contrast to NK cells exposed to L-MICA-129Met targets (0.142 pg/ml per MFI unit, $P = 0.0001$ for interaction between MICA-129 variant and MICA expression intensity, ANCOVA). IFNγ production of NK cells cultured in the absence of target cells or secretion of NK cells exposed to the L-con cells was either not detectable or < 25 pg/ml.

The MICA-129Met variant leads to stronger down-regulation of NKG2D on the plasma membrane of NK cells than the MICA-129Val variant

Next, we asked why increasing expression of the high-avidity MICA-129Met isoform did not trigger continuously stronger functional responses as the low-avidity MICA-129Val isoform did. Since MICA can be cleaved from the cell surface (Groh *et al*, 2002; Salih *et al*, 2002; Waldhauer *et al*, 2008), one possibility was that higher expression of MICA leads to higher concentrations of soluble MICA (sMICA), which can inhibit NKG2D signaling (Groh *et al*, 2002). However, L-MICA-129Met and L-MICA-129Val clones did not release MICA (Appendix Table S1).

Sustained exposure of NK cells to NKG2D ligand-expressing cells can also down-regulate NKG2D (Coudert *et al*, 2005; Ogasawara *et al*, 2005; Oppenheim *et al*, 2005; Wiemann *et al*, 2005). Thus, we investigated NKG2D expression on NK cells exposed for 4 and 24 h to L-con, L-MICA-129Met, or L-MICA-129Val clones (Fig 5, Appendix Fig S9A). The percentage of $NKG2D^{+}$ NK cells decreased by 9.5%-points for the MICA-129Val ($P = 0.0309$) and by 19.4%-points for the MICA-129Met variant ($P < 0.0001$) compared to the control (co-culture with L-con cells; two-way ANCOVA adjusted for MICA expression intensity on different clones). The MFI of NKG2D decreased by 11.8 units for the MICA-129Val ($P = 0.0006$) and by 13.7 units for the MICA-129Met variant ($P = 0.0001$) compared to the control (two-way ANCOVA). Notably, the percentage of $NKG2D^{+}$ cells decreased more among NK cells encountering L-MICA-129Met than L-MICA-129Val targets (−9.3%-points, $P = 0.0008$, two-way ANCOVA). In addition, the MFI of NKG2D was significantly different between NK cells exposed to L-MICA-129Met and L-MICA-129Val targets ($P = 0.0225$, two-way ANCOVA). In these analyses as in the previous analyses, we adjusted for the MICA expression intensity on different clones although it had little effect on the NKG2D down-regulation on NK cells (Appendix Fig S10). NK cells co-cultured with L-MICA cells did not show differences in CD94 expression indicating the specificity of the effect (Appendix Fig S9B and C).

Notably, the NKG2D expression was significantly reduced on all three NK-cell subpopulations 4 and 24 h after exposure to MICA-expressing targets (Fig EV4A). After adjustment to MICA expression intensities, the NKG2D expression was on average 19.5 ($P = 8.04 \times 10^{-6}$, $CD56^{dim}CD16^{+}$), 16.2 ($P = 2.26 \times 10^{-8}$, $CD56^{bright}CD16^{+}$), or 15.8%-points ($P = 1.02 \times 10^{-4}$, $CD56^{bright}CD16^{-}$) lower on NK cells exposed to L-MICA-129Met than L-MICA-129Val clones (Fig EV4B). Hence, the MICA-129Met variant induced a stronger down-regulation of NKG2D than the MICA-129Val variant. This counter-regulation appears to limit the initially stronger functional effects of the MICA-129Met variant on NKG2D signaling.

The MICA-129Met variant leads to an earlier antigen-specific activation of $CD8^{+}$ T cells

NKG2D on $CD8^{+}$ T cells functions as a co-stimulatory molecule (Groh *et al*, 2001), and stimulation of NKG2D alone was indeed not sufficient to induce a proliferation of purified $CD8^{+}$ T cells even at high concentrations of anti-NKG2D or MICA-129Met/Val-Fc proteins (Appendix Fig S11). At low concentrations of anti-CD3 (0.005 and 0.01 μg/ml), co-stimulation of $CD8^{+}$ T cells by

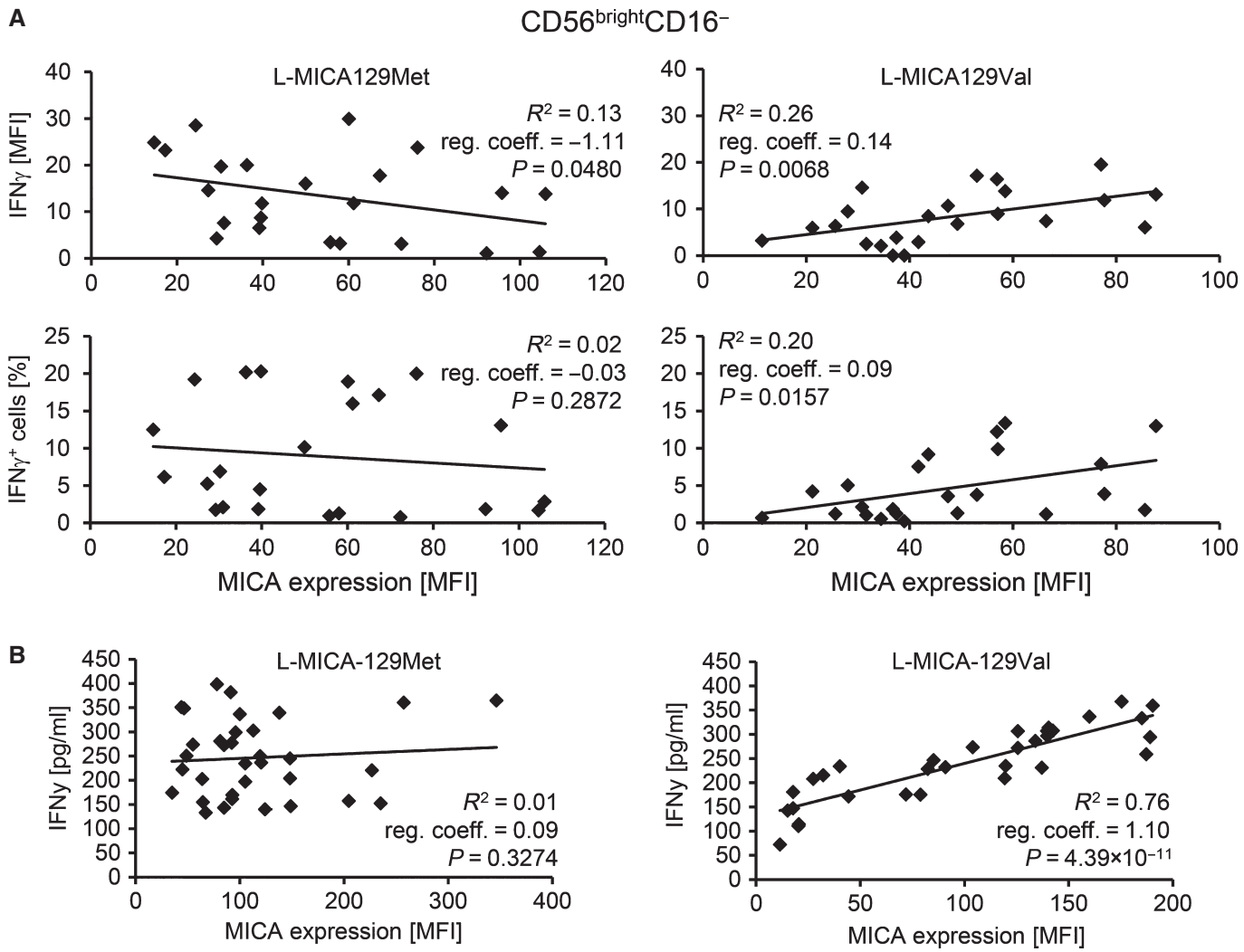

Figure 4. IFNγ production of NK cells in response to the MICA-129Met and MICA-129Val isoforms.

A The IFNγ expression of purified IL-2-stimulated (100 U/ml for 4 days) NK cells exposed for 4 h to L-MICA-129Met (n = 23) or L-MICA-129Val clones (n = 23) was determined by flow cytometry. The IFNγ expression was analyzed after gating on $CD56^{bright}CD16^{-}$ NK cells. In parallel, the MICA expression on target cells was determined. Displayed are the linear regressions of the MFI of IFNγ in $CD56^{bright}CD16^{-}$ NK cells (upper panels) or the proportion of $IFN\gamma^{+}$ $CD56^{bright}CD16^{-}$ NK cells (lower panels) and the MICA expression intensity on target cells (MFI) for the L-MICA-129Met (left panels) and L-MICA-129Val clones (right panels). The coefficients of determination (R^2), the regression coefficients (reg. coeff.), and the P-values for Pearson correlation are indicated.

B The IFNγ release of purified IL-2-stimulated NK cells (100 U/ml for 4 days) co-cultured with L-MICA-129Met (n = 34) or L-MICA-129Val clones (n = 32) for 24 h was measured in the supernatant by ELISA. In parallel, the MICA expression intensity on target cells was determined by flow cytometry. The linear regressions of IFNγ release (pg/ml) by NK cells and MICA expression on targets (MFI) are displayed for the L-MICA-129Met clones (left panel) and the L-MICA-129Val clones (right panel). The coefficients of determination (R^2), the regression coefficients (reg. coeff.), and the P-values for Pearson correlation are indicated.

anti-NKG2D induced proliferation and IL-2 production as expected but less efficiently than co-stimulation by anti-CD28 (Appendix Fig S12). Both, the MICA-129Met-Fc and MICA-129Val-Fc proteins provided co-stimulatory signals but did not differ in their capacity to induce proliferation or IL-2 production when measured after 96 h (Fig 6A). However, at 72 h after stimulation, $CD8^{+}$ T cells had proliferated more in response to the MICA-129Met-Fc than MICA-129Val-Fc or OVA-Fc proteins (P = 0.0277, Wilcoxon test), suggesting a slightly earlier activation by NKG2D-mediated co-stimulation via the MICA-129Met-Fc protein (Fig 6B and C). The effects of co-stimulation by anti-CD28 and anti-NKG2D are shown for comparison (Fig 6D).

The MICA-129Met variant leads to stronger down-regulation of NKG2D on $CD8^{+}$ T cells than the MICA-129Val variant impairing subsequent co-stimulation

NKG2D was strongly down-regulated on $CD8^{+}$ T cells co-cultured with L-MICA-129Met but hardly after co-culture with L-MICA-129Val clones (Fig EV5). The proportion of $NKG2D^{+}CD3^{+}CD8^{+}$ cells decreased by 35.8%-points more when exposed to L-MICA-129Met clones compared to those encountering the L-MICA-129Val clones ($P = 7.8 \times 10^{-8}$ two-way ANOVA adjusted for MICA expression intensity on different clones), and the MFI of NKG2D decreased by 12.1 units more ($P = 2.6 \times 10^{-5}$; Fig 7A). Notably, on $CD8^{+}$

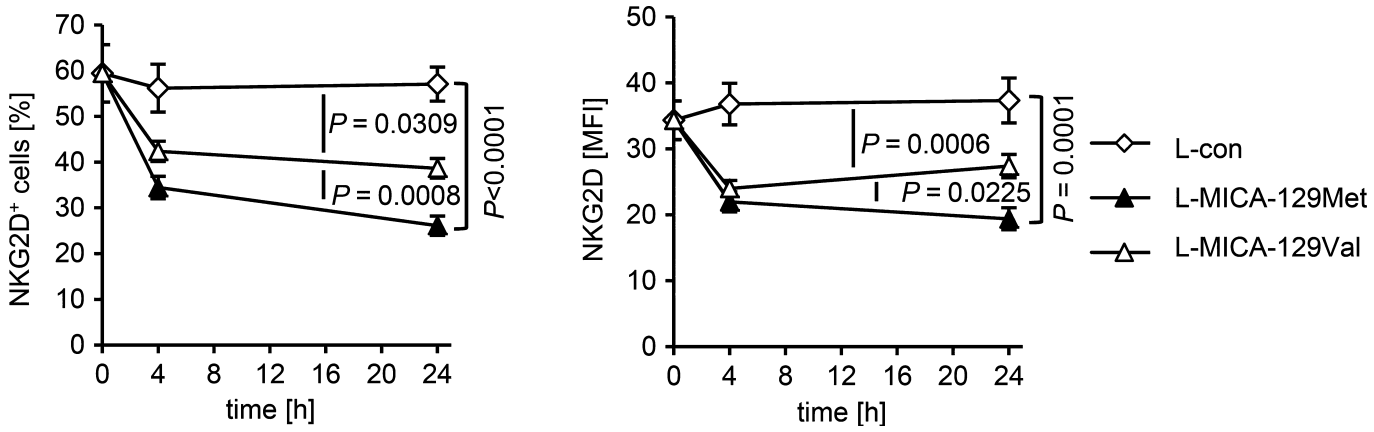

Figure 5. Down-regulation of NKG2D on NK cells in response to the MICA-129Met and MICA-129Val isoforms.
NKG2D expression on purified IL-2-stimulated NK cells (100 U/ml for 4 days) exposed to L-MICA-129Met (n = 25) or L-MICA-129Val clones (n = 25) for 0, 4, and 24 h was analyzed by flow cytometry. NK cells (2.5×10^5) were co-cultured with 5×10^4 target cells and analyzed for NKG2D expression after gating of $CD3^-CD56^+$ cells. The means and SD of the percentage of $NKG2D^+$ NK cells (left panel) and of the MFI of NKG2D (right panel) are shown. Differences between the groups were analyzed by repeated measures ANOVA, and P-values for pairwise comparisons are indicated.

T cells, the MFI of NKG2D decreased clearly more when exposed to clones with higher MICA-129Met expression intensity ($P = 0.016$, two-way ANCOVA), whereas CD8 expression was not altered indicating the specificity of the effect (Appendix Fig S13). The down-regulation of NGK2D on $CD8^+$ T cells was functionally relevant. Exposure of $CD8^+$ T cells to anti-NKG2D for 24 h reduced NKG2D expression (Fig 7B) and impaired their capability to proliferate subsequently in response to NKG2D-mediated co-stimulation (Fig 7C and D and Appendix Fig S14). The strong down-regulation of NKG2D on $CD8^+$ T cells by MICA-129Met variants appears to be important for the association of this polymorphism with the outcome of HSCT.

Discussion

Numerous studies have demonstrated the impact of SNPs on the outcome of HSCT (Dickinson, 2008; Harris *et al*, 2013). Those SNPs, which alter gene regulation or protein function, might not only be useful as biomarkers but also identify new targets for therapy. We focused on the MICA-129Val/Met dimorphism, which has been previously associated with the risk of cGVHD and relapse (Boukouaci *et al*, 2009).

We generated MICA-129Met and MICA-129Val variants differing only in amino acid position 129 to enable testing of effects of this single amino acid variation that was reported to distinguish MICA variants with high and low binding avidity to NKG2D (Steinle *et al*, 2001). Natural *MICA* alleles usually combine several polymorphisms, and homozygosity is infrequent, making it impossible to study effects of a single amino acid exchange using patient-derived cells or materials. Using MICA-transfected L cells, we confirmed the previous report by Steinle and colleagues (Steinle *et al*, 2001) that the MICA-129Met variant binds NKG2D better than the MICA-129Val isoform. Replacement of valine by methionine affects NKG2D binding indirectly likely by a conformational change since this position is not directly involved in NKG2D binding (Li *et al*, 1999, 2001). We show here that both MICA isoforms differed also in their efficacy to elicit NKG2D-mediated cellular responses. Notably, the greater

Figure 6. Co-stimulation of $CD8^+$ T cells by the MICA-129Met and MICA-129Val isoforms.

A MACS-separated $CD8^+$ T cells were cultured in triplicate on an immobilized anti-CD3 mAb (0.005 μg/ml [upper panel] or 0.01 μg/ml [lower panel]) in combination with recombinant MICA-129Met-Fc, MICA-129Val-Fc, and OVA-Fc proteins at various concentrations (1.0, 0.5, 0.1, 0.0 μg/ml). After 72 h, 25% of the supernatant was harvested and IL-2 concentrations were measured by ELISA. The harvested medium was replaced by the same volume containing 1 μCi ^{3}H-labeled thymidine. After 12 h, the plates were completely harvested and the DNA-bound radioactivity was determined. The means and SD of the stimulation index (SI) are displayed (n = 4). Significant differences between MICA-129Met/Val-Fc and OVA-Fc proteins were found when the antigen-specific signal (anti-CD3) was limited (*$P < 0.05$, t-test; upper left panel: 1.0 μg/ml: MICA-129Met-Fc versus OVA-Fc $P = 0.0372$ and MICA-129Val-Fc versus OVA-Fc $P = 0.0366$; upper right panel: 1.0 μg/ml: MICA-129Met-Fc versus OVA-Fc $P = 0.0499$ and MICA-129Val-Fc versus OVA-Fc $P = 0.0192$; 0.5 μg/ml: MICA-129Met-Fc versus OVA-Fc $P = 0.0164$ and MICA-129Val-Fc versus OVA-Fc $P = 0.0357$; lower left panel: 0.5 μg/ml: MICA-129Met-Fc versus OVA-Fc $P = 0.0287$ and MICA-129Val-Fc versus OVA-Fc $P = 0.0232$; lower right panel: 1.0 μg/ml: MICA-129Met-Fc versus OVA-Fc $P = 0.0171$ and MICA-129Val-Fc versus OVA-Fc $P = 0.0484$).

B Purified CFSE-stained $CD8^+$ T cells were stimulated by immobilized anti-CD3 (0.005 μg/ml) in combination with recombinant MICA-129Met-Fc, MICA-129Val-Fc, OVA-Fc proteins, or co-stimulatory mAb (anti-CD28, anti-NKG2D) or an isotype control ($mIgG_1$). The proliferation of $CD3^+CD8^+$ T cells was assessed at 60 h by flow cytometry. Results of a representative out of 6 experiments are displayed. Untreated CFSE-stained $CD8^+$ T cells are included for comparison. The percentage of proliferating cells and MFI for CFSE are indicated.

C The MFI of CFSE in unstimulated $CD8^+$ T cells (control) was set to 100% in individual experiments (n = 6), and the relative decrease due to proliferation was calculated. Means + SD are shown. Significant differences (*$P = 0.0277$, Wilcoxon test) between MICA-129Met-Fc versus MICA-129Val-Fc and OVA-Fc proteins were found at slightly higher anti-CD3 concentrations (0.1 and 0.05 μg/ml) than at later time points (see A).

D Anti-CD28 and anti-NKG2D mAb were used in parallel as a positive control, mean + SD are shown, and significant differences (*$P = 0.0277$, Wilcoxon test) to the isotype control ($mIgG_1$) are indicated (n = 6).

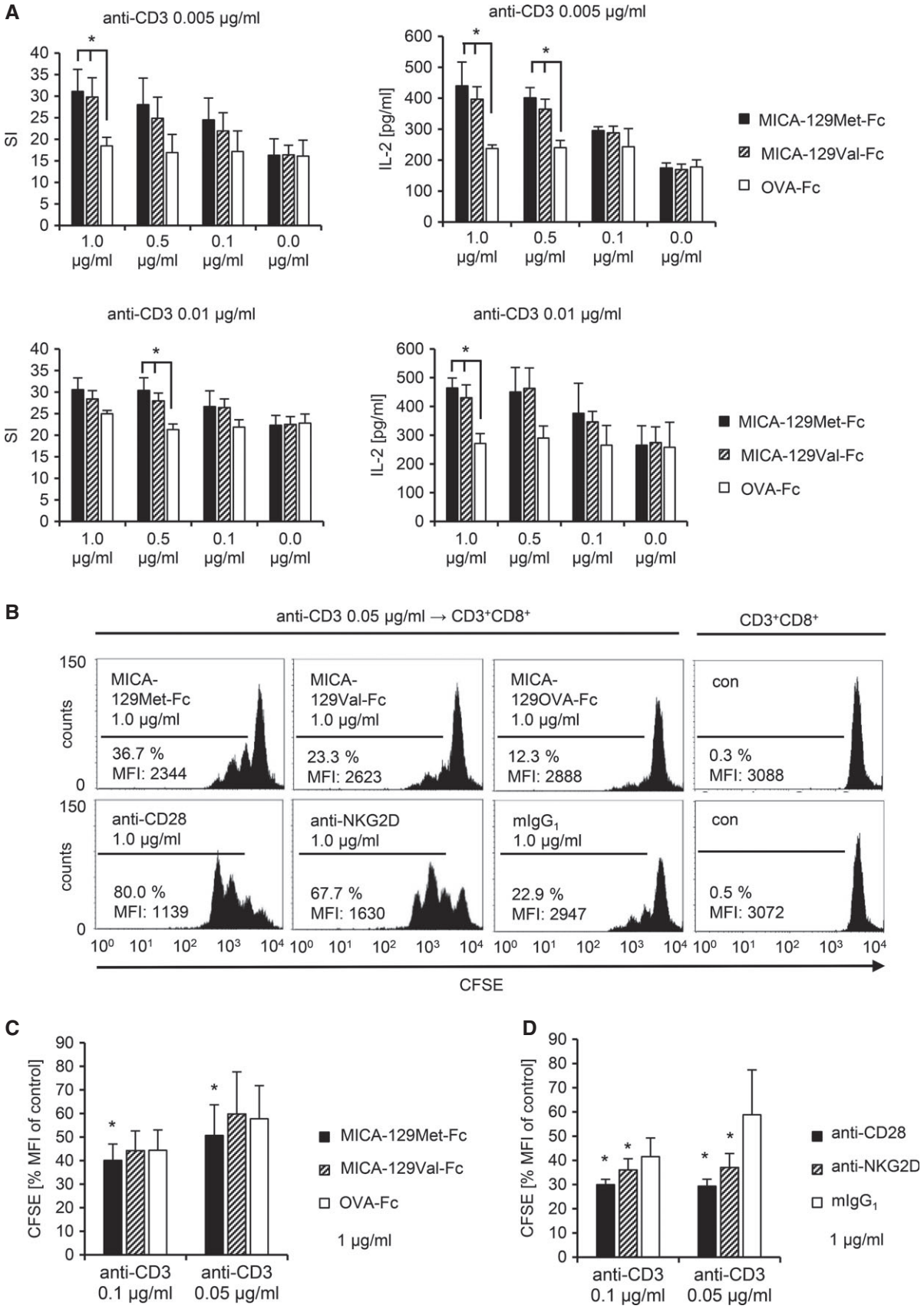

Figure 6.

efficacy of the MICA-129Met variant to elicit down-stream signals was not explained alone by its higher NKG2D binding avidity. Recombinant MICA-129Met-Fc and MICA-129Val-Fc proteins also elicited different functional responses but did not significantly differ in binding avidity to NKG2D. Thus, both variants varied also in their efficacy to elicit NKG2D signal transduction after binding.

The first alteration downstream of NKG2D binding was a stronger phosphorylation of SRC family kinases in NK cells stimulated by the MICA-129Met compared to the MICA-129Val variant. This included tyrosine residue Y419, which is auto-phosphorylated during activation. SRC kinases are essential for NKG2D-triggered cytotoxicity in human NK cells (Billadeau *et al*, 2003), and the SCR family kinase inhibitor PP2 indeed completely abolished degranulation and IFNγ release induced by the recombinant MICA-129Met/Val proteins. MICA-129Met ligands triggered more degranulation of $CD56^{dim}CD16^{+}$ NK cells and IFNγ production of $CD56^{bright}CD16^{-}$ NK cells than MICA-129Val ligands. The amount of degranulation and IFNγ secretion correlated positively with the MICA expression intensity on target cells but only for the MICA-129Val variant. In contrast, the expression intensity of MICA-129Met ligands had either none or even a negative effect on the magnitude of degranulation and IFNγ expression or release. It also inversely influenced the killing of target cells, whereas killing increased steadily with expression intensity of the MICA-129Val variant. On $CD8^{+}$ T cells, the MICA-129Met variant led to a slightly earlier co-stimulatory activation than the MICA-129Val variant. Importantly, the MICA-129Met variant induced a stronger down-regulation of NKG2D on NK cells and even more on $CD8^{+}$ T cells than the MICA-129Val isoform. Down-regulation of NKG2D on $CD8^{+}$ T cells impaired their capability to receive co-stimulatory signals via NKG2D. Hence, the stronger capacity of the MICA-129Met variant to signal via NKG2D itself limited the biological effects of an increased MICA-129Met expression intensity by a reduction in NKG2D expression. In other words, MICA-129Met variants, which elicit strong NKG2D responses, stimulate in parallel a robust negative feedback signal.

The counter-regulation of NKG2D could be a fairly uncomplicated mechanism contributing to the tuning of NKG2D responses with respect to MICA expression intensities, which has been reported recently (Shafi *et al*, 2011). In this study investigating several MICA-129Met but no MICA-129Val isoforms, the highest functional responses of NK and γδT cells were also not elicited by targets with highest MICA expression intensities. It has been suggested that NKG2D-mediated responses are tuned to an optimum against the MICA expression intensity that is most commonly induced by cellular dysregulation in an individual (Shafi *et al*, 2011).

In summary, the degree of NK-cell cytotoxicity and cytokine production increased steadily with the MICA expression intensity, if the MICA-129Val variant was present on target cells. Augmented expression of the MICA-129Met isoform, in contrast, had no or even a negative effect on NK-cell function (Fig 8A). On $CD8^{+}$ T cells, co-stimulation with the MICA-129Met variant allowed for an earlier antigen-dependent activation than the MICA-129Val variant, but a rapid down-regulation of NKG2D impaired any subsequent NKG2D-dependent co-stimulation (Fig 8B). This interaction between MICA-129 genotype and MICA expression intensity is likely important for understanding of MICA-129 disease associations. Notably, these data show that the MICA-129Met/Val dimorphism affects differently NKG2D signaling and NKG2D expression at the plasma membrane (see Table 3 for a summary). On the basis of this model, we could build hypotheses on clinical outcomes expected to be associated with this SNP after HSCT (Table 3).

After HSCT, NKG2D-mediated co-stimulation of $CD8^{+}$ T cells presumably contributes to both GVHD and graft-versus-leukemia (GVL) reactions and similarly, NKG2D-mediated NK-cell activation potentially contributes to GVL effects and to protection against pathogens such as cytomegalovirus (Leung, 2011). MICA-129Met variants eliciting immediately a stronger $CD8^{+}$ T- and NK-cell activation might therefore contribute to the occurrence of aGVHD. MICA is constitutively expressed in gastrointestinal epithelium (Groh *et al*, 1996), a target organ of GVHD, and can be up-regulated in other tissues under conditions of inflammation (Raulet *et al*, 2013). Inflammation is known to occur frequently after preconditioning, and MICA/B expression was indeed found in skin and liver during aGVHD (Gannage *et al*, 2008). Non-professional antigen-presenting cells that express MICA upon cellular stress become able to activate $CD8^{+}$ T cells directly. This pathway presumably contributes to the initiation of aGVHD, if MICA is expressed on normal cells, such as endothelial or epithelial cells, and alloreactive $CD8^{+}$ T cells become activated. MICA on leukemic cells could help to initiate GVL reactions by co-stimulation of anti-leukemic $CD8^{+}$ T cells. However, the severity of aGVHD and the risk of cGVHD but also the probability of strong GVL effects could be limited by down-regulation of NKG2D on $CD8^{+}$ T cells. In a murine model of HSCT, it has been recently demonstrated that NKG2D indeed contributes to aGVHD and graft-versus-tumor effects (Karimi *et al*, 2015).

Figure 7. Down-regulation of NKG2D by the MICA-129Met and the MICA-129Val isoforms on $CD8^{+}$ T cells and impairment of subsequent co-stimulation via NKG2D.

A NKG2D expression on purified $CD8^{+}$ T cells exposed to L-MICA-129Met (n = 19) or L-MICA-129Val clones (n = 19) for 0, 4, and 24 h was analyzed by flow cytometry. $CD8^{+}$ T cells (2.5×10^{5}) were co-cultured with 5×10^{4} target cells and analyzed for NKG2D expression after gating on $CD3^{+}CD8^{+}$ T cells. The means and SD of the MFI of NKG2D (left panel) and of the percentage of $NKG2D^{+}CD8^{+}$ T cells (right panel) are displayed. Differences between the groups were analyzed by repeated measures ANOVA, and the P-values are indicated.

B Purified $CD8^{+}$ T cells were cultured on plate-bound anti-NKG2D (1 μg/ml) or isotype control ($mIgG_1$) for 24 h before the NKG2D expression was measured by flow cytometry. Means and SD of MFI (upper panel) and percentage of $NKG2D^{+}$ cells (lower panel) are shown (n = 6). Differences between the groups were analyzed by t-tests, and the P-values are indicated.

C These $CD8^{+}$ T cells were subsequently CFSE-stained and cultured on plates coated with anti-CD3 (0.005 μg/ml) in combination with anti-CD28 (0.5 μg/ml) as a positive control or anti-NKG2D (0.5 μg/ml). Proliferation was measured after 60 h by flow cytometry. Untreated CFSE-stained $CD8^{+}$ T cells are included for comparison. The percentage of proliferating cells and the MFI for CFSE are indicated.

D The MFI of CFSE in unstimulated $CD8^{+}$ T cells (control) was set to 100% in individual experiments (n = 6), and the relative decrease due to proliferation was calculated. Means + SD are shown. Significant differences (Wilcoxon test) between $CD8^{+}$ T cells pre-exposed to anti-NKG2D and isotype control ($mIgG_1$) were found in these experiments at anti-CD3 concentrations of 0.01 and 0.005 μg/ml.

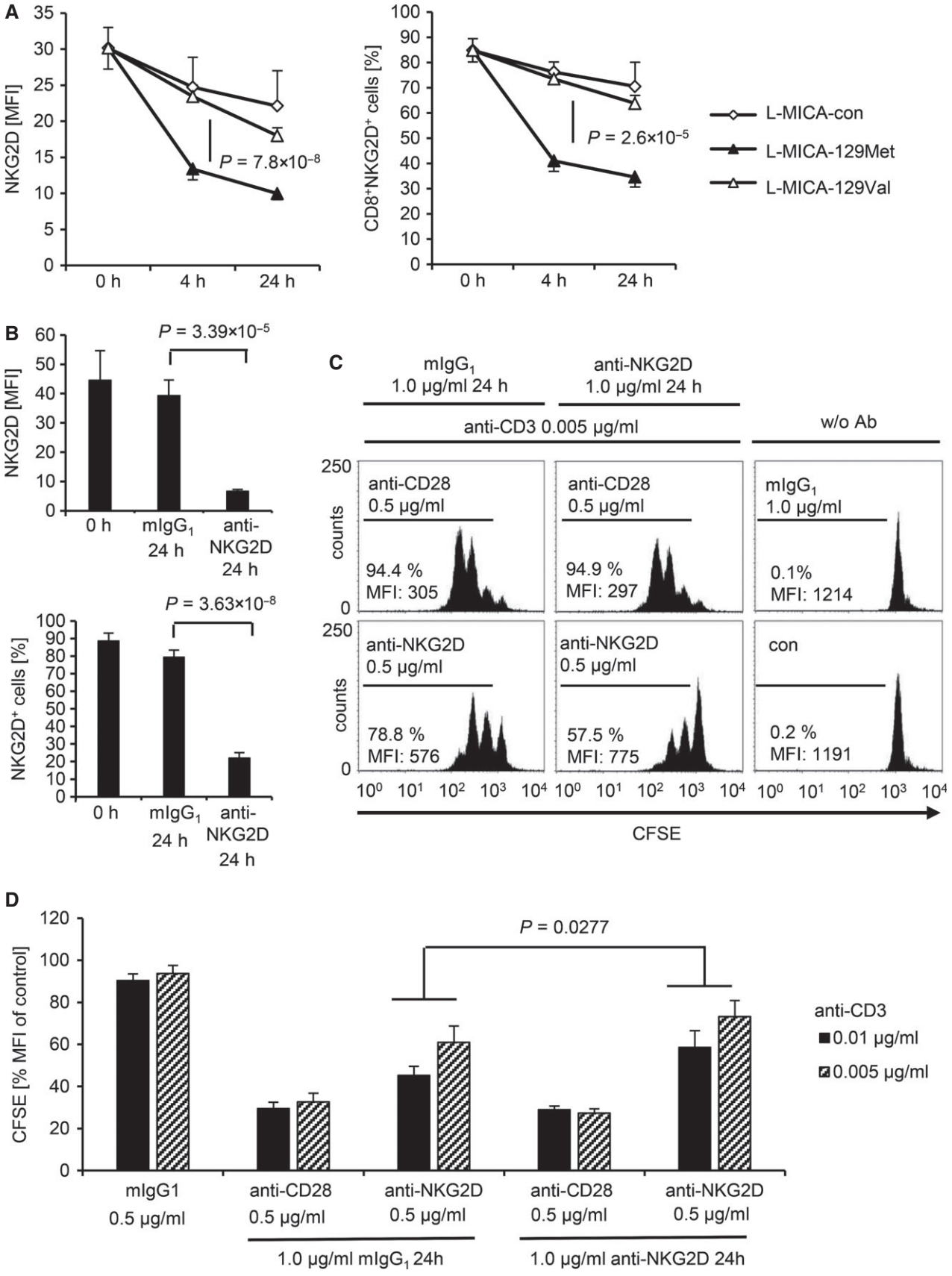

Figure 7.

MICA can be expressed on leukemic (Salih *et al*, 2003; Sconocchia *et al*, 2005; Boissel *et al*, 2006; Kato *et al*, 2007; Diermayr *et al*, 2008; Nückel *et al*, 2010; Sanchez-Correa *et al*, 2011; Hilpert *et al*, 2012) and on lymphoma cells (Dulphy *et al*, 2009; Reiners *et al*, 2013). MICA-129Met variants eliciting earlier or stronger $CD8^+$ T- and NK-cell activation could in principal also allow for faster eradication of those malignant cells. However, the loss of NKG2D expression in response to engagement of a MICA-129Met variant would likely be more important over time. Therefore, a decreased NK and $CD8^+$ T-cell activity against malignant cells expressing NKG2D ligands would be expected to increase the risk of a relapse in carriers of a *MICA-129Met* allele. Notably, not only NK cells but also *in vitro*-activated $CD8^+$ T cells were reported to kill malignant cells expressing NKG2D ligands in an T-cell receptor-independent but NKG2D-dependent manner (Dhanji *et al*, 2004; Verneris *et al*, 2004; Karimi *et al*, 2005) and such cells have even been used in adoptive immunotherapy after HSCT (Laport *et al*, 2011; Meehan *et al*, 2013).

In our cohort, the homozygous carriers of MICA-129Met alleles had indeed an increased risk to experience aGVHD, which could be the consequence of immediate effects of MICA-129Met variants on NKG2D signaling (Table 3). The *MICA-129Met* alleles appeared to support the initiation of aGVHD in homozygous carriers especially in patients receiving ATG. In this subgroup with an overall substantially reduced risk to develop aGVHD, the faster co-stimulatory activation of residual $CD8^+$ T cells by the MICA-129Met variant could be important, whereas this difference might not matter if a full $CD8^+$ T cell repertoire is present in patients. Alternatively, pro-inflammatory cytokines, such as IFNγ released by NK cells in response to stimulation of NKG2D, could contribute to aGVHD (Ferrara *et al*, 1989). On the other hand, having at least one *MICA-129Met* allele conferred a lower probability to develop a severe or fatal aGVHD. When the patients were stratified according to treatment with ATG, this beneficial *MICA-129Met* association was attributed to the subgroup not receiving ATG. This finding appears to be explainable by a rapid NKG2D down-regulation on alloreactive $CD8^+$ T cells mediated by engagement of at least one high-avidity MICA-129Met variant limiting the NKG2D-mediated co-stimulation of alloreactive donor $CD8^+$ T cells. In heterozygous patients, also the risk of occurrence of aGVHD was reduced, suggesting that the effect of MICA-129Met variants on the expression of NKG2D is decisive for this outcome. In consequence, we found overall an increased probability of survival after HSCT for patients carrying a *MICA-129Met* allele in our cohort. Consistently, patients who carried two *MICA-129Val* alleles were at risk to develop a severe or fatal aGVHD and they appeared to particularly profit from ATG treatment. This could be explained by a failure to efficiently down-regulate NKG2D on alloreactive $CD8^+$ T cells, and this finding is potentially of therapeutic relevance for patients carrying two *MICA-129Val* alleles. However, ATG can affect in addition to T cells also other immune cell types including NK cells and B cells (Hoegh-Petersen *et al*, 2013), which also might have contributed to the effects observed in our cohort.

It has been previously reported that the risk of cGVHD was increased for recipients with the *MICA-129Val/Val* genotype, whereas the MICA-129Met/Met genotype was associated with the risk of relapse (Boukouaci *et al*, 2009). In our cohort, the *MICA-129Met/Met* genotype was similarly associated with a trend toward a higher mortality due to relapse in patients not treated with ATG (HR = 3.43, $P = 0.1450$). Notably, the associations reported (Boukouaci *et al*, 2009) are also well explainable by effects on NKG2D (Table 3). Sustained NKG2D-mediated activation of alloreactive $CD8^+$ T cells would be expected if only a MICA-129Val variant is present, and this could increase the risk of cGVHD. Sustained NKG2D-mediated activation of anti-leukemic $CD8^+$ T cells and NK cells would be expected to reduce the risk of relapse. Thus, the different risk associations reported herein and the previous study by Boukouaci *et al* are not arguing against the relevance of the MICA-129 dimorphism for the outcome of HSCT. They rather point toward differences in the relative importance of specific outcomes such as aGVHD, cGVHD, and relapse in the two cohorts due to clinical reasons. The incidence of cGVHD, for example, was 47% (Boukouaci *et al*, 2009) versus 30.5%, and effects on a specific outcome are of course more likely detectable if the respective outcome is more frequent. Similarly, the effect of the SNP on overall survival could vary in different cohorts depending on the relative importance of aGVHD, cGVHD, and relapse for survival in a cohort. The principal relevance of NKG2D signaling for the outcome of allogeneic HSCT is further emphasized by studies demonstrating an effect of the genotype of the NKG2D ligand *RAET1L* (Antoun *et al*, 2012) and *NKG2D* (Espinoza *et al*, 2009) itself on overall survival of patients.

The MICA-129 dimorphism could also be relevant for the success of immunotherapies using NK cells to treat MICA-positive malignancies (Laport *et al*, 2011; Leung, 2011; Meehan *et al*, 2013). Moreover, it might be highly important when NKG2D signaling is targeted by new therapies aiming at up-regulation of MICA by histone deacetylase inhibitors (Kato *et al*, 2007; Diermayr *et al*, 2008) or blocking of signaling by soluble NKG2D (Hilpert *et al*, 2012).

Our experimental data showed that the MICA-129Met variant triggers more NKG2D signals at low expression intensities, whereas MICA-129Val variant elicits more NKG2D effects at high expression, at which the MICA-129Met variant already down-regulates NKG2D leading to impaired function. Thus, expression intensity can change the biological effect of this SNP. Both variants may confer advantages and disadvantages in certain situations, such as virus infections, suggesting balancing evolution of *MICA* alleles. Differences in MICA expression intensities in GVHD-affected tissues (Gannage *et al*, 2008) and on malignant cells (Sconocchia *et al*, 2005; Boissel *et al*, 2006; Nückel *et al*, 2010; Hilpert *et al*, 2012) could therefore affect the association of the SNP with specific outcome parameters after HSCT. Notably, MICA expression intensities can vary for certain *MICA* alleles (Shafi *et al*, 2011). A further modifying factor is sMICA (Boukouaci *et al*, 2009), which was found in variable amounts in patient sera (Salih *et al*, 2002; Boissel *et al*, 2006; Nückel *et al*, 2010; Hilpert *et al*, 2012). Moreover, anti-MICA Ab (Boukouaci *et al*, 2009), neutralizing sMICA but also sensitizing MICA-expressing cells to complement-dependent cellular cytotoxicity (Zou *et al*, 2002; Jinushi *et al*, 2006; Zou & Stastny, 2010), might additionally modulate the effects of the SNP MICA-129.

In conclusion, we have shown that the MICA-129Val/Met dimorphism affects the strength and kinetics of NKG2D signaling resulting in differences of NK-cell cytotoxicity and cytokine secretion as well as $CD8^+$ T-cell co-stimulation. It also affects NKG2D expression on NK and even more on $CD8^+$ T cells. These functional effects of the dimorphism were critically modulated by the MICA expression intensity. The MICA-129 dimorphism had a significant impact on

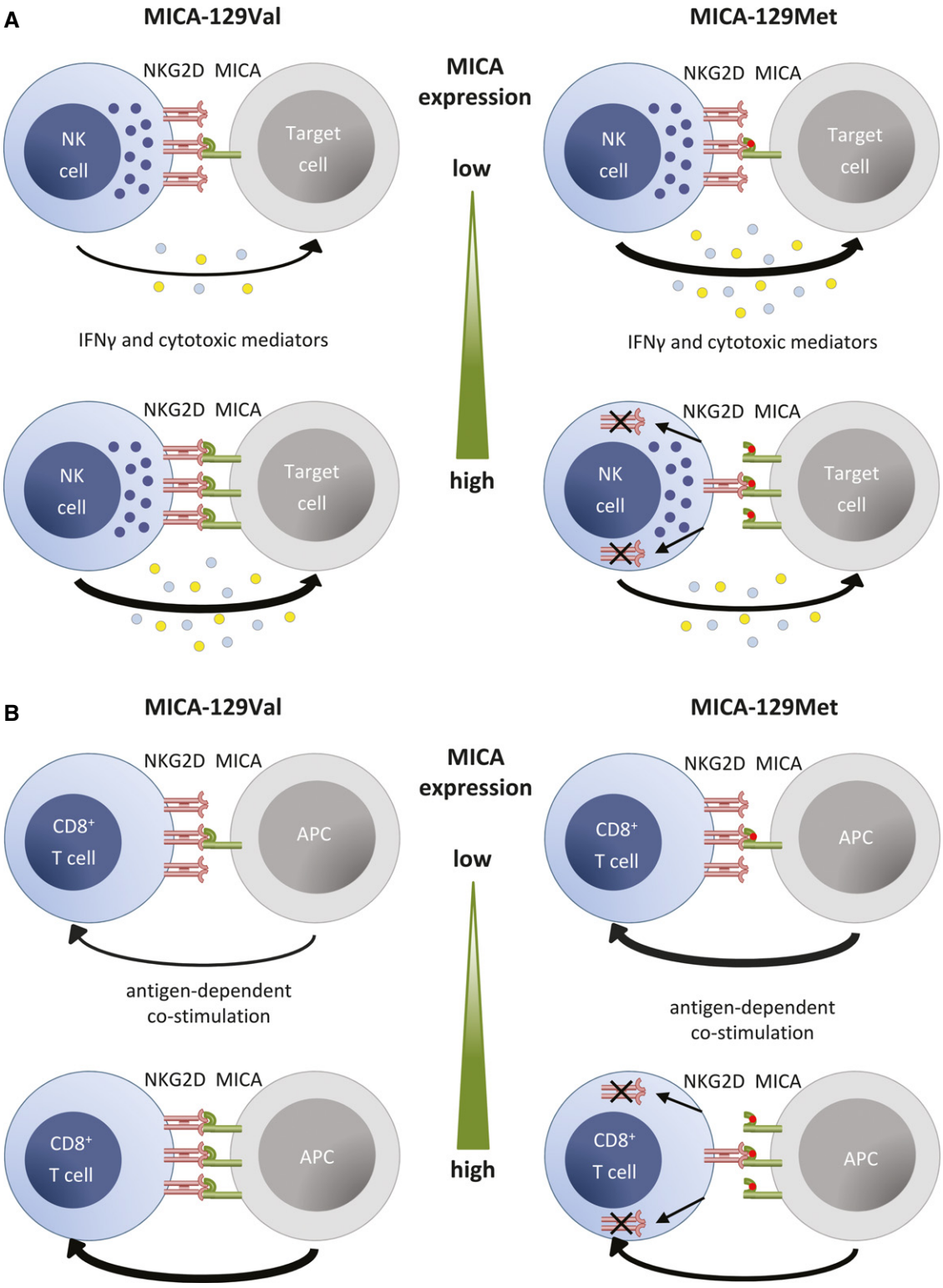

Figure 8. Summary of functional effects of MICA-129 variants depending on expression intensity.

A For target cells expressing the MICA-129Val variant, the degree of NK-cell cytotoxicity and IFNγ production increased steadily with the MICA expression intensity. Augmented expression of the high-avidity MICA-129Met isoform, in contrast, had no or even a negative effect on these NK-cell functions due to a rapid down-regulation of NKG2D on NK cells.

B Antigen-dependent co-stimulation of $CD8^+$ T cells with the MICA-129Met variant allowed for an earlier antigen-dependent activation than co-stimulation with the MICA-129Val variant. However, the down-regulation of NKG2D in response to MICA-129Met ligands impaired any subsequent NKG2D-dependent co-stimulation and T-cell activation. The down-regulation of NKG2D on $CD8^+$ T cells was augmented with MICA-129Met expression intensity.

Table 3. Summary of biological effects of *MICA-129* genotypes and their relation to expected and observed clinical outcomes after HSCT.

MICA-129 genotype	NKG2D signaling	NKG2D cell surface expression over time	HSCT outcomes	Clinical outcomes expected in view of biological function	Clinical outcomes observed
Met/Met	strong	reduced	aGVHD	↑[a] or ↓	↑ occurrence[b] ↓ fatal[c]
			cGVHD	↓	↓[d]
			relapse	↑	↑[d]
			overall survival	variable	↑[c]
Met/Val	intermediate	reduced	aGVHD	→ or ↓	↓ occurrence[b] ↓ fatal[c]
			cGVHD	↓	
			relapse	↑	
			overall survival	variable	↑[c]
Val/Val	weak	preserved	aGVHD	↓ or ↑	↓ occurrence[b] ↑ fatal[c]
			cGVHD	↑	↑[d]
			relapse	↓	↓[d]
			overall survival	variable	↓[c]

[a]↑ increased, → unchanged, ↓ decreased.
[b]Attributable to the group receiving a T-cell-depleting treatment with ATG in our study.
[c]Attributable to the group not treated with ATG in our study.
[d]Data from Boukouaci *et al* (2009).

the outcome of HCST in this and in a previous independent study (Boukouaci *et al*, 2009). Our data suggest that patients carrying a MICA-129Met allele have a reduced risk of fatal aGVHD, whereas carriers of a MICA-129Val/Val genotype are at high risk and appear to profit from ATG treatment. Potentially, NKG2D itself could be a target for prevention or therapy of GVHD.

Materials and Methods

Patients and treatments

Approval for the analysis has been obtained from the Institutional Review Board of UMG, and it has been conducted according to the Declaration of Helsinki. Informed consents to transplantation and retrospective outcome analysis have been obtained from all patients. The patient materials and clinical data are owned by UMG. Their use requires Institutional Review Board approval. Transplantation indications and conditioning protocols followed European Group for Blood and Marrow Transplantation (EBMT) guidelines or clinical trial protocols, whenever pertinent. The MICA-129 genotyping results were obtained retrospectively and not taken into consideration for any treatment decisions. Prophylaxis of GVHD started on day −1 and consisted of cyclosporine (target trough level 100–300 μg/l) or tacrolimus (target trough level 8–12 μg/l) and mycophenolate mofetil (1 g twice a day until day 28 or day 50, depending on the protocol). ATG was applied to patients mismatched and most unrelated transplantations. Either 10 mg/kg bw (body weight) ATG-Fresenius S (Fresenius Biotech, Grafelfing, Germany) or 2.0 mg/kg bw thymoglobuline (Genzyme Europe, Naarden, the Netherlands) was given from day −3 to day 1. Acute and chronic GVHD were scored according to international standards (Przepiorka *et al*, 1995). Cases of aGVHD were categorized into groups of overall grades 0 and I–IV, and cases of cGVHD were categorized into absent, mild, moderate, and severe, respectively (Filipovich *et al*, 2005).

Statistical analyses

Statistical analyses of clinical and genotyping data were performed with R software (http://www.R-project.org). The influence of the MICA-129 dimorphism on the following outcome parameters were evaluated: overall mortality (time to event analysis with Cox proportional hazard models), TRM, mortality due to aGVHD, mortality due to relapse, occurrence of aGVHD (0 versus grades I–IV), severity of aGVHD (grades I and II versus grades III and IV), occurrence of cGVHD (absent versus mild, moderate, or severe), and occurrence of relapse (probability of event analyses with logistic regression). The analyses were performed after adjustment for the relevant clinical covariates: T-cell depletion, total body irradiation, HLA-matched unrelated donor, female donor for male recipient, and diagnosis group (Table 2). In addition, all analyses were adjusted for a binary indicator distinguishing whether patient and donor had the same MICA-129 genotype or not. Other parameters, including having a less than 8/8 HLA-matched unrelated donor, reduced intensity conditioning, and disease status, were considered but not identified as significant covariates. The co-dominant model was employed to determine the most appropriate inheritance risk model (additive, dominant, or recessive). Reported are the results of the most appropriate genetic model. Power for detected effects ranged between 52% (recessive model) and 86% (additive model) at the 5% significance level.

Sample sizes for *in vitro* experiments were estimated based on previous experiences with similar assays. Typical group sizes for MICA-129 strata such as L-MICA-129Met and L-MICA-129Val clones were ≥ 20 and balanced, yielding a power ≥ 80% for the detected main effects of MICA-129. No samples were excluded from analysis. The experimental data were evaluated with the WinStat software (R. Fitch Software, Bad Krozingen, Germany) employing the Kolmogorov–Smirnov test to determine normal distribution and Pearson correlation, *t*-tests, or two-way ANCOVAs with interactions

for subsequent analyses. The nonparametric Wilcoxon test was used to compare non-normally distributed target variables. A *P*-value of < 0.05 in two-sided tests was considered significant. The SAS software (Cary, North Carolina, USA) was used to estimate ANOVA or ANCOVA-like linear mixed models with adjustment of parameters for the interaction with MICA expression intensity. Dependent on the experimental design, random effects were included into the models to account for longitudinal correlation (cell surface expression of NKG2D and CD94; relative cell lysis) or a random trial effect (IFNγ). While *t*-tests allowed for different group variances where appropriate, ANCOVA-like models used a pooled estimate of standard deviation (SD) for robust inference.

Materials and antibodies

Unless specified otherwise, all chemicals were from Sigma-Aldrich (Taufkirchen, Germany) or Merck (Darmstadt, Germany), all enzymes from New England Biolabs (Ipswich, MA, USA), and all cell culture plastic materials from Nunc (Roskilde, Denmark) or Sarstedt (Nümbrecht, Germany). Antibodies (Ab) used are listed in the Appendix Table S2.

MICA-129 genotyping

The SNP rs1051792 (G/A) leading to a substitution of Val (G) by Met (A) at position 129 of MICA was genotyped by a TaqMan assay (Applied Biosystems, Foster City, CA, USA) containing the forward primer 5′-GCTCTTCCTCTCCCAAAACCT-3′ and the reverse primer 5′-CGTTCATGGCCAAGGTCTGA-3′ and the two allele-specific dye-labeled probes FAM-5′-AATGGACA**G**TGCCCC-3′ and VIC-5′-AATG GACA**A**TGCCCC-3′.

MICA-129 expression constructs

A pCMV6-AC expression vector containing the *MICA* gene (Origene, Rockville, ML, USA) was altered by site-directed mutagenesis at two positions (codons for amino acids 24 and 360) to obtain the *MICA*00701* allele. This allele has a methionine at amino acid position 129. The MICA-129Val variant (pCMV6-AC-MICA-129Val) was generated by mutagenesis of the pCMV6-AC-MICA-129Met construct. To obtain MICA proteins as mouse IgG_{2a}-Fc fusion proteins (MICA-129Met-mIgG_{2a}-Fc and MICA-129Val-mIgG_{2a}-Fc), the extracellular parts of MICA were amplified by polymerase chain reaction (PCR) from pCMV6-AC-MICA-129Met and pCMV6-AC-MICA-129Val vectors. As control, an ovalbumin (OVA) fusion protein construct (OVA-mIgG_{2a}-Fc) was generated. Primers with restriction sites for *Kpn*I (MICA-129-Fc_fwd: 5′-TGGTACCATG GGGCTGGGCCCGGTCTTCCTGC-3′; OVA-Fc_fwd: 5′-CAGGTACC ATGGGCTCCATCGGCGCAGCAA-3′) or *BamH*I (MICA-129-Fc_rev: 5′-CGGATCCTGAAGCACCAGCACTTTCCCAGA-3′; OVA-Fc_rev: 5′-TGAGGATCCATAGGGGAAACACATCTGCCAAAG-3′) were used, and the PCR products were inserted into the pcDNA3.1/*myc*-His A (+) expression vector (Invitrogen, Darmstadt, Germany) that already contained the mouse IgG_{2a}-Fc cDNA, including the hinge and the CH2 and CH3 regions, derived from the pFUSE-mIgG_{2a}-Fc1 vector (InvivoGen, Toulouse, France). All constructs were sequenced before use.

Cell culture and transfections

Mouse fibroblast L cells, human embryonic kidney (HEK) 293 cells, and K562 cells were maintained in $NaHCO_3$-buffered Dulbecco's modified Eagle's medium (DMEM) supplemented with 10% fetal calf serum (FCS; Biochrom, Berlin, Germany), 2 mM L-glutamine, 1 mM sodium pyruvate, 50 μM 2-mercaptoethanol, 100 U/ml penicillin, and 100 μg/ml streptomycin. All cell lines were tested routinely by PCR to exclude mycoplasma contamination. L cells were transfected by electroporation with 50 μg of *Pvu*I-linearized pCMV6-AC-MICA-129Met or pCMV6-AC-MICA-129Val constructs or the empty pCMV6-AC vector. After selection (1 mg/ml G418, Biochrom, Berlin, Germany), clones (L-con, L-MICA-129Met, and L-MICA-129Val) were obtained by limiting dilution. HEK293 cells were transfected with 50 μg *Pvu*I-linearized DNA of MICA-129Met-Fc, MICA-129Val-Fc, or OVA-Fc constructs. After selection (0.5 mg/ml G418), fusion protein secretion into the supernatant was analyzed by an ELISA for mouse IgG.

NK cells and $CD8^+$ T cells

Peripheral blood mononuclear cells (PBMC) were obtained from blood of healthy donors by centrifugation on Biocoll separating solution (Biochrom). PBMC were cultured for 4 days with 100 U/ml human IL-2 (Proleukin, Chiron, Amsterdam, the Netherlands) to obtain LAK cells. NK cells were isolated from PBMC by magnetic-activated cell sorting (MACS) using a negative selection kit (NK cell isolation kit II, Miltenyi Biotec, Bergisch-Gladbach, Germany) and either used directly or cultured for 4 days with 100 U/ml IL-2. Purity of NK cells was evaluated by flow cytometry (Appendix Fig S15A). $CD8^+$ T cells were isolated from PBMC by MACS using a negative selection kit ($CD8^+$ T cell isolation kit, Miltenyi Biotec). Purity of $CD8^+$ T cells was evaluated by flow cytometry (Appendix Fig S15B).

Enzyme-linked immuno-sorbent assay (ELISA)

To measure the secretion of MICA-129Met/Val-mIgG_{2a}-Fc and OVA-mIgG_{2a}-Fc proteins from transfected clones of HEK293 cells, 96-well Nunc MaxiSorp microtiter plates were coated overnight at 4°C with 10 μg/ml goat anti-mouse IgG Ab in sodium carbonate buffer (pH 8.5; 50 μl/well). After blocking with 1% gelatin in phosphate-buffered saline (PBS), cell culture supernatants (50 μl/well) were added and the plates were incubated for 1 h at 37°C. For detection, a goat anti-mouse horseradish peroxidase (HRP)-conjugated Ab diluted 1:4,000 in PBS with 0.05% Tween-20 was used. After incubation (1 h at 37°C), 50 μl 2,2′-azino-bis(3-ethylbenzothiazoline-6-sulfonic acid; ABTS) substrate solution was added to each well and the optical density was immediately determined using a BioTek PowerWave 340 microplate spectrophotometer (BioTek, Bad Friedrichshall, Germany) set to 405 nm. IFNγ, TNF-α, IL-10, and IL-13 concentrations in the supernatant of NK cells co-cultured with L-con, L-MICA-129Met, or L-MICA-129Val clones (5×10^4 targets plus 2.5×10^5 NK cells in 200 μl medium) for 4–24 h or cultured on plate-bound MICA-129Met-Fc, MICA-129Val-Fc, or OVA-Fc proteins (2.5×10^5 NK cells in 200 μl medium) were determined by human IFNγ, TNF-α, IL-10, and IL-13 ELISA sets (ImmunoTools, Friesoythe, Germany). IL-2

release from $CD8^+$ T cells was measured by human IL-2 ELISA set (MAX Standard, Biolegend, Fell, Germany). Concentrations of sMICA in the supernatants of L-MICA-129Met/Val cells (1×10^6 cells, 10 ml medium, 24 h) were determined using the human MICA DuoSet (R&D Systems, Wiesbaden, Germany). These assays were performed according to the manufacturer's protocols. All samples were analyzed in duplicate or triplicates in comparison to a standard curve of IFNγ, TNF-α, IL-2, IL-10, IL-13, MICA, or mouse IgG protein, respectively.

Production and purification of recombinant MICA-129Met-Fc and MICA-129Val-Fc fusion proteins

To obtain supernatant containing the fusion proteins, 5×10^7 HEK293-MICA-129Met-Fc, HEK293-MICA-129Val-Fc, or HEK293-OVA-Fc cells were cultured in 75 ml FCS-free DMEM for 3 days. The cell culture supernatants were dialyzed in 20 mM sodium phosphate buffer (pH 7.0) overnight at 4°C in a dialysis tubing with a molecular weight cutoff (MWCO) of 12–14 kDa (SERVA Electrophoresis GmbH, Heidelberg, Germany). Subsequently, the fusion proteins were purified using 1-ml HiTrap-Protein-G-HP columns (GE Healthcare, Freiburg, Germany) according to the manufacturer's instructions. After buffer exchange in PBS (pH 7.2), the proteins were concentrated using Amicon filter units with 30-kDa MWCO (Merck Millipore, Darmstadt, Germany). Bradford assays (Bio-Rad Laboratories GmbH, Munich, Germany) and reducing sodium dodecyl sulfate-polyacrylamide gel electrophoresis (SDS–PAGE) were performed to determine the concentration and purity of the MICA-129Met-Fc, MICA-129Val-Fc, and OVA-Fc proteins. Glycosylation was tested by digestion with Endo H (New England Biolabs, Ipswich, MA, USA).

Surface plasmon resonance (SPR) analysis

SPR measurements were done using a Reichert SPR Biosensor SR7500DC with a HC 1000 m sensorchip (Xantec Bioanalytics, Düsseldorf, Germany). All measurements were performed in running buffer containing PBS, pH 7.4, at a flow rate of 40 µl/min. NKG2D-Fc was covalently immobilized on the EDC/NHS-activated left channel (sample channel) of the sensorchip, at a concentration of 200 nM, at a flow rate of 30 µl/min, to a response level of 2,500 response units (RU). The right channel of the chip served as a reference. Increasing concentrations of analyte (MICA-129Met-Fc or MICA-129Val-Fc) were injected for 270 s over both channels, and dissociation was followed for 15 min. Kinetic analysis was performed using Scrubber 2.0 (BioLogic Software, Campbell, Australia). The recorded responses were double referenced (right channel, buffer blank) and normalized using the molecular weight of the analyte (in kDa).

SDS–PAGE and immunoblotting

NK cells were stimulated with the fusion proteins as described below (CD107a degranulation assay), before Nonidet P-40 (NP-40) lysates were prepared for Western blot analyses. A total of 1×10^6 NK cells were harvested at 4°C for each time point either unstimulated or stimulated at 37°C with MICA-129Met-Fc, MICA-129Val-Fc, or OVA-Fc proteins for 3, 10, or 30 min, respectively. The cells were lysed in 25 µl NP-40 buffer (1%) before 25 µl reducing loading buffer was added. After incubation for 4 min at 95°C, the lysates were loaded on 4–12% SDS gels for electrophoresis at 20 to 40 mA for approximately 3 h. Then, the proteins were blotted onto a nitrocellulose membrane (Roth, Karlsruhe, Germany) for 1 h using a semi-dry blotting technique (1 mA/cm^2). The membrane was blocked in Tris-buffered saline with 0.1% Tween-20 (TBS-T) with 5% bovine serum albumin (BSA) for 1 h, washed, and then incubated with specific primary Ab in TBS-T together with 1% BSA overnight at 4°C. After being washed three times for 10 min in TBS-T, the membrane was incubated with a HRP-labeled secondary Ab or, for the detection of MICA, with HRP-conjugated streptavidin (BioLegend). Detection was done using an enhanced chemiluminescence (ECL) kit (GE Healthcare), and chemiluminescence was measured using a digital image acquisition system (Intas Chemilux Entry, Intas, Göttingen, Germany). The MICA-129Met-Fc, MICA-129Val-Fc, and OVA-Fc fusion proteins were separated by SDS–PAGE together with BSA or OVA as control proteins. The gels were stained with Coomassie Brilliant Blue R250 for 15 min followed by a 30-min wash with 10% acetic acid and 30% methanol and documented using the Intas gel manager (Intas, Göttingen, Germany).

Flow cytometry

Flow cytometry was performed with a FACSCalibur flow cytometer and CellQuestPro software (BD Biosciences, Heidelberg, Germany). Cell surface expression of MICA on propidium iodide (PI)-negative cells was examined using the anti-MICA monoclonal antibody (mAb) AMO1 (1 µg/10^6 cells in 100 µl PBS; for Ab see Appendix Table S2) and fluorescein isothiocyanate (FITC)-conjugated goat anti-mouse IgG Ab as secondary reagent. This secondary Ab was also used to detect the binding of the recombinant MICA-129Met-Fc, MICA-129Val-Fc, or OVA-Fc fusion proteins to NK cells. Binding of a recombinant human NKG2D-Fc fusion protein (139-NK, R&D Systems) to MICA-expressing cells (0.2 µg/10^6 cells in 100 µl PBS) was assessed using a polyclonal FITC-conjugated goat anti-human IgG Ab as secondary reagent. PBMC and NK cells were characterized using mAb against CD3, CD14, CD16, CD19, CD56, CD94, NKp30 (CD337), NKp44 (CD336), NKp46 (CD335), NKG2D (CD314), and γ/δ T-cell receptor (TCR). $CD8^+$ T cells were characterized with mAb against CD3, CD8, CD28, and NKG2D. All stainings were done at 4°C in the dark. Isotype controls were purchased from ImmunoTools or BioLegend. NKG2D expression and CD94 expression were also measured after co-culture for 4 or 24 h of 2.5×10^5 purified IL-2-stimulated NK cells with 5×10^4 target cells per well of a 96-well plate. NKG2D expression and CD8 expression were measured after co-culture for 4 or 24 h of 2.5×10^5 purified $CD8^+$ T cells with 5×10^4 target cells per well of a 96-well plate. A potential cytotoxic effect of the SRC kinase inhibitor PP2 (25 µM; Sigma-Aldrich, #P0042) was determined by staining of NK cells with Annexin V-FITC (BD Biosciences) in combination with PI in binding buffer according to the manufacturer's protocol.

CD107a degranulation assay

To determine the degranulation of NK cells exposed to L-con, L-MICA-129Met, or L-MICA-129Val target cells, 10^6 LAK cells and

4×10^4 targets were co-cultured for 1 h at 37°C in 100 µl medium (E:T ratio 25:1), and an anti-CD107a mAb (4 µl) or the respective isotype control (mouse IgG_1) was added. Alternatively, 2×10^5 purified NK cells were co-cultured in 100 µl medium with 5×10^4 target cells (E:T ratio 4:1). Afterward, the cells were harvested and stained at 4°C with anti-CD16 and anti-CD56 mAb to identify $CD107a^+$ NK cells. To elicit degranulation of purified IL-2-stimulated NK cells with immobilized MICA-129Met/Val-$mIgG_{2a}$-Fc or OVA-$mIgG_{2a}$-Fc fusion proteins, MaxiSorp microtiter plates (Nunc) were pre-coated with 1 µg/well of a goat anti-mouse $F(ab')_2$ fragment in 100 µl sodium carbonate coating buffer (pH 8.5) overnight at 4°C. After washing with PBS, the MICA-129Met-Fc, MICA-129Val-Fc, or OVA-Fc proteins were added at different concentrations in 100 µl PBS/well and incubated for 1 h at room temperature. Then, the plates were washed before IL-2-stimulated NK cells (2.5×10^5/well in 100 µl medium) and the CD107a mAb or the isotype control were added. The plates were incubated at 37°C for 1 h before the cells were harvested and stained to identify $CD107a^+$ NK cells. In some assays, the SRC kinase inhibitor PP2 (25 µM) or dimethyl sulfoxide (DMSO) as solvent was given to the NK cells 30 min before being added to the plates.

Intracellular staining of IFNγ

To determine the IFNγ expression in NK cells exposed to L-con, L-MICA-129Met, or L-MICA-129Val target cells, 2×10^5 NK cells were co-cultured in 100 µl medium for 4 h at 37°C with 5×10^4 targets (E:T ratio 4:1). Afterward, the cells were harvested and counterstained at 4°C with anti-CD16 and anti-CD56 mAb before fixation and permeabilization with Cytofix/Cytoperm and Perm/Wash solutions (BD Biosciences) according to the manufacturer's protocol. The cells were then stained with an anti-IFNγ mAb or an isotype control suitable for intracellular staining experiments ($mIgG_1$, MOPC-21; Biolegend) for 30 min at 4°C. To elicit IFNγ expression of purified IL-2-stimulated NK cells with immobilized MICA-129Met/Val-$mIgG_{2a}$-Fc or OVA-$mIgG_{2a}$-Fc fusion proteins, microtiter plates were prepared as described above. IL-2-stimulated NK cells (2.5×10^5/well in 100 µl medium) were added, and the plates were incubated at 37°C for 4 h before the cells were harvested, stained at 4°C with anti-CD56 and anti-CD16 mAbs, and analyzed by flow cytometry.

^{51}Cr release assay

Target cells were labeled by incubating 1×10^6 cells in 200 µl DMEM containing 100 µl FCS and 50 µCi $Na_2{}^{51}CrO_4$ (CrRA8, Hartmann Analytic, Braunschweig, Germany) for 1 h at 37°C and washed three times with DMEM. Effector cells were added to 5×10^3 ^{51}Cr-labeled target cells in triplicate at various ratios in 200 µl DMEM with 10% FCS per well of round-bottomed microtiter plates. Spontaneous release was determined by incubation of target cells in the absence of effector cells. The microtiter plates were centrifuged for 5 min at $40 \times g$, incubated at 37°C for 4 h, and then centrifuged again. Supernatant and sediment were separately taken to determine radioactivity in each well using a MicroBeta^2 counter (PerkinElmer Life Sciences, Köln, Germany). Percentage of specific lysis was calculated by subtracting percent spontaneous ^{51}Cr release.

The paper explained

Problem
Allogeneic hematopoietic stem cell transplantation offers a chance to cure several hematological malignancies but has a high risk of post-transplant complications including graft-versus-host disease and relapse of malignancy.

Results
An amino acid exchange from valine to methionine at position 129 in MICA, a ligand of the activating natural killer (NK) cell receptor NKG2D, was associated with an increased chance of survival and a reduced risk to die from acute graft-versus-host disease (GVHD) in a cohort of 452 patients. Nonetheless, carriers of the *MICA-129Met/Met* genotype had an increased risk to experience acute GVHD. The survival of *MICA-129Val/Val* genotype carriers was improved when treated with antithymocyte globulin (ATG) to reduce alloreactive T-cell numbers. On the one site, the MICA-129Met isoform triggered more cytotoxicity and interferon-γ production by NK cells and it activated cytotoxic T cells faster. On the other site, the MICA-129Met variant induced a faster and stronger down-regulation of NKG2D on NK and cytotoxic T cells than the MICA-129Val isoform. The reduced cell surface expression of NKG2D in response to engagement by MICA-129Met variants appeared to reduce the severity of acute GVHD.

Impact
These results demonstrate how the MICA-129 polymorphism affects the function of NK cells and cytotoxic T cells. With respect to the risk of acute GVHD, homozygous carriers of the MICA-129Val variant may specifically profit from a T-cell-depleting treatment with ATG since this MICA variant has a lower ability to down-regulate NKG2D and to limit thereby the activation of alloreactive T cells.

Proliferation assays

Proliferation of $CD8^+$ T cells was analyzed after stimulation by a plate-bound anti-CD3 mAb delivering a first signal in combination with anti-CD28, anti-NKG2D, or MICA-129Met-Fc or MICA-129Val-Fc proteins delivering second or co-stimulatory signal. OVA-Fc (having a $mIgG_{2a}$ Fc fragment), $mIgG_{2a}$ (A111-3, BD Biosciences), and $mIgG_1$ (C76-47, BD Biosciences) served as controls. 96-well Nunc MaxiSorp microtiter plates were coated overnight at 4°C with 10 µg/ml goat anti-mouse IgG $F(ab')_2$ fragments in sodium carbonate buffer (pH 8.5; 100 µl/well). After washing with PBS, stimulatory mAb or recombinant Fc fusion proteins or isotype controls were added at the indicated concentrations and incubated at room temperature for 2 h. Then, the plates were washed again with PBS before 1×10^5 freshly isolated $CD8^+$ T cells per well were added in 200 µl medium with 10% FCS. After 72 h, 50 µl medium was harvested for IL-2 measurements and replaced by the same volume containing 1 µCi [methyl-^{3}H]thymidine (MT 6031, Hartmann Analytic). Following a further incubation of 12 h, the DNA-bound radioactivity was harvested with a FilerMate Harvester (Perkin Elmer) and measured with MicroBeta^2 Counter (Perkin Elmer). The SI was calculated by dividing the measured counts per minute (cpm) by the cpm of the negative control (unstimulated $CD8^+$ T cells). In other experiments, purified $CD8^+$ T cells were labeled by the dye CFSE (C-1157, Invitrogen, Karlsruhe, Germany) before culture on the coated plates. Cells were incubated for 5 min with 5 µM CFSE in PBS/0.1% BSA at 37°C. After being washed 3 times

with DMEM containing 10% FCS, the cells were cultured as described above. The cells were harvested at the indicated time points, stained by anti-CD3 and anti-CD8 mAbs, and analyzed by flow cytometry.

Expanded View for this article is available online:
http://emmm.embopress.org

Acknowledgements
This work was supported by the Deutsche Forschungsgemeinschaft (GRK 1034) providing stipends for A.I. and E.V, the SFB 1002 (TP C05), and the European Union grant FP7-PEOPLE-2012-ITN-315963 (CELLEUROPE). We thank Prof. Blanche Schwappach, Institute of Molecular Biology, UMG, for supporting SPR analyses (FOR1086/2, grant SCHW823/2-1). Furthermore, we acknowledge support by the Open Access Publication Funds of the Göttingen University.

Author contributions
AI and LE performed most of the experiments. SM did CD107a and intracellular IFNγ stainings, FvB the *MICA* genotyping, and MK the SPR analysis. ME, LW, and CSH provided reagents and analyzed data. JMW, NW, DK, and GW provided clinical samples and data. DM, EV, YB, and HB performed statistical analyses. RD designed the study. AI, DM, and RD wrote the manuscript. All authors approved the manuscript.

Conflict of interest
The authors declare that they have no conflict of interest.

For more information
http://www.ebi.ac.uk/imgt/hla/

References

Amroun H, Djoudi H, Busson M, Allat R, El Sherbini SM, Sloma I, Ramasawmy R, Brun M, Dulphy N, Krishnamoorthy R *et al* (2005) Early-onset ankylosing spondylitis is associated with a functional MICA polymorphism. *Hum Immunol* 66: 1057 – 1061

Anderson E, Grzywacz B, Wang H, Wang T, Haagenson M, Spellman S, Blazar BR, Miller JS, Verneris MR (2009) Limited role of MHC class I chain-related gene A (MICA) typing in assessing graft-versus-host disease risk after fully human leukocyte antigen-matched unrelated donor transplantation. *Blood* 114: 4753 – 4754; author reply 4754–4755

Andre P, Castriconi R, Espeli M, Anfossi N, Juarez T, Hue S, Conway H, Romagne F, Dondero A, Nanni M *et al* (2004) Comparative analysis of human NK cell activation induced by NKG2D and natural cytotoxicity receptors. *Eur J Immunol* 34: 961 – 971

Antoun A, Vekaria D, Salama RA, Pratt G, Jobson S, Cook M, Briggs D, Moss P (2012) The genotype of RAET1L (ULBP6), a ligand for human NKG2D (KLRK1), markedly influences the clinical outcome of allogeneic stem cell transplantation. *Br J Haematol* 159: 589 – 598

Askar M, Sun Y, Rybicki L, Zhang A, Thomas D, Kalaycio M, Pohlman B, Dean R, Duong H, Hanna R *et al* (2014) Synergistic effect of major histocompatibility complex class I-related chain a and human leukocyte antigen-DPB1 mismatches in association with acute graft-versus-host disease after unrelated donor hematopoietic stem cell transplantation. *Biol Blood Marrow Transplant* 20: 1835 – 1840

Ayo CM, de Oliveira AP, Camargo AV, Brandao de Mattos CC, Bestetti RB, de Mattos LC (2015) Association of the functional MICA-129 polymorphism with the severity of chronic Chagas heart disease. *Clin Infect Dis* 61: 1310 – 1313

Bahram S, Bresnahan M, Geraghty DE, Spies T (1994) A second lineage of mammalian major histocompatibility complex class I genes. *Proc Natl Acad Sci USA* 91: 6259 – 6263

Bauer S, Groh V, Wu J, Steinle A, Phillips JH, Lanier LL, Spies T (1999) Activation of NK cells and T cells by NKG2D, a receptor for stress-inducible MICA. *Science* 285: 727 – 729

Billadeau DD, Upshaw JL, Schoon RA, Dick CJ, Leibson PJ (2003) NKG2D-DAP10 triggers human NK cell-mediated killing via a Syk-independent regulatory pathway. *Nat Immunol* 4: 557 – 564

Boissel N, Rea D, Tieng V, Dulphy N, Brun M, Cayuela JM, Rousselot P, Tamouza R, Le Bouteiller P, Mahon FX *et al* (2006) BCR/ABL oncogene directly controls MHC class I chain-related molecule A expression in chronic myelogenous leukemia. *J Immunol* 176: 5108 – 5116

Boukouaci W, Busson M, Peffault de Latour R, Rocha V, Suberbielle C, Bengoufa D, Dulphy N, Haas P, Scieux C, Amroun H *et al* (2009) MICA-129 genotype, soluble MICA, and anti-MICA antibodies as biomarkers of chronic graft-versus-host disease. *Blood* 114: 5216 – 5224

Bryceson YT, Ljunggren HG, Long EO (2009) Minimal requirement for induction of natural cytotoxicity and intersection of activation signals by inhibitory receptors. *Blood* 114: 2657 – 2666

Champsaur M, Lanier LL (2010) Effect of NKG2D ligand expression on host immune responses. *Immunol Rev* 235: 267 – 285

Choy MK, Phipps ME (2010) MICA polymorphism: biology and importance in immunity and disease. *Trends Mol Med* 16: 97 – 106

Coudert JD, Zimmer J, Tomasello E, Cebecauer M, Colonna M, Vivier E, Held W (2005) Altered NKG2D function in NK cells induced by chronic exposure to NKG2D ligand-expressing tumor cells. *Blood* 106: 1711 – 1717

Dhanji S, Teh SJ, Oble D, Priatel JJ, Teh HS (2004) Self-reactive memory-phenotype CD8 T cells exhibit both MHC-restricted and non-MHC-restricted cytotoxicity: a role for the T-cell receptor and natural killer cell receptors. *Blood* 104: 2116 – 2123

Dickinson AM (2008) Non-HLA genetics and predicting outcome in HSCT. *Int J Immunogenet* 35: 375 – 380

Diermayr S, Himmelreich H, Durovic B, Mathys-Schneeberger A, Siegler U, Langenkamp U, Hofsteenge J, Gratwohl A, Tichelli A, Paluszewska M *et al* (2008) NKG2D ligand expression in AML increases in response to HDAC inhibitor valproic acid and contributes to allorecognition by NK-cell lines with single KIR-HLA class I specificities. *Blood* 111: 1428 – 1436

Douik H, Ben Chaaben A, Attia Romdhane N, Romdhane HB, Mamoghli T, Fortier C, Boukouaci W, Harzallah L, Ghanem A, Gritli S *et al* (2009) Association of MICA-129 polymorphism with nasopharyngeal cancer risk in a Tunisian population. *Hum Immunol* 70: 45 – 48

Dulphy N, Berrou J, Campillo JA, Bagot M, Bensussan A, Toubert A (2009) NKG2D ligands expression and NKG2D-mediated NK activity in Sezary patients. *J Invest Dermatol* 129: 359 – 364

Elsner L, Flügge PF, Lozano J, Muppala V, Eiz-Vesper B, Demiroglu SY, Malzahn D, Herrmann T, Brunner E, Bickeböller H *et al* (2010) The endogenous danger signals HSP70 and MICA cooperate in the activation of cytotoxic effector functions of NK cells. *J Cell Mol Med* 14: 992 – 1002

Espinoza JL, Takami A, Onizuka M, Sao H, Akiyama H, Miyamura K, Okamoto S, Inoue M, Kanda Y, Ohtake S *et al* (2009) NKG2D gene polymorphism has a significant impact on transplant outcomes after HLA-fully-matched unrelated bone marrow transplantation for standard risk hematologic malignancies. *Haematologica* 94: 1427 – 1434

Fang M, Lanier LL, Sigal LJ (2008) A role for NKG2D in NK cell-mediated resistance to poxvirus disease. *PLoS Pathog* 4: e30

Ferrara JL, Guillen FJ, van Dijken PJ, Marion A, Murphy GF, Burakoff SJ (1989) Evidence that large granular lymphocytes of donor origin mediate acute graft-versus-host disease. *Transplantation* 47: 50 – 54

Filipovich AH, Weisdorf D, Pavletic S, Socie G, Wingard JR, Lee SJ, Martin P, Chien J, Przepiorka D, Couriel D *et al* (2005) National Institutes of Health consensus development project on criteria for clinical trials in chronic graft-versus-host disease: I. Diagnosis and staging working group report. *Biol Blood Marrow Transplant* 11: 945 – 956

Gannage M, Buzyn A, Bogiatzi SI, Lambert M, Soumelis V, Dal Cortivo L, Cavazzana-Calvo M, Brousse N, Caillat-Zucman S (2008) Induction of NKG2D ligands by gamma radiation and tumor necrosis factor-alpha may participate in the tissue damage during acute graft-versus-host disease. *Transplantation* 85: 911 – 915

Gasser S, Orsulic S, Brown EJ, Raulet DH (2005) The DNA damage pathway regulates innate immune system ligands of the NKG2D receptor. *Nature* 436: 1186 – 1190

Groh V, Bahram S, Bauer S, Herman A, Beauchamp M, Spies T (1996) Cell stress-regulated human major histocompatibility complex class I gene expressed in gastrointestinal epithelium. *Proc Natl Acad Sci USA* 93: 12445 – 12450

Groh V, Rhinehart R, Randolph-Habecker J, Topp MS, Riddell SR, Spies T (2001) Costimulation of CD8alphabeta T cells by NKG2D via engagement by MIC induced on virus-infected cells. *Nat Immunol* 2: 255 – 260

Groh V, Wu J, Yee C, Spies T (2002) Tumour-derived soluble MIC ligands impair expression of NKG2D and T-cell activation. *Nature* 419: 734 – 738

Guerra N, Tan YX, Joncker NT, Choy A, Gallardo F, Xiong N, Knoblaugh S, Cado D, Greenberg NM, Raulet DH (2008) NKG2D-deficient mice are defective in tumor surveillance in models of spontaneous malignancy. *Immunity* 28: 571 – 580

Harris AC, Ferrara JL, Levine JE (2013) Advances in predicting acute GVHD. *Br J Haematol* 160: 288 – 302

Hilpert J, Grosse-Hovest L, Grunebach F, Buechele C, Nuebling T, Raum T, Steinle A, Salih HR (2012) Comprehensive analysis of NKG2D ligand expression and release in leukemia: implications for NKG2D-mediated NK cell responses. *J Immunol* 189: 1360 – 1371

Hoegh-Petersen M, Amin MA, Liu Y, Ugarte-Torres A, Williamson TS, Podgorny PJ, Russell JA, Grigg A, Ritchie D, Storek J (2013) Anti-thymocyte globulins capable of binding to T and B cells reduce graft-vs-host disease without increasing relapse. *Bone Marrow Transplant* 48: 105 – 114

Jinushi M, Hodi FS, Dranoff G (2006) Therapy-induced antibodies to MHC class I chain-related protein A antagonize immune suppression and stimulate antitumor cytotoxicity. *Proc Natl Acad Sci USA* 103: 9190 – 9195

Karimi M, Cao TM, Baker JA, Verneris MR, Soares L, Negrin RS (2005) Silencing human NKG2D, DAP10, and DAP12 reduces cytotoxicity of activated $CD8^+$ T cells and NK cells. *J Immunol* 175: 7819 – 7828

Karimi MA, Bryson JL, Richman LP, Fesnak AD, Leichner TM, Satake A, Vonderheide RH, Raulet DH, Reshef R, Kambayashi T (2015) NKG2D expression by $CD8^+$ T cells contributes to GVHD and GVT effects in a murine model of allogeneic HSCT. *Blood* 125: 3655 – 3663

Kato N, Tanaka J, Sugita J, Toubai T, Miura Y, Ibata M, Syono Y, Ota S, Kondo T, Asaka M *et al* (2007) Regulation of the expression of MHC class I-related chain A, B (MICA, MICB) via chromatin remodeling and its impact on the susceptibility of leukemic cells to the cytotoxicity of NKG2D-expressing cells. *Leukemia* 21: 2103 – 2108

Kirsten H, Petit-Teixeira E, Scholz M, Hasenclever D, Hantmann H, Heider D, Wagner U, Sack U, Hugo Teixeira V, Prum B *et al* (2009) Association of MICA with rheumatoid arthritis independent of known HLA-DRB1 risk alleles in a family-based and a case control study. *Arthritis Res Ther* 11: R60

Kitcharoen K, Witt CS, Romphruk AV, Christiansen FT, Leelayuwat C (2006) MICA, MICB, and MHC beta block matching in bone marrow transplantation: relevance to transplantation outcome. *Hum Immunol* 67: 238 – 246

Laport GG, Sheehan K, Baker J, Armstrong R, Wong RM, Lowsky R, Johnston LJ, Shizuru JA, Miklos D, Arai S *et al* (2011) Adoptive immunotherapy with cytokine-induced killer cells for patients with relapsed hematologic malignancies after allogeneic hematopoietic cell transplantation. *Biol Blood Marrow Transplant* 17: 1679 – 1687

Leelayuwat C, Townend DC, Degli-Esposti MA, Abraham LJ, Dawkins RL (1994) A new polymorphic and multicopy MHC gene family related to nonmammalian class I. *Immunogenetics* 40: 339 – 351

Leung W (2011) Use of NK cell activity in cure by transplant. *Br J Haematol* 155: 14 – 29

Li P, Morris DL, Willcox BE, Steinle A, Spies T, Strong RK (2001) Complex structure of the activating immunoreceptor NKG2D and its MHC class I-like ligand MICA. *Nat Immunol* 2: 443 – 451

Li P, Willie ST, Bauer S, Morris DL, Spies T, Strong RK (1999) Crystal structure of the MHC class I homolog MIC-A, a gammadelta T cell ligand. *Immunity* 10: 577 – 584

Lopez-Hernandez R, Valdes M, Lucas D, Campillo JA, Martinez-Garcia P, Salama H, Lopez M, Salgado G, Botella C, Minguela A *et al* (2010) Association analysis of MICA gene polymorphism and MICA-129 dimorphism with inflammatory bowel disease susceptibility in a Spanish population. *Hum Immunol* 71: 512 – 514

Meehan KR, Talebian L, Tosteson TD, Hill JM, Szczepiorkowski Z, Sentman CL, Ernstoff MS (2013) Adoptive cellular therapy using cells enriched for $NKG2D^+CD3^+CD8^+$T cells after autologous transplantation for myeloma. *Biol Blood Marrow Transplant* 19: 129 – 137

Nückel H, Switala M, Sellmann L, Horn PA, Dürig J, Duhrsen U, Küppers R, Grosse-Wilde H, Rebmann V (2010) The prognostic significance of soluble NKG2D ligands in B-cell chronic lymphocytic leukemia. *Leukemia* 24: 1152 – 1159

Ogasawara K, Benjamin J, Takaki R, Phillips JH, Lanier LL (2005) Function of NKG2D in natural killer cell-mediated rejection of mouse bone marrow grafts. *Nat Immunol* 6: 938 – 945

Oppenheim DE, Roberts SJ, Clarke SL, Filler R, Lewis JM, Tigelaar RE, Girardi M, Hayday AC (2005) Sustained localized expression of ligand for the activating NKG2D receptor impairs natural cytotoxicity in vivo and reduces tumor immunosurveillance. *Nat Immunol* 6: 928 – 937

Parmar S, Del Lima M, Zou Y, Patah PA, Liu P, Cano P, Rondon G, Pesoa S, de Padua Silva L, Qazilbash MH *et al* (2009) Donor-recipient mismatches in MHC class I chain-related gene A in unrelated donor transplantation lead to increased incidence of acute graft-versus-host disease. *Blood* 114: 2884 – 2887

Pollock RA, Chandran V, Pellett FJ, Thavaneswaran A, Eder L, Barrett J, Rahman P, Farewell V, Gladman DD (2013) The functional MICA-129 polymorphism is associated with skin but not joint manifestations of psoriatic disease independently of HLA-B and HLA-C. *Tissue Antigens* 82: 43 – 47

Przepiorka D, Weisdorf D, Martin P, Klingemann HG, Beatty P, Hows J, Thomas ED (1995) 1994 Consensus Conference on Acute GVHD Grading. *Bone Marrow Transplant* 15: 825 – 828

Raache R, Belanteur K, Amroun H, Benyahia A, Heniche A, Azzouz M, Mimouni S, Gervais T, Latinne D, Boudiba A *et al* (2012) Association of

major histocompatibility complex class 1 chain-related gene a dimorphism with type 1 diabetes and latent autoimmune diabetes in adults in the Algerian population. *Clin Vaccine Immunol* 19: 557 – 561

Raulet DH, Gasser S, Gowen BG, Deng W, Jung H (2013) Regulation of ligands for the NKG2D activating receptor. *Annu Rev Immunol* 31: 413 – 441

Reiners KS, Kessler J, Sauer M, Rothe A, Hansen HP, Reusch U, Hucke C, Kohl U, Durkop H, Engert A *et al* (2013) Rescue of impaired NK cell activity in hodgkin lymphoma with bispecific antibodies in vitro and in patients. *Mol Ther* 21: 895 – 903

Rincon-Orozco B, Kunzmann V, Wrobel P, Kabelitz D, Steinle A, Herrmann T (2005) Activation of V gamma 9V delta 2 T cells by NKG2D. *J Immunol* 175: 2144 – 2151

Salih HR, Antropius H, Gieseke F, Lutz SZ, Kanz L, Rammensee HG, Steinle A (2003) Functional expression and release of ligands for the activating immunoreceptor NKG2D in leukemia. *Blood* 102: 1389 – 1396

Salih HR, Rammensee HG, Steinle A (2002) Cutting edge: down-regulation of MICA on human tumors by proteolytic shedding. *J Immunol* 169: 4098 – 4102

Sanchez-Correa B, Morgado S, Gayoso I, Bergua JM, Casado JG, Arcos MJ, Bengochea ML, Duran E, Solana R, Tarazona R (2011) Human NK cells in acute myeloid leukaemia patients: analysis of NK cell-activating receptors and their ligands. *Cancer Immunol Immunother* 60: 1195 – 1205

Sconocchia G, Lau M, Provenzano M, Rezvani K, Wongsena W, Fujiwara H, Hensel N, Melenhorst J, Li J, Ferrone S *et al* (2005) The antileukemia effect of HLA-matched NK and NK-T cells in chronic myelogenous leukemia involves NKG2D-target-cell interactions. *Blood* 106: 3666 – 3672

Shafi S, Vantourout P, Wallace G, Antoun A, Vaughan R, Stanford M, Hayday A (2011) An NKG2D-mediated human lymphoid stress surveillance response with high interindividual variation. *Sci Transl Med* 3: 113ra124

Steinle A, Li P, Morris DL, Groh V, Lanier LL, Strong RK, Spies T (2001) Interactions of human NKG2D with its ligands MICA, MICB, and homologs of the mouse RAE-1 protein family. *Immunogenetics* 53: 279 – 287

Tong HV, Toan NL, Song LH, Bock CT, Kremsner PG, Velavan TP (2013) Hepatitis B virus-induced hepatocellular carcinoma: functional roles of MICA variants. *J Viral Hepat* 20: 687 – 698

Verneris MR, Karami M, Baker J, Jayaswal A, Negrin RS (2004) Role of NKG2D signaling in the cytotoxicity of activated and expanded CD8 + T cells. *Blood* 103: 3065 – 3072

Waldhauer I, Goehlsdorf D, Gieseke F, Weinschenk T, Wittenbrink M, Ludwig A, Stevanovic S, Rammensee HG, Steinle A (2008) Tumor-associated MICA is shed by ADAM proteases. *Cancer Res* 68: 6368 – 6376

Warren EH, Zhang XC, Li S, Fan W, Storer BE, Chien JW, Boeckh MJ, Zhao LP, Martin PJ, Hansen JA (2012) Effect of MHC and non-MHC donor/recipient genetic disparity on the outcome of allogeneic HCT. *Blood* 120: 2796 – 2806

Wesselkamper SC, Eppert BL, Motz GT, Lau GW, Hassett DJ, Borchers MT (2008) NKG2D is critical for NK cell activation in host defense against Pseudomonas aeruginosa respiratory infection. *J Immunol* 181: 5481 – 5489

Wiemann K, Mittrücker HW, Feger U, Welte SA, Yokoyama WM, Spies T, Rammensee HG, Steinle A (2005) Systemic NKG2D down-regulation impairs NK and CD8 T cell responses in vivo. *J Immunol* 175: 720 – 729

Yoshida K, Komai K, Shiozawa K, Mashida A, Horiuchi T, Tanaka Y, Nose M, Hashiramoto A, Shiozawa S (2011) Role of the MICA polymorphism in systemic lupus erythematosus. *Arthritis Rheum* 63: 3058 – 3066

Zhao J, Jiang Y, Lei Y, Zou K, Wang C, Huang S, Yi F, Xia B (2011) Functional MICA-129 polymorphism and serum levels of soluble MICA are correlated with ulcerative colitis in Chinese patients. *J Gastroenterol Hepatol* 26: 593 – 598

Zou Y, Mirbaha F, Lazaro A, Zhang Y, Lavingia B, Stastny P (2002) MICA is a target for complement-dependent cytotoxicity with mouse monoclonal antibodies and human alloantibodies. *Hum Immunol* 63: 30 – 39

Zou Y, Stastny P (2010) Role of MICA in the immune response to transplants. *Tissue Antigens* 76: 171 – 176

Expanded View Figures

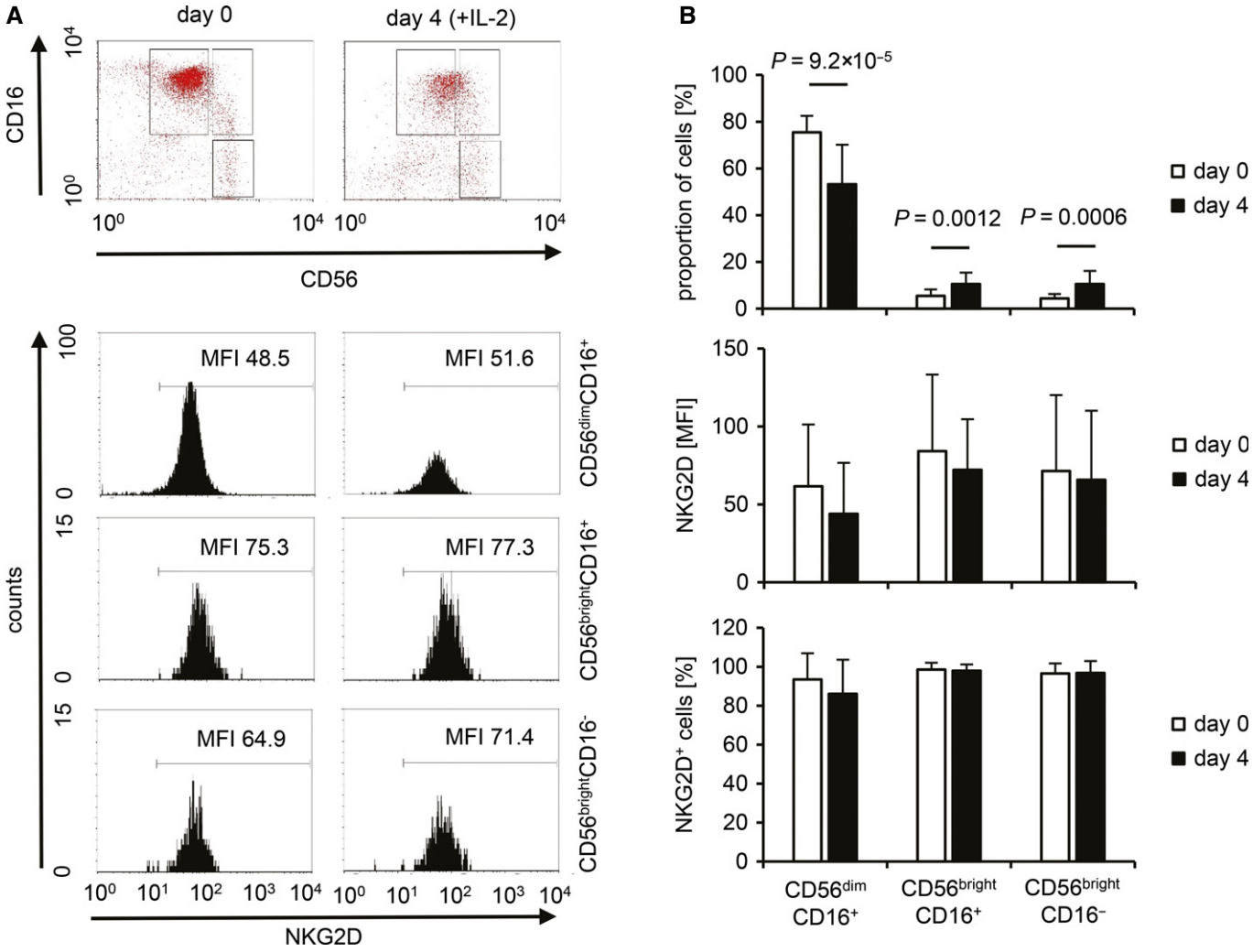

Figure EV1. NKG2D expression on freshly isolated and IL-2-stimulated NK-cell populations.

A Three populations ($CD56^{dim}CD16^{+}$, $CD56^{bright}CD16^{+}$, $CD56^{bright}CD16^{-}$) were gated on freshly isolated NK cells (day 0) and NK cells stimulated for 4 days with IL-2 (100 U/ml) as exemplified in the upper panel. The NKG2D expression on these NK-cell populations is displayed in the lower panel, and the MFI for NKG2D is indicated.

B Summaries (means + SD) of the proportion of the three NK-cell populations and their NKG2D expression intensity (MFI and percentage $NKG2D^{+}$ cells) at day 0 (n = 21) and 4 days after IL-2 stimulation (n = 16) are shown. The data were analyzed by t-test, and the P-values of significant differences are indicated.

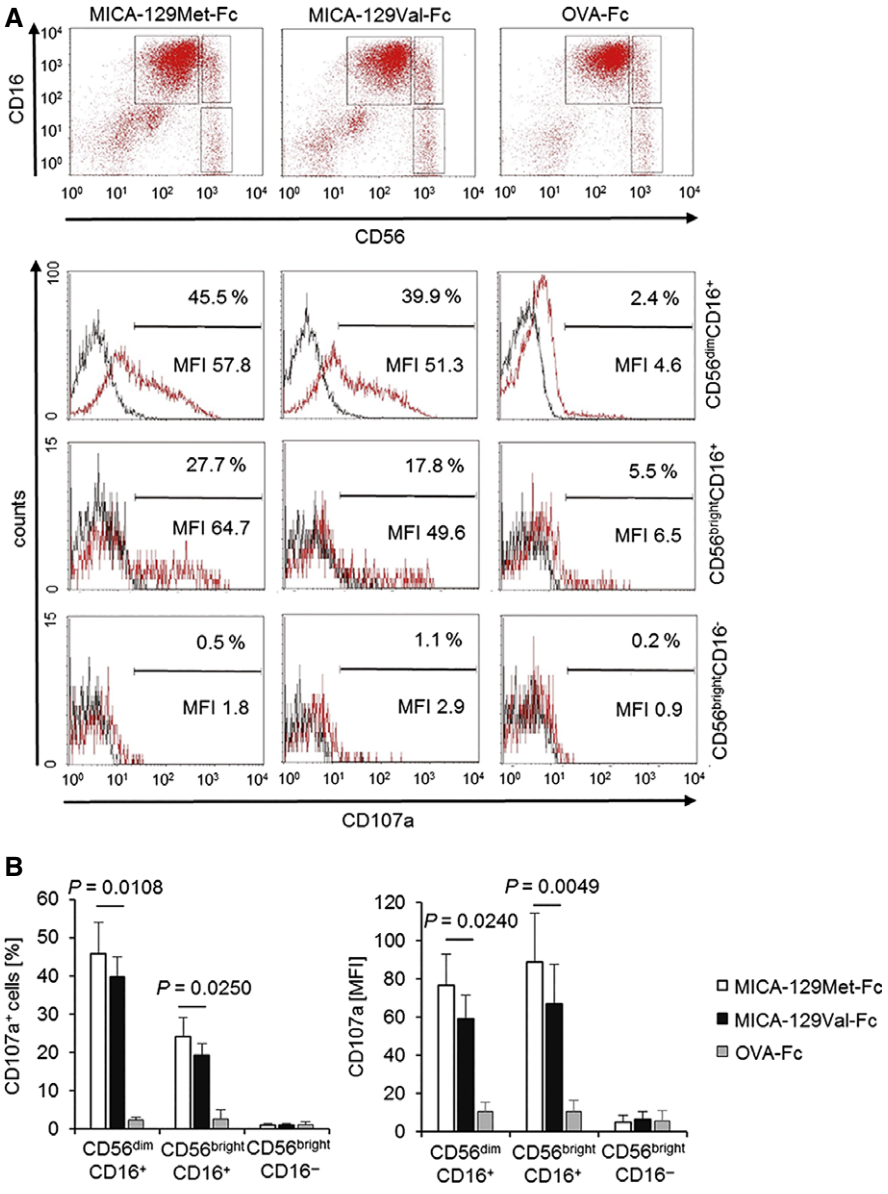

Figure EV2. Degranulation of CD56^{dim}CD16^{+} and CD56^{bright}CD16^{+} NK cells in response to the MICA-129Met and the MICA-129Val isoforms.

A Purified IL-2-stimulated NK cells (100 U/ml for 4 days) were cultured for 2 h on plates coated with MICA-129Met-Fc, MICA-129Val-Fc, or OVA-Fc proteins (10 μg/ml) before flow cytometry. The NK-cell populations were gated as illustrated in the upper panel (CD56^{dim}CD16^{+}, CD56^{bright}CD16^{+}, CD56^{bright}CD16^{-}), and CD107a expression was determined as displayed in the lower panel (red: CD107a, black: isotype control). The specific MFI (MFI CD107a minus MFI isotype control) and the percentage of CD107a^{+} cells are indicated.

B A summary (means + SD) of 5 experiments is shown. The data were analyzed by *t*-test, and the *P*-values of significant differences are indicated.

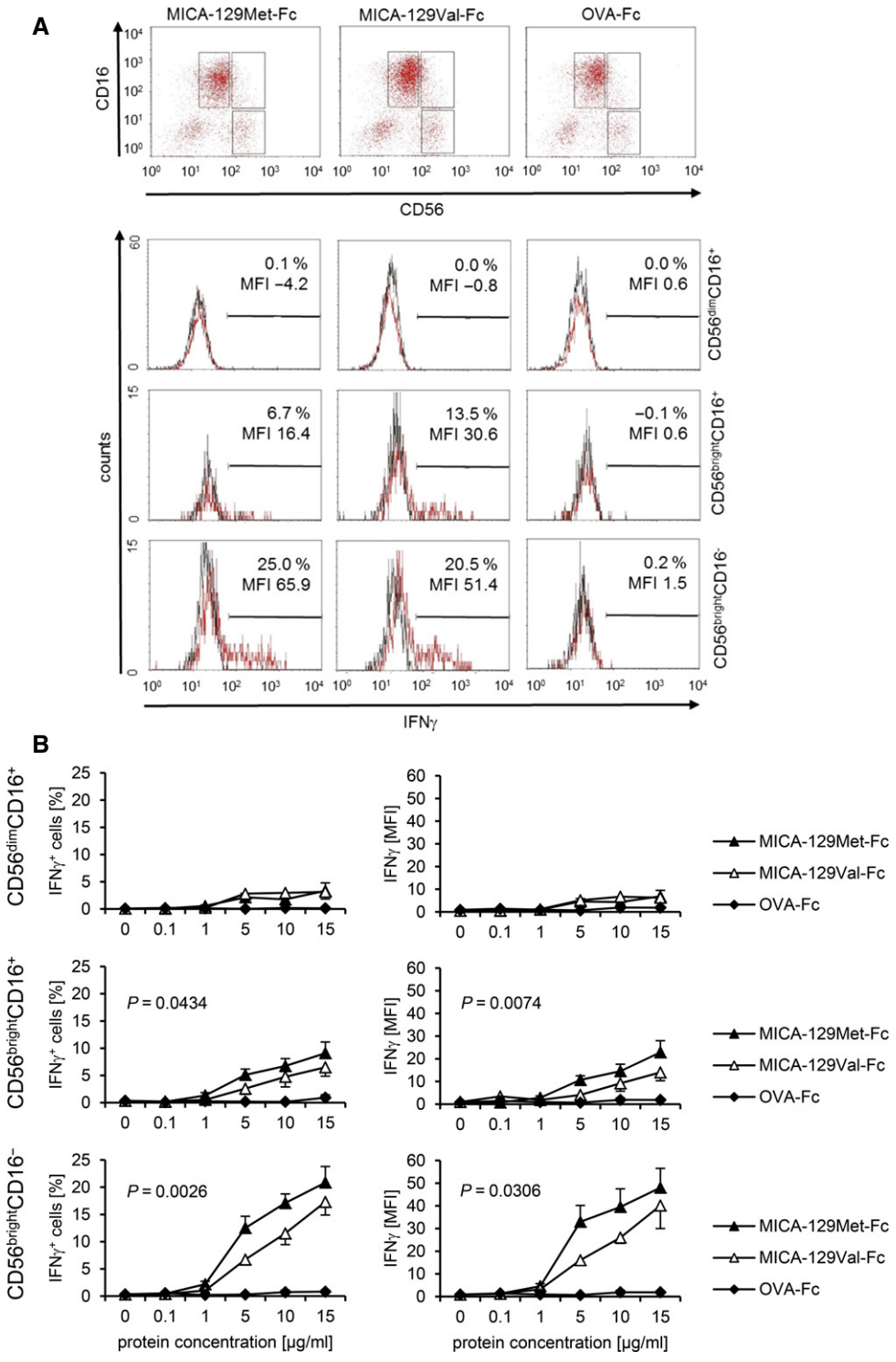

Figure EV3. Expression of IFNγ in CD56^{bright}CD16^{-} and CD56^{bright}CD16^{+} NK cells in response to the MICA-129Met and the MICA-129Val isoforms.

A Purified IL-2-stimulated NK cells (100 U/ml for 4 days) were cultured for 4 h on plates coated with MICA-129Met-Fc, MICA-129Val-Fc, or OVA-Fc proteins (0, 0.1, 1, 5, 10, 15 µg/ml) before flow cytometry. The NK-cell populations were gated as exemplified in the upper panel (CD56^{dim}CD16^{+}, CD56^{bright}CD16^{+}, CD56^{bright}CD16^{-}). The intracellular IFNγ expression in these populations is displayed in the lower panel (red: IFNγ, black: isotype control). The specific MFI (MFI IFNγ minus MFI isotype control) and the percentage of IFNγ^{+} cells are indicated.

B A summary (means + SEM) of 9 experiments is shown. The data were analyzed by two-way ANCOVA adjusted for the protein concentration (5, 10, 15 µg/ml), and the *P*-values of significant differences between the MICA-129Met-Fc and MICA-129Val-Fc proteins are indicated.

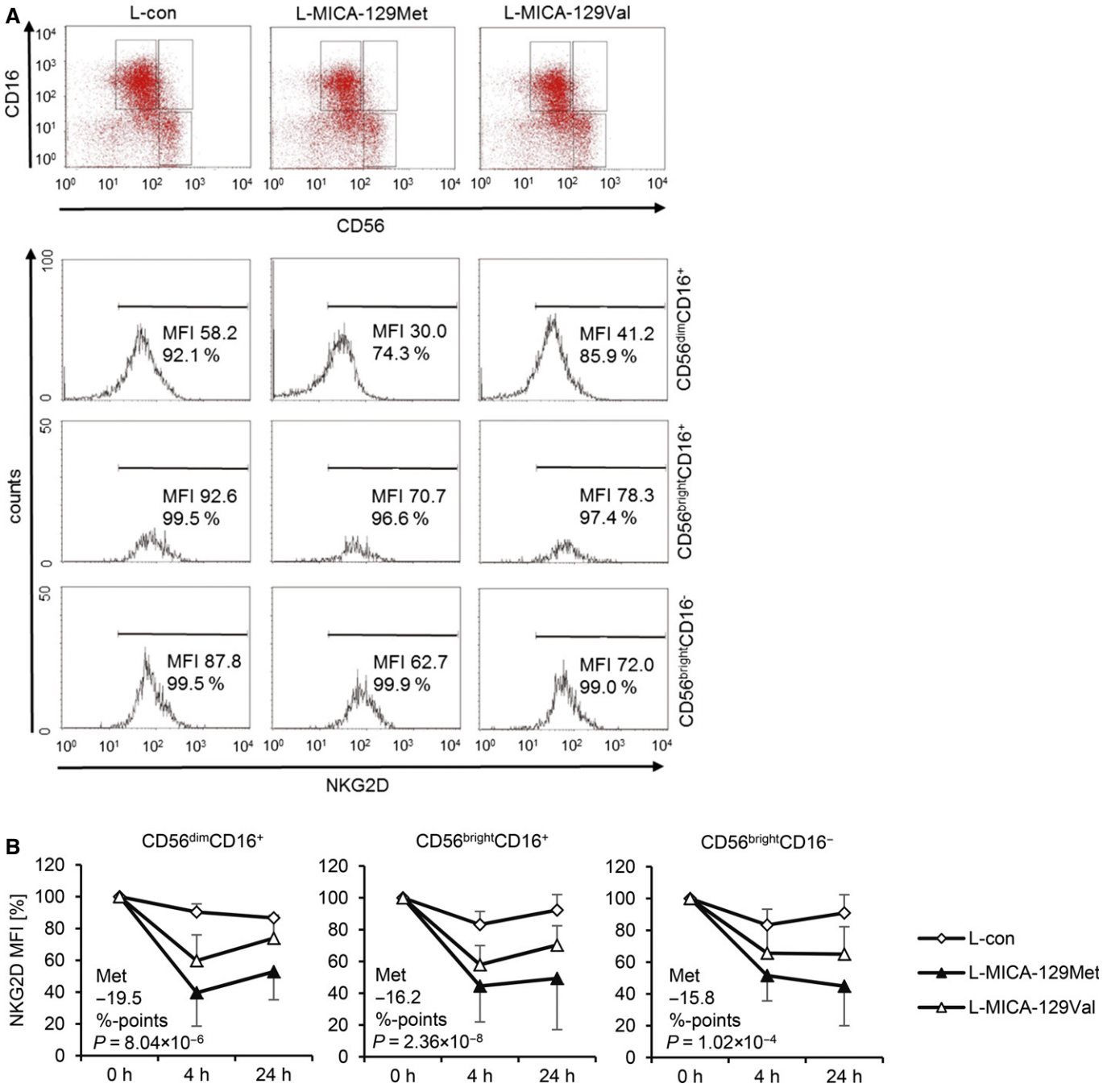

Figure EV4. Down-regulation of NGK2D on CD56^{dim}CD16^{+}, CD56^{bright}CD16^{+}, and CD56^{bright}CD16^{-} NK cells in response to the MICA-129Met and the MICA-129Val isoforms.

A Purified IL-2-stiumlated NK cells (100 U/ml for 4 days) were co-cultured with L-con, L-MICA-129Met, or L-MICA-129Val clones for 4 h. Three NK-cell populations (CD56^{dim}CD16^{+}, CD56^{bright}CD16^{+}, CD56^{bright}CD16^{-}) were gated as illustrated in the upper panel. The NKG2D expression on these NK-cell populations is displayed in the lower panel, and the MFI of NKG2D and the percentages of NKG2D^{+} cells are indicated.

B A summary (means + SD) of NKG2D expression on the three NK-cell populations 4 and 24 h after co-culture with L-con (n = 3), L-MICA-129Met (n = 17), and L-MICA-129Val clones (n = 18) is displayed. The NKG2D expression (MFI) at the beginning (0 h) was set to 100%. The average reduction of NKG2D on NK cells in response to L-MICA-129Met compared to L-MICA-129Val clones at 4 and 24 h (%-points) is indicated in the panels. The differences were analyzed by repeated measures ANOVA, and P-values are indicated.

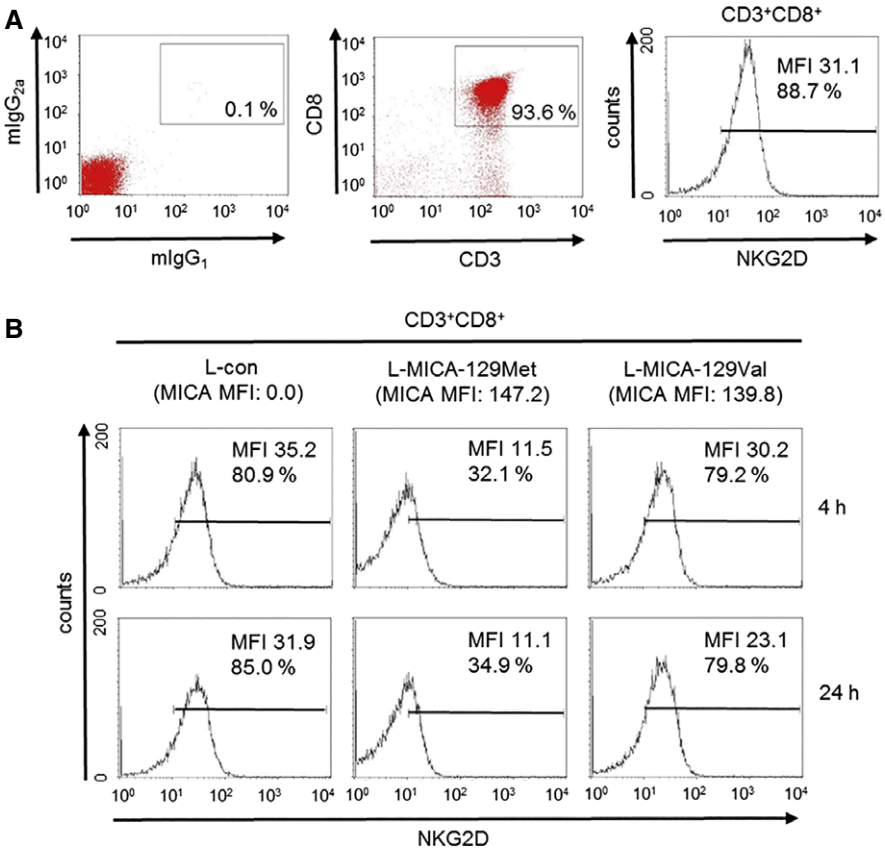

Figure EV5. Down-regulation of NGK2D on CD8$^+$ T cells in response to the MICA-129Met and MICA-129Val isoforms.

A Purified CD8$^+$ T cells were analyzed by flow cytometry for NKG2D expression as illustrated here. The MFI for NKG2D and the percentage of NKG2D$^+$CD8$^+$ T cells are indicated.

B The NK cells were subsequently co-cultured with an L-con, L-MICA-129Met, or L-MICA-129Val clone (the MFI values for MICA on these clones are indicated above the histograms in brackets). NKG2D expression was determined as illustrated in (A) after 4 and 24 h. The MFI for NKG2D and the percentages of NKG2D$^+$CD8$^+$ T cells are indicated.

EMBO Molecular Medicine

Antje Isernhagen, Dörthe Malzahn, Elena Viktorova, Leslie Elsner, Sebastian Monecke, Frederike von Bonin, Markus Kilisch, Janne Marieke Wermuth, Neele Walther, Yesilda Balavarca, Christiane Stahl-Hennig, Michael Engelke, Lutz Walter, Heike Bickeböller, Dieter Kube, Gerald Wulf, & Ralf Dressel

The MICA-129 dimorphism affects NKG2D signaling and outcome of hematopoietic stem cell transplantation

Appendix

Table of content

Legends for Appendix Figures

Appendix Figure S1. L-MICA-129Met cells bind NKG2D with higher avidity than L-MICA-129Val cells. (**A**) The expression of MICA was analyzed by flow cytometry on L-con, L-MICA-129Met, and L-MICA-129Val cells using a FITC-conjugated goat anti-mouse IgG as secondary Ab. In parallel, the binding of a recombinant human NKG2D-Fc fusion protein was measured using FITC-conjugated goat anti-human IgG as secondary Ab. Staining with the respective primary reagent plus secondary Ab (blue or red line) and FITC-labeled secondary Ab only (black line) is shown. The MFI of MICA expression and NKG2D binding determined by these measurements are indicated. (**B**) The MICA expression intensity on L-MICA-129Met (n=79) and L-MICA-129Val clones (n=81) was determined as MFI by flow cytometry as illustrated in panel A and is displayed in box-and-whisker plots. The data were compared by a t-test. (**C**) In parallel, the binding of a recombinant NKG2D-Fc fusion protein to the L-MICA-129Met and L-MICA-129Val clones was measured by flow cytometry and the MFIs are shown in box-and-whisker plots. A difference between the cell lines was assessed by a t-test. (**D**) The ratios of the NKG2D binding and MICA expression for the L-MICA-129Met and L-MICA-129Val clones are summarized in box-and-whisker plots revealing a difference between the MICA-129 variants in NKG2D binding avidity (t-test).

Appendix Figure S2. MICA-129Met-Fc and L-MICA-129Val-Fc proteins, in contrast to an OVA-Fc protein, bind to NK cells. (**A**) MICA-129Met-Fc and L-MICA-129Val-Fc proteins were separated together with a bovine serum albumin (BSA) standard and a marker (M) by SDS-PAGE and stained with Coomassie blue (left panel) to demonstrate the integrity of the recombinant fusion proteins. Both fusions proteins (5 µg) were separated by SDS-PAGE and blotted. The blot was probed with a biotinylated anti-MICA Ab (right panel). (**B**) The OVA-Fc protein was separated with a marker (M) by SDS-PAGE and stained with Coomassie blue (left panel). The OVA-Fc fusion protein (1 µg) was separated together with OVA (1 µg) by SDS-PAGE and blotted. The blot was probed with an anti-OVA Ab. (**C**) The binding of MICA-129Met-Fc, MICA-129Val-Fc, and as negative control OVA-Fc fusion proteins to purified IL-2- stimulated (100 U/ml for 4 days) NK cells was determined by flow cytometry.

The histograms illustrate the staining with the fusion proteins (10 µg/ml) plus secondary Ab in bold and with the secondary Ab only in light. The percentage of cells binding to the proteins and the MFI are indicated. (**D**) The binding of MICA-129Met-Fc, MICA-129Val-Fc, and OVA-Fc fusion proteins to NK cells was determined by flow cytometry at various concentrations and is shown as means (n=3) and SD of the MFI (left panel) and the percentage of positive cells (right panel) . Notably, the binding decreased at very high concentrations of MICA proteins (100 µg/ml). Binding of MICA129Met-Fc and MICA-129Val-Fc proteins to NK cells was not significantly different. In contrast, we had observed a higher avidity of the MICA-129Met than MICA-129Val isoform for NKG2D using L cells expressing the MICA-129Met or MICA-129Val variants (see Appendix Fig S1D). This might be due to slight differences in the conformation or glycosylation of MICA molecules expressed in L cells or produced as IgG_{2a}-Fc fusion proteins in HEK293 cells. Notably, the MICA-129Met-Fc and MICA-129Val-Fc proteins varied in their efficacy to elicit downstream biological effects (see Fig 2B, Fig 2C, Fig 3A, Fig EV2, Fig EV3) similarly as MICA-129Met/Val molecules expressed on L cells.

Appendix Figure S3. MICA-129Met-Fc and MICA-129Val-Fc proteins bind with similar avidity to NKG2D in SPR analysis. (**A**) NKG2D-Fc was covalently immobilized on an activated HC 1000m SPR sensorchip and the SPR response was recorded after injecting 2, 4, 8, 16, 32, 64, 125, 250, and 500 nM of MICA-129Val-Fc or MICA-129Met-Fc fusion proteins. A typical sensogram of MICA129Val-Fc binding obtained via SPR is shown with observed binding (black lines) and global fit of SPR data using kinetic parameters k_a and k_d (orange lines). (**B**) Equilibrium binding analysis of NKG2D-Fc binding to MICA-129Met-Fc at 20 °C. (**C**) Equilibrium binding analysis of NKG2D-Fc binding to MICA-129Val-Fc at 20°C. (**D**) The equilibrium binding constants (K_D) of the MICA-129Met-Fc and MICA-129Val-Fc proteins to NKG2D-Fc were obtained using a nonlinear curve fit. The results of four experiments are summarized (means ± SD) and compared by a t-test.

Appendix Figure S4. **Resting NK cells fail to respond to L-MICA-129Met and L-MICA-129Val clones.** (**A**) A summary of 3 independent experiments is shown demonstrating the very low cytotoxic activity of freshly isolated NK cells against an L-MICA-129Met and an L-MICA-129Val clone. L-con cells served as negative and K562 cells as a positive control. The means of specific lysis plus SD at different E:T ratios (16:1 to 0.25:1) were measured in ^{51}Chromium-release assays. (**B**) The MICA expression intensity to the L target cells was determined in parallel by flow cytometry and the MFI as well as the percentage of MICA$^+$ cells are displayed. (**C**) Freshly isolated NK cells were co-cultured with K562 target cells before measuring CD107a$^+$ (2 h) and IFNγ^+ cells (4 h) by flow cytometry on CD56^{dim}CD16$^+$, CD56^{bright}CD16$^+$, and CD56^{bright}CD16$^-$ NK cells. In the shown experiment, 10.7% of the CD56^{dim}CD16$^+$ NK cells were CD107a$^+$ whereas very few NK cells responded to K562 cells by IFNγ production. (**D**) A summary (mean plus SD) of 3 independent flow cytometry experiments performed in parallel to the experiments in panels A and B is shown. (**E**) The release of cytokines (IFNγ, TNFα, IL-10, and IL-13) into the supernatant was determined in parallel to these experiments by ELISA after 4 and 24 h of co-culture ($2.5x10^5$ NK cells plus $5x10^4$ targets). The means plus SD of 3 experiments are shown.

Appendix Figure S5. Inhibition of SRC family kinases by PP2 abolishes lysis of MICA expressing target cells and release of cytokines but does not induce apoptosis in NK cells. (**A**) One of 2 experiments with in principal identical results is shown demonstrating the inhibition of cytotoxic activity of purified IL-2-stimulated (100 U/ml for 4 days) NK cells against an L-MICA-129Met and an L-MICA-129Val clone by PP2 (25 μM). The means of specific lysis of triplicates plus SD at different E:T ratios (4:1 to 0.06:1) are shown as measured in a ^{51}Chromium-release assay. The MICA expression intensity and the percentage of MICA$^+$ target cells was determined in parallel by flow cytometry and is indicated. As controls untreated cells (con) and cells treated with the solvent only (DMSO) are included. (**B**) The release of IFNγ and TNFα into the supernatant was determined by ELISA after 4 h of culture of $2.5x10^5$ purified IL-2-stimulated (100 U/ml for 4 days) NK cells (con) on plate-bound MICA-129Met-Fc, MICA-129Val-Fc, or OVA-Fc proteins (10 μg/ml). PP2 (25 μM) or the solvent only (DMSO) was added to the

cultures. Means plus SD of 3 experiments are displayed. (**C**) Purified IL-2-stimulated (100 U/ml for 4 days) NK cells (con) were cultured for 4 h in presence of PP2 (25 µM) or the solvent only (DMSO). The cells were stained by AnnexinV-FITC and PI and the percentage of early apoptotic cells ($AnnexinV^+/PI^-$) is indicated. (**D**) A summary (means plus SD) of 7 independent experiments is shown.

Appendix Figure S6. **NK cells degranulate in response to L-MICA-129Met and L-MICA-129Val clones.** (**A**) PBMC were stimulated *in vitro* for 4 days with IL-2 (100 U/ml) and then characterized by flow cytometry for expression of the indicated cell surface markers. The percentage of cells positive for the various markers (mean plus SD, n=6) is displayed. (**B**) NK cells among the PBMC were identified by staining of CD16 and CD56. The $CD56^+$ NK cells were gated as illustrated in this dot plot for subsequent analysis of CD107a expression. In these experiments using unseparated IL-2-stimulated PBMC as effector cells, $CD56^{bright}$ NK cells were too rare to analyze them separately. (**C**) The degranulation of $CD56^+$ NK cells exposed to L-con, L-MICA-129Met or L-MICA-129Val clones for 1 h was determined by flow cytometry after staining of CD107a. Black lines indicate CD107a staining while gray-lined histograms show the isotype control. The percentages of $CD107a^+$ cells and the MFI of CD107a of these measurements are indicated in the histograms.

Appendix Figure S7. The expression of IFNγ in $CD56^{bright}CD16^+$ and $CD56^{dim}CD16^+$ NK cells in response to the MICA-129Met and MICA-129Val isoforms.

The IFNγ expression of $CD56^{bright}CD16^+$ (**A**) and $CD56^{dim}CD16^+$ (**B**) NK cells exposed to L-MICA-129Met (n=23) or L-MICA-129Val clones (n=23) for 4 h was determined by flow cytometry as MFI of IFNγ (upper panels) and as percentage of $IFN\gamma^+$ cells (lower panels). The purified NK cells had been stimulated *in vitro* for 4 days with IL-2 (100 U/ml). In parallel, the MICA expression on target cells was determined. Displayed is the linear regression of IFNγ and MICA expression on targets, both determined as MFI, for the L-MICA-129Met (upper left panel) and L-MICA-129Val clones (upper right panel). The linear regression of the percentage of $IFN\gamma^+$ NK cells and MICA expression on targets (determined as MFI) is

shown for the L-MICA-129Met (lower left panel) and L-MICA-129Val clones (lower right panel). The coefficients of determination (R^2), the regression coefficients (reg. coeff.) and the *P*-values for Pearson correlation are indicated.

Appendix Figure S8. Cytokine release of NK cells in response to the MICA-129Met and MICA-129Val isoforms.

The release of IFNγ, TNFα, IL-10, and IL-13 into the supernatant was determined by ELISA after 4 h of culture of $2.5x10^5$ purified IL-2-stimulated (100 U/ml, 4 days) NK cells on plate-bound MICA-129Met-Fc, MICA-129Val-Fc, and OVA-Fc proteins (0, 5, 10, 15 µg/ml). Means plus SEM of 6 experiments are displayed. The data were analyzed by ANCOVA adjusted for the protein concentration (5, 10, 15 µg/ml) and the *P*-values of significant differences between the MICA-129Met-Fc and MICA-129Val-Fc proteins are indicated in the panels for IFNγ and TNFα. In the panel for IL-13, the *P*-values indicate significant differences between the OVA-Fc and the MICA-129Met-Fc (red) or MICA-129Val-Fc (blue) proteins, respectively.

Appendix Figure S9. Down-regulation of NKG2D but not of CD94 on NK cells co-cultured with L-MICA-129Val and L-MICA-129Met clones. (**A**) NKG2D expression on purified IL-2-stimulated NK cells (100 U/ml for 4 days) co-cultured with L-con, L-MICA-129Met or L-MICA-129Val target cells for 24 h was analyzed by flow cytometry. NKG2D expression was analyzed after gating on $CD3^-CD56^+$ NK cells. Black-lined histograms represent the NKG2D staining while gray-lined histograms show the isotype control. The percentages of $NKG2D^+$ cells and the MFI of NKG2D are indicated in the histograms. (**B**) In parallel, the CD94 expression on the NK cells was determined. Black-lined histograms represent CD94 staining while gray lines show the isotype control. The percentages of $CD94^+$ cells and the MFI of CD94 of these measurements are indicated in the histograms. (**C**) CD94 expression on purified IL-2-stimulated NK cells (100 U/ml for 4 days) exposed to L-MICA-129Met (n=25) or L-MICA-129Val clones (n=25) for 0, 4,

and 24 h was analyzed by flow cytometry. The means and SD of the percentage of $CD94^+$ NK cells (left panel) and of the MFI of CD94 (right panel) are shown.

Appendix Figure S10. Correlation of NKG2D expression on NK cells with L-MICA-129Val and L-MICA-129Met expression on target cells. NKG2D expression on purified IL-2-stimulated NK cells (100 U/ml for 4 days) exposed to L-MICA-129Met (n=25) or L-MICA-129Val clones (n=25) for 0, 4, and 24 h was analyzed by flow cytometry. The linear regression of MICA expression on target cells and NKG2D expression on NK cells both determined as MFI is shown for the L-MICA-129Met (left panels) and L-MICA-129Val cells (right panels) 4 h (upper panels) and 24 h (lower panels) after co-culture. The coefficient of determination (R^2), the regression coefficient (reg. coeff.) and the *P*-value for Pearson correlation are indicated for both MICA variants.

Appendix Figure S11. Stimulation of NKG2D by MICA-129Met-Fc and MICA-129Val-Fc proteins alone is not sufficient to induce proliferation of $CD8^+$ T cells or IL-2 release. (**A**) MACS-separated $CD8^+$ T cells were cultured in triplicates in 96-well-plates with an immobilized anti-CD3 mAb (1.0 to 0.0 µg/ml). After 72h, 25 % of the supernatant were harvested and IL-2 concentrations were measured by ELISA (see panel B). The harvested medium was replaced by the same volume containing 1 µCi ^{3}H-labeled thymidine. After 12h, the plates were completely harvested and the DNA-bound radioactivity was determined. The SI was calculated by dividing the measured cpm by the cpm of the negative control (only $CD8^+$ T cells). The means and SD of SI determined in 4 independent experiments are displayed. (**B**) The means and SD of IL-2 concentrations determined in triplicates in 4 independent experiments are shown. The anti-CD3 mAb alone can induce proliferation and IL-2 production. (**C**) The means and SD of SI after stimulation with co-stimulatory mAb (anti-CD28, anti-NKG2D), MICA-129Met-Fc, MICA-129Val-Fc proteins, and controls (OVA-Fc, mIgG1, mIgG2a) alone as determined in triplicates in 4 independent experiments are displayed. Thus, these reagents alone did not induce proliferation. (**D**) The means and SD of IL-2 release after stimulation with co-stimulatory mAb (anti-CD28, anti-NKG2D),

MICA-129Met-Fc, MICA-129Val-Fc proteins, and controls (OVA-Fc, mIgG1, mIgG2a) alone as determined in triplicates in 4 independent experiments are shown. Thus, these reagents alone did not induce IL-2 release. (**E**) MACS-separated CFSE-stained $CD8^+$ T cells were stimulated in the same way by anti-CD3, anti-CD28, anti-NKG2D, MICA-129Met-Fc, MICA-129Val-Fc proteins, and controls (OVA-Fc, mIgG1, mIgG2a) alone. The proliferation was assessed at 72h by flow cytometry after gating of $CD3^+CD8^+$ T cells. The MFI of CFSE in unstimulated $CD8^+$ T cells (control) was set to 100 % in individual experiments and the relative decrease due to proliferation was calculated (upper panel). In parallel, the proportion of dividing cells was determined (lower panel). Thus, only the anti-CD3 mAb induced proliferation.

Appendix Figure S12. NKG2D signaling provides a co-stimulatory signal for $CD8^+$ T cells when anti-CD3 is limited to 0.01 or 0.005 µg/ml. (**A**) The threshold of CD3 signaling was determined that requires co-stimulatory signals to induce proliferation and IL-2 release by $CD8^+$ T cells. Purified $CD8^+$ T cells were cultured in triplicates in 96-well-plates coated with an immobilized anti-CD3 in combination with an anti-CD28 mAb. After 72h, 25 % of the supernatant were harvested and IL-2 concentrations were measured by ELISA. The harvested medium was replaced by the same volume containing 1 µCi ^{3}H-labeled thymidine. After 12h, the plates were completely harvested and the DNA-bound radioactivity was determined in triplets. The means and SD of SI and IL-2 release as determined in triplicates in 4 independent experiments are shown (* P<0.05, ** P<0.01, t-test; left panel: anti-CD3 0.01 µg/ml: 1.0 µg/ml anti-CD28 versus 0.0 µg/ml anti-CD28 P=0.0145 and 0.5 µg/ml anti-CD28 versus 0.0 µg/ml anti-CD28 P=0.0002, anti-CD3 0.005 µg/ml: 1.0 µg/ml anti-CD28 versus 0.0 µg/ml anti-CD28 P=0.0048 and 0.5 µg/ml anti-CD28 versus 0.0 µg/ml anti-CD28 P=0.0023; right panel: anti-CD3 0.05 µg/ml: 1.0 µg/ml anti-CD28 versus 0.0 µg/ml anti-CD28 P=0.0091 and 0.5 µg/ml anti-CD28 versus 0.0 µg/ml anti-CD28 P=0.0091, anti-CD3 0.01 µg/ml: 1.0 µg/ml anti-CD28 versus 0.0 µg/ml anti-CD28 P=0.0091 and 0.5 µg/ml anti-CD28 versus 0.0 µg/ml anti-CD28 P=0.0091, anti-CD3 0.005 µg/ml: 1.0 µg/ml anti-CD28 versus 0.0 µg/ml anti-CD28 P=0.0073 and 0.5 µg/ml anti-CD28 versus 0.0 µg/ml anti-CD28 P=0.0073)

(**B**) In parallel, an anti-NKG2D mAb was used for co-stimulation (* P<0.05, t-test; left panel: anti-CD3 0.01 µg/ml: 1.0 µg/ml anti-NKG2D versus 0.0 µg/ml anti-NKG2D P=0.0036 and 0.5 µg/ml anti-NKG2D versus 0.0 µg/ml anti-NKG2D P=0.0060 and 0.1 µg/ml anti-NKG2D versus 0.0 µg/ml anti-NKG2D P=0.0005, anti-CD3 0.005 µg/ml: 0.5 µg/ml anti-NKG2D versus 0.0 µg/ml anti-NKG2D P=0.0309; right panel: anti-CD3 0.005 µg/ml: 0.5 µg/ml anti-NKG2D versus 0.0 µg/ml anti-NKG2D P=0.0205) (**C**) A $mIgG_1$ isotype control was also used in parallel. Thus, NKG2D-mediated co-stimulation was effective when the anti-CD3 mAb was limited (0.01 and 0.005 µg/ml). The anti-NKG2D mAb induced more proliferation and IL-2 release when used in lower concentration (0.5 µg/ml compared to 1.0 µg/ml). Notably, anti-NKG2D co-stimulation induced a proliferation even at 0.1 µg/ml were the anti-CD28 mAb was not able anymore to elicit a significant proliferation.

Appendix Figure S13. Correlation of NKG2D expression on $CD8^+$ T cells with L-MICA-129Val and L-MICA-129Met expression on target cells. (**A**) NKG2D expression on purified $CD8^+$ T cells co-cultured with L-con, L-MICA-129Met (n=19) or L-MICA-129Val clones (n=19) for 24 h was analyzed by flow cytometry. NKG2D expression was analyzed after gating of $CD3^+CD8^+$ T cells. The linear regression of MICA expression on target cells and NKG2D expression on $CD8^+$ T cells, both determined as MFI, is displayed for the L-MICA-129Met (left panels) and L-MICA-129Val cells (right panels) 4 h (upper panels) and 24 h (lower panels) after co-culture. The coefficient of determination (R^2), the regression coefficient (reg. coeff.), and the P-value for Pearson correlation are indicated for both MICA variants. (**B**) In parallel, the CD8 expression on the $CD8^+$ T cells was determined. The means and SD of the percentage of $CD8^+$ T cells (left panel) and of the MFI of CD8 (right panel) are shown demonstrating the specificity of the effect of MICA engagement for NKG2D expression.

Appendix Figure S14. Impairment of NKG2D-mediated co-stimulation of $CD8^+$ T cells by NKG2D-counter-regulation. Purified $CD8^+$ T cells were cultured on plate-bound anti-NKG2D (1 µg/ml) or an isotype control (IgG_1) for 24 h before the NKG2D expression was measured by flow cytometry. These

$CD8^+$ T cells were subsequently stained with CFSE and cultured on plates coated with anti-CD3 mAb (0.005 or 0.01 µg/ml) in combination with anti-CD28 (0.5 µg/ml) mAb as positive control or anti-NKG2D mAb (0.5 µg/ml). Proliferation was measured after 72 h by flow cytometry. The means and SD (n=6) of cell divisions is shown as evaluated in parallel to the MFI (see Fig 7D). Differences between $CD8^+$ T cells pre-exposed to anti-NKG2D and isotype control ($mIgG_1$) were obvious in these experiments (red boxes).

Appendix Figure S15. Characterization of purified IL-2-stimulated NK cells and purified $CD8^+$ T cells. (**A**) NK cell markers (CD16, CD56, CD94, NKp44, NKG2D) and the T cell marker CD3 were always determined by flow cytometry on the surface of MACS-isolated human NK cells, stimulated for 4 days with IL-2 (100 U/ml), before the cells were used in experiments. The means and SD of the percentage of cells positive for the respective markers are shown (n=26). (B) MACS-isolated human $CD8^+$ T cells, were always controlled by flow cytometry before the cells were used in experiments. The means and SD of the percentage of cells positive for the respective marker combinations are shown (n=11).

Appendix Figure S1

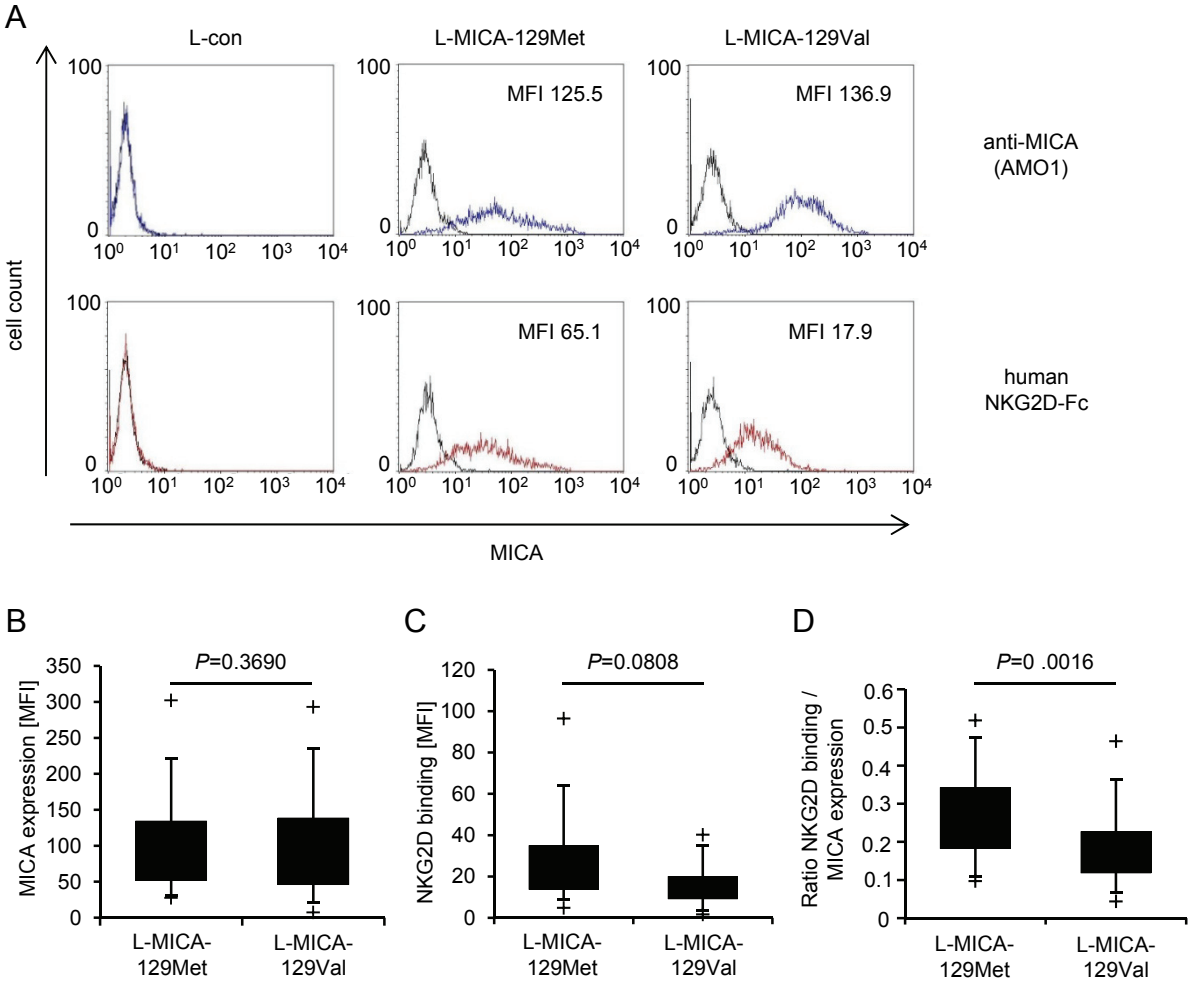

Appendix Figure S2

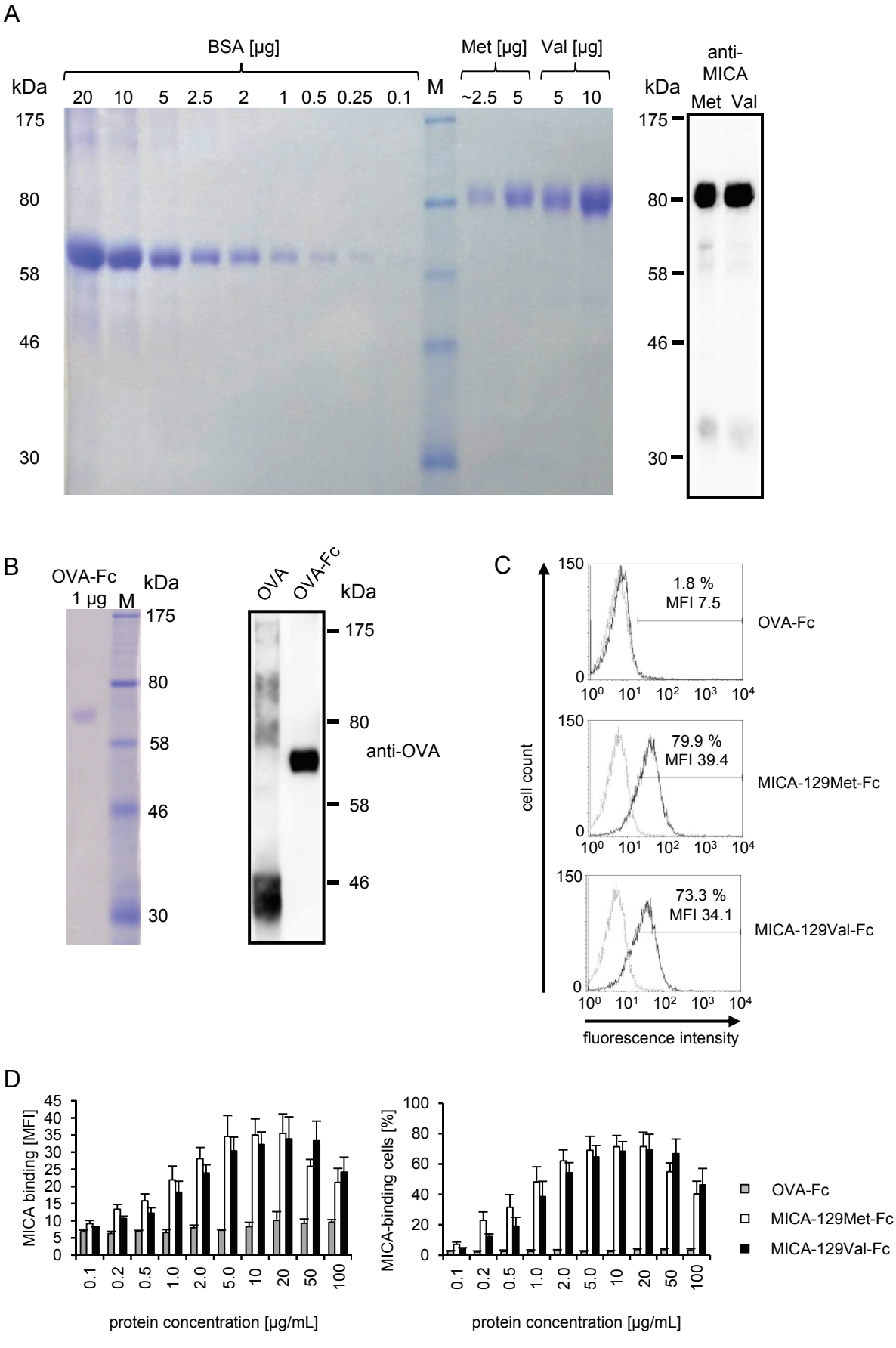

Appendix Figure S3

A

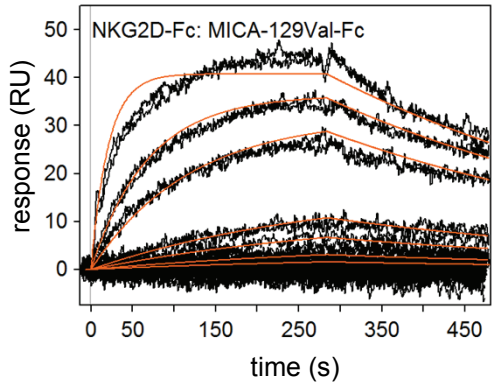

D

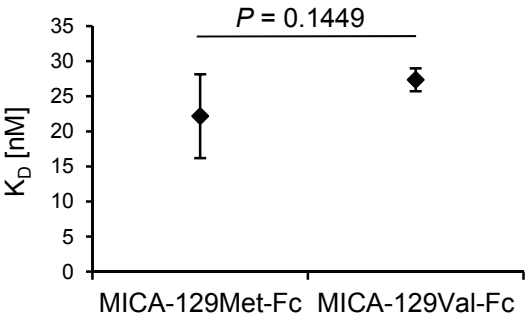

B

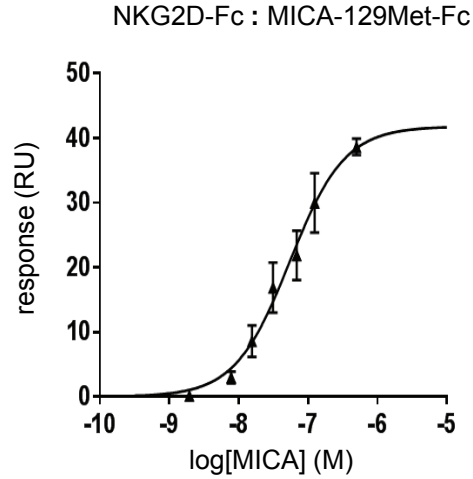

C

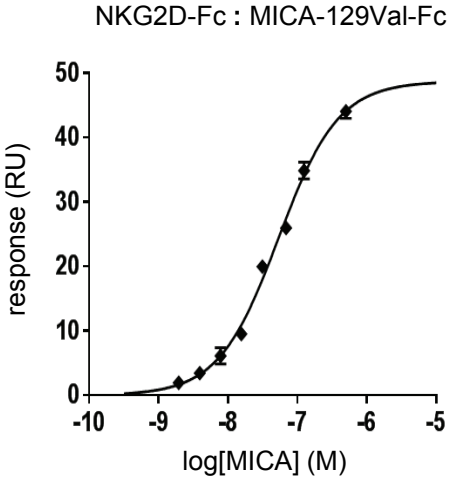

Appendix Figure S4

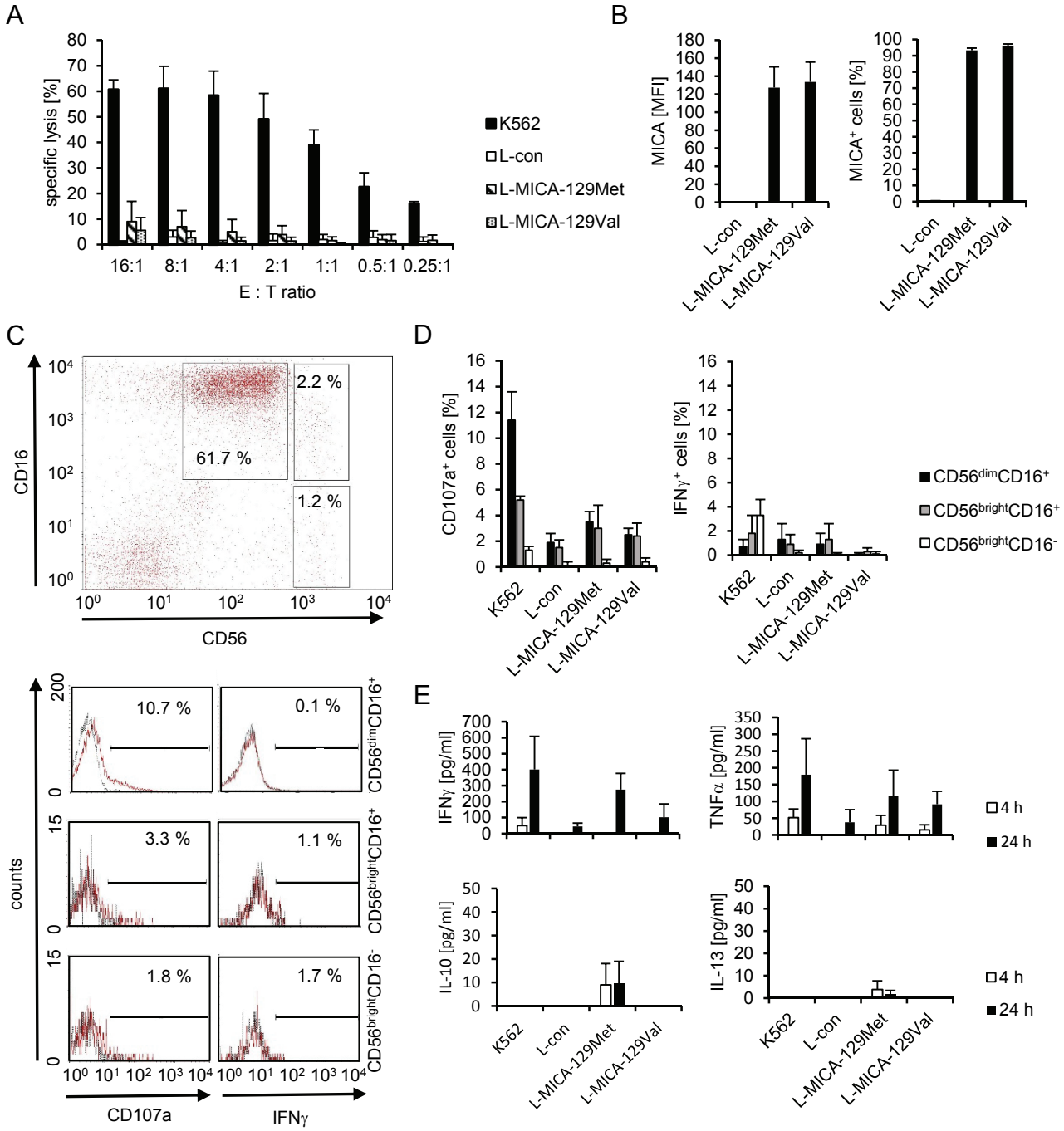

Appendix Figure S5

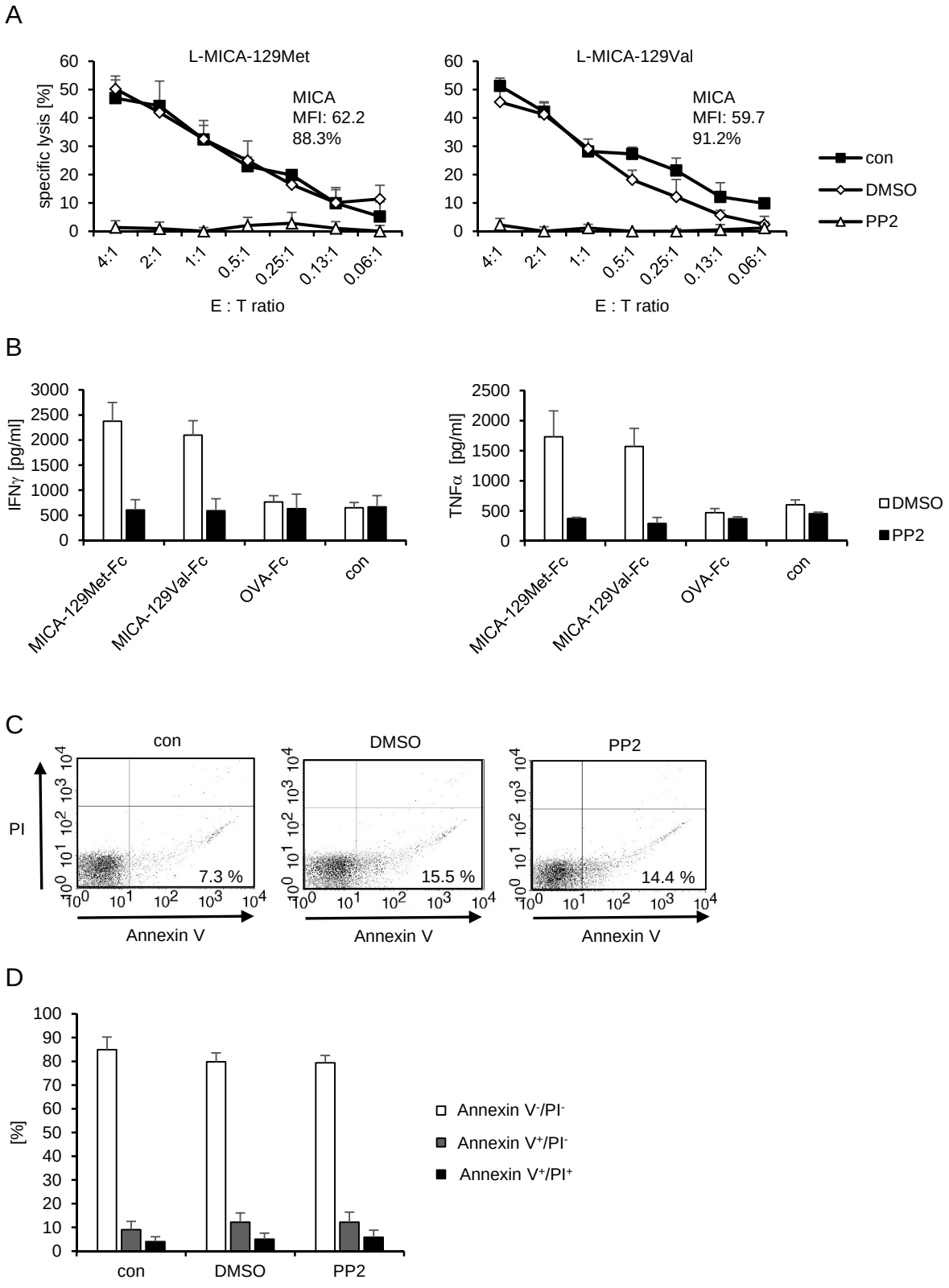

Appendix Figure S6

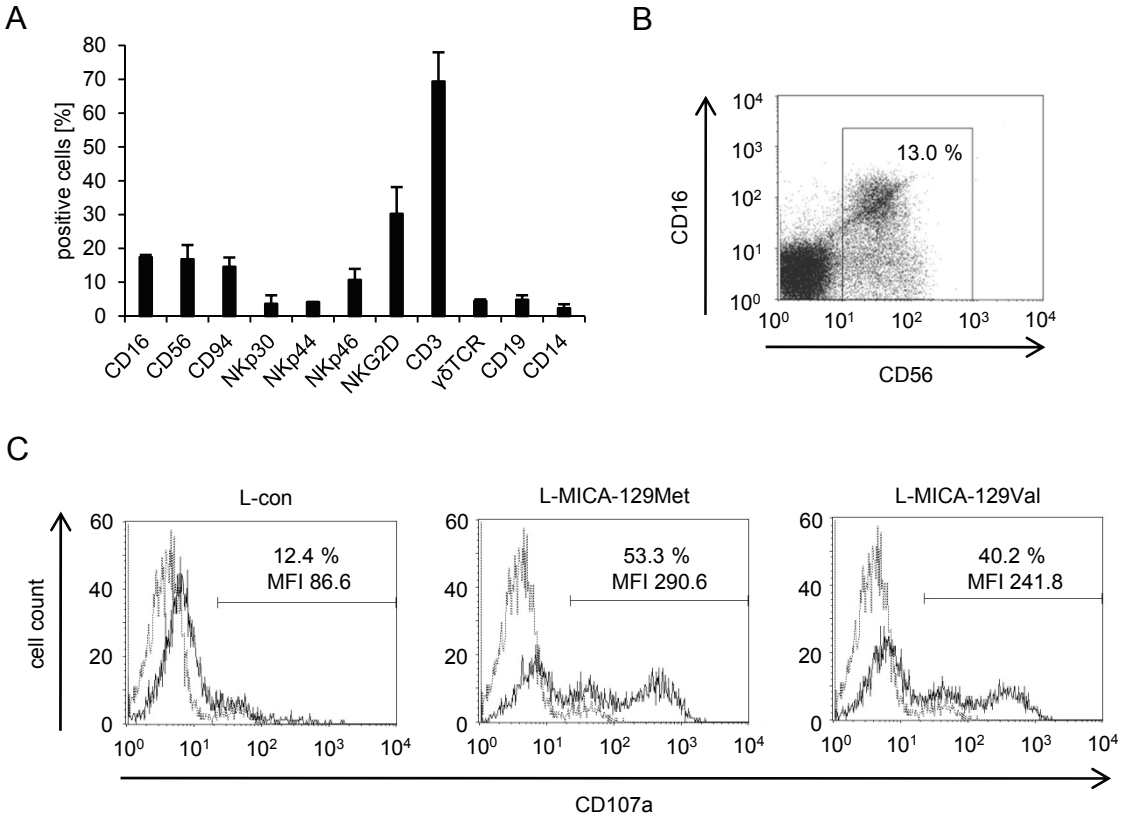

Appendix Figure S7

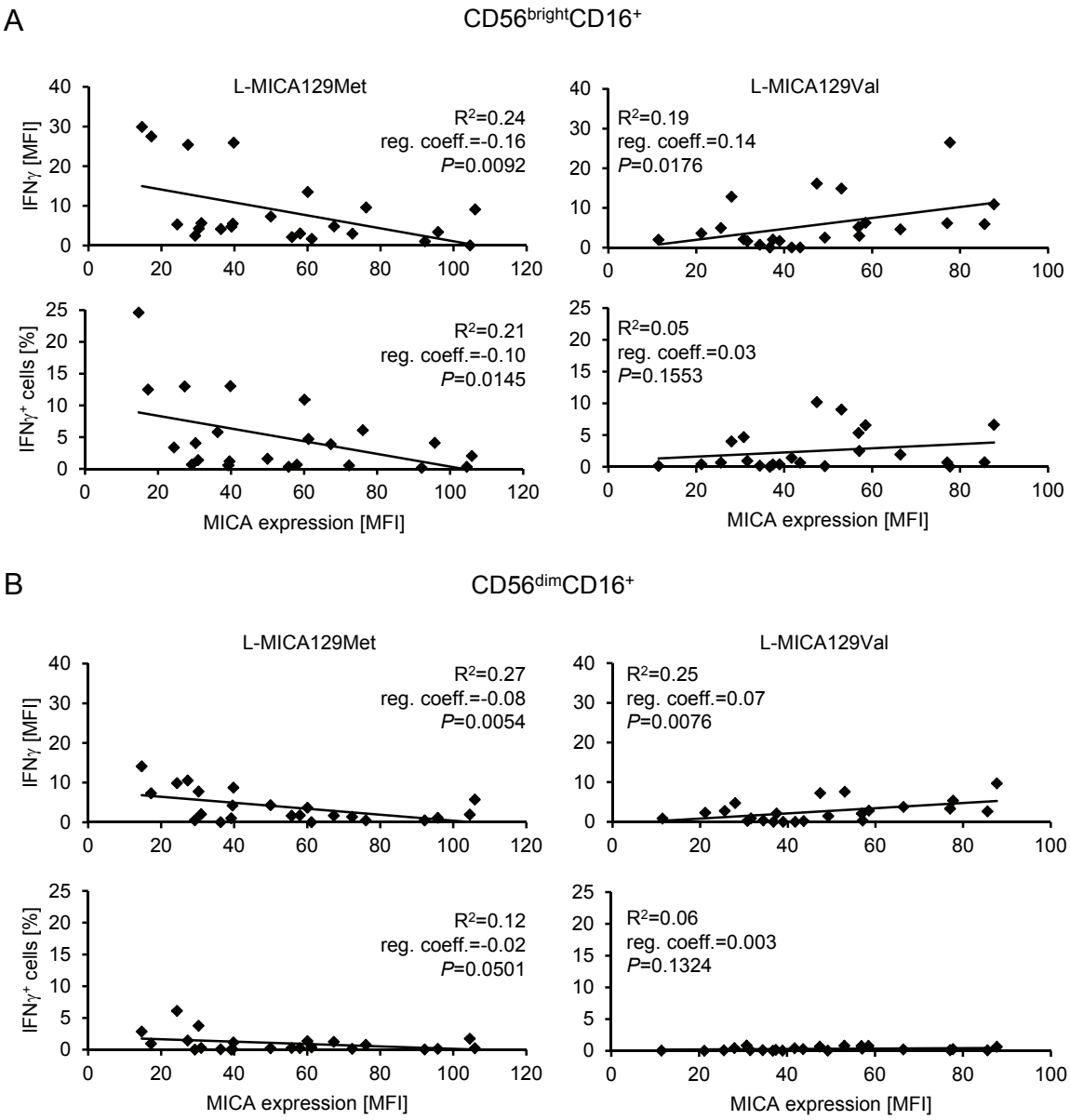

Appendix Figure S8

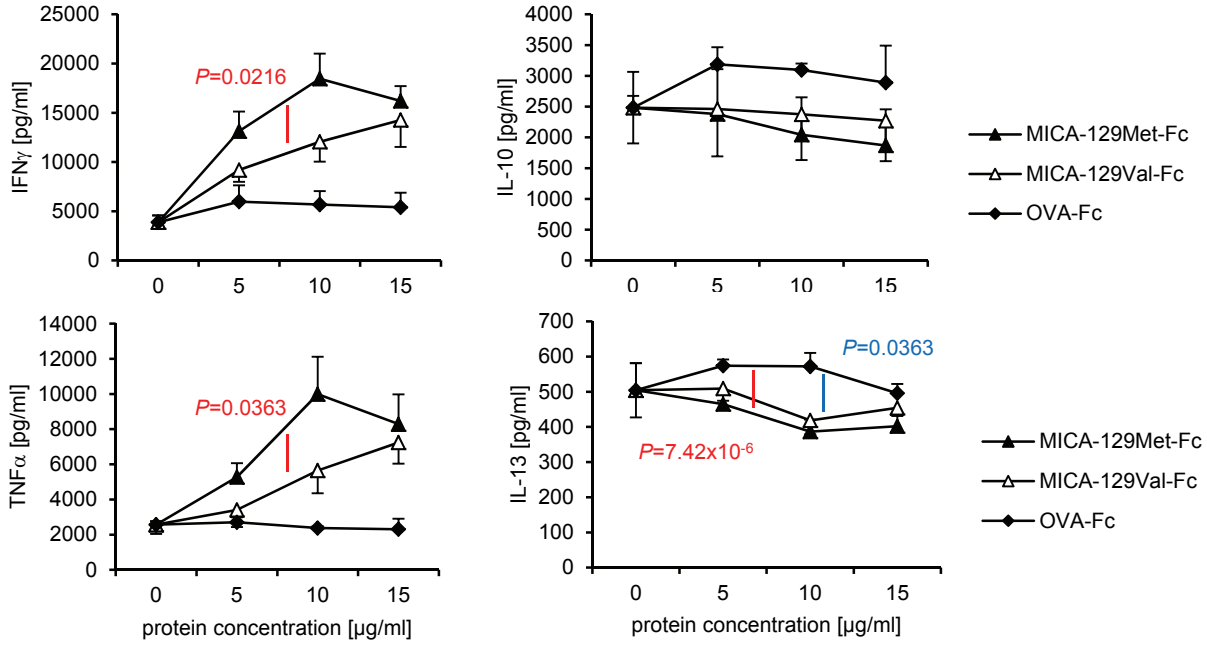

Appendix Figure S9

A

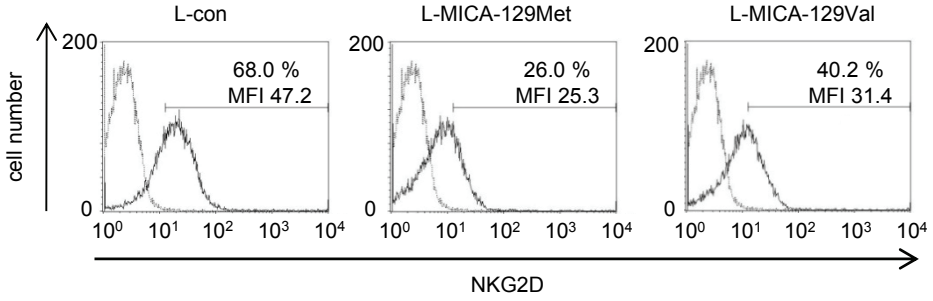

B

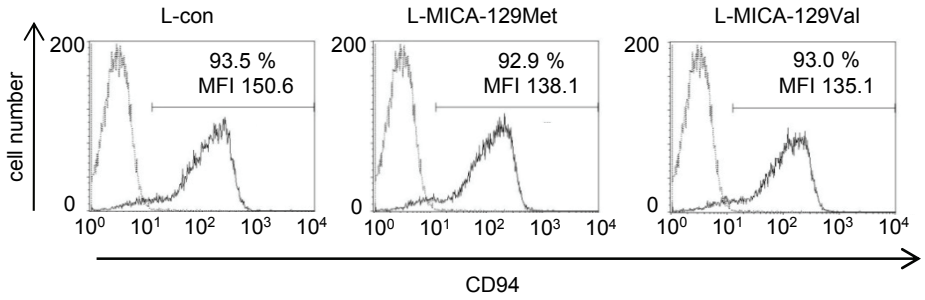

C

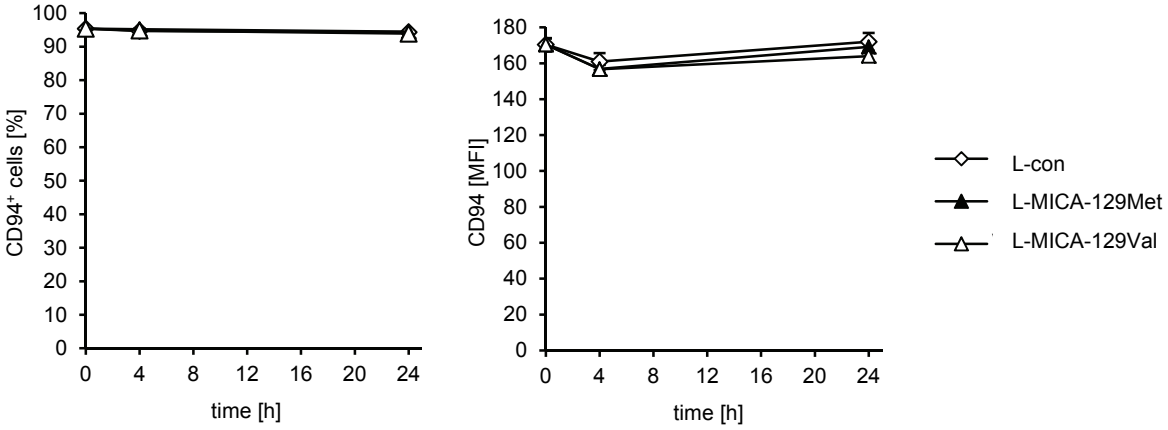

Appendix Figure S10

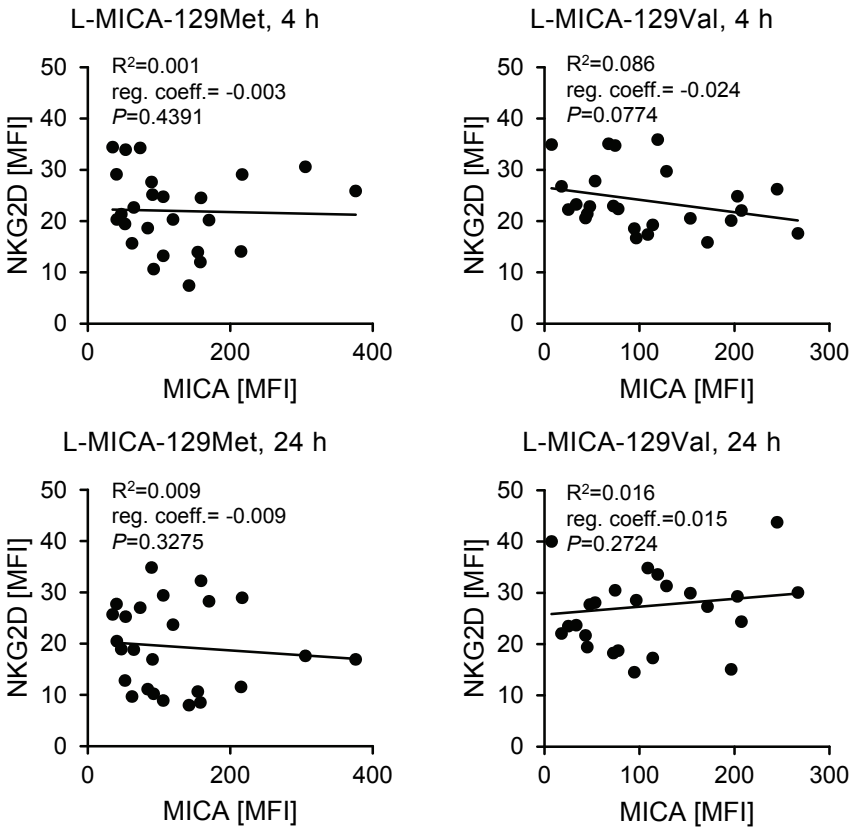

Appendix Figure S11

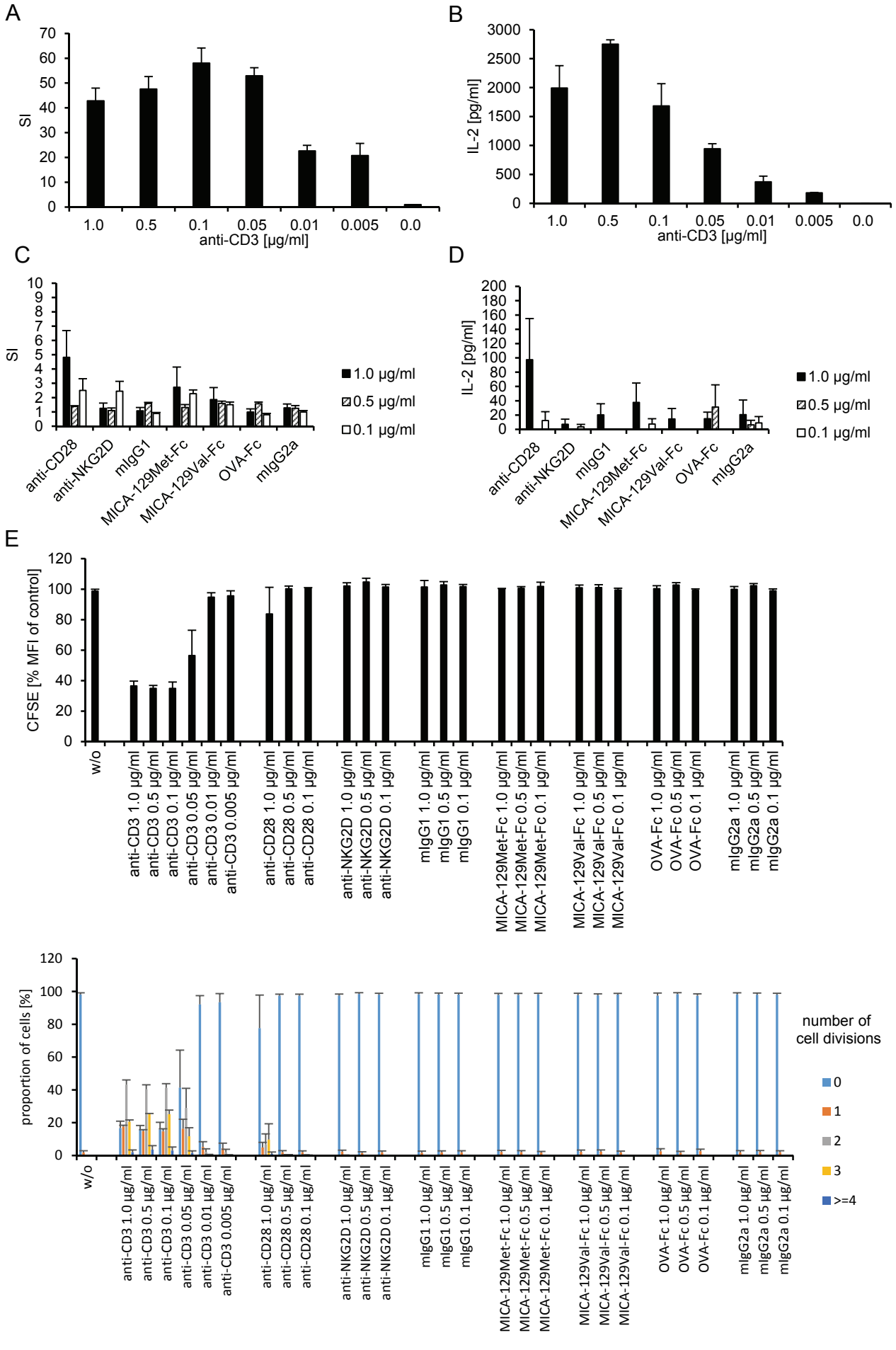

Appendix Figure S12

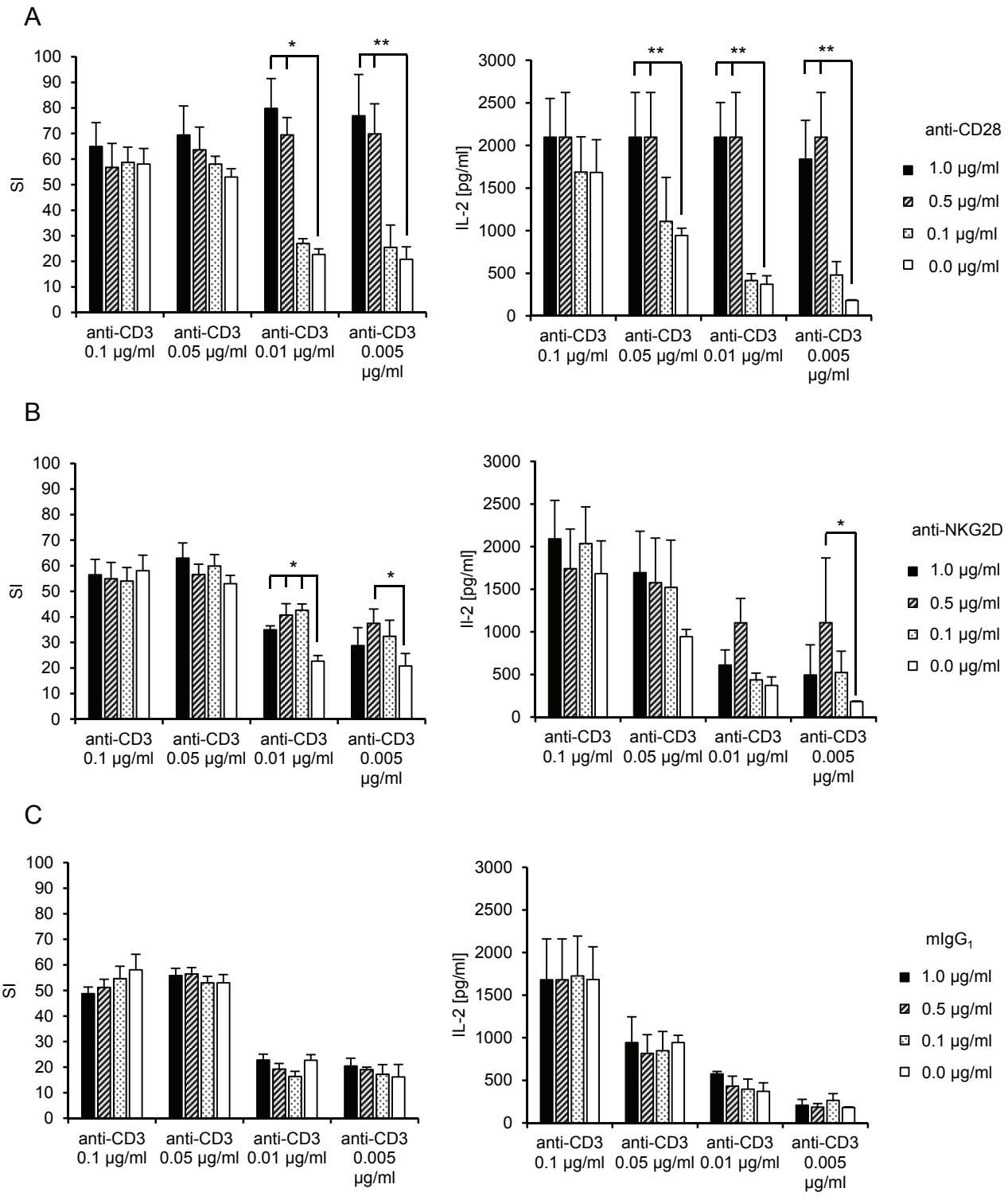

Appendix Figure S13

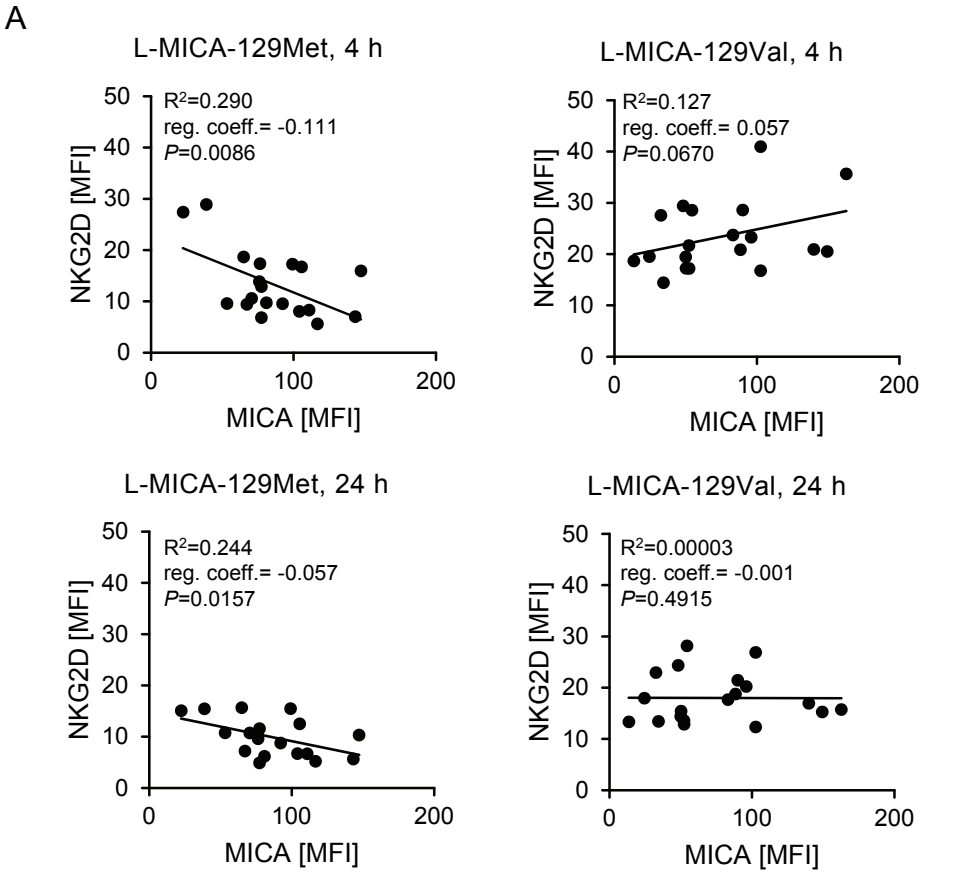

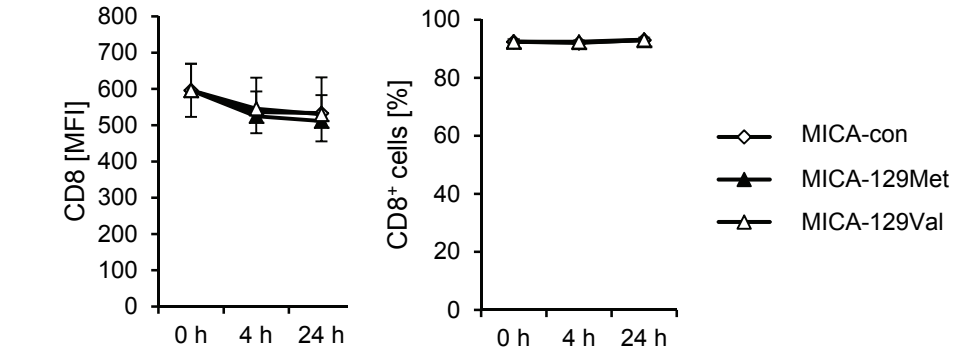

Appendix Figure S14

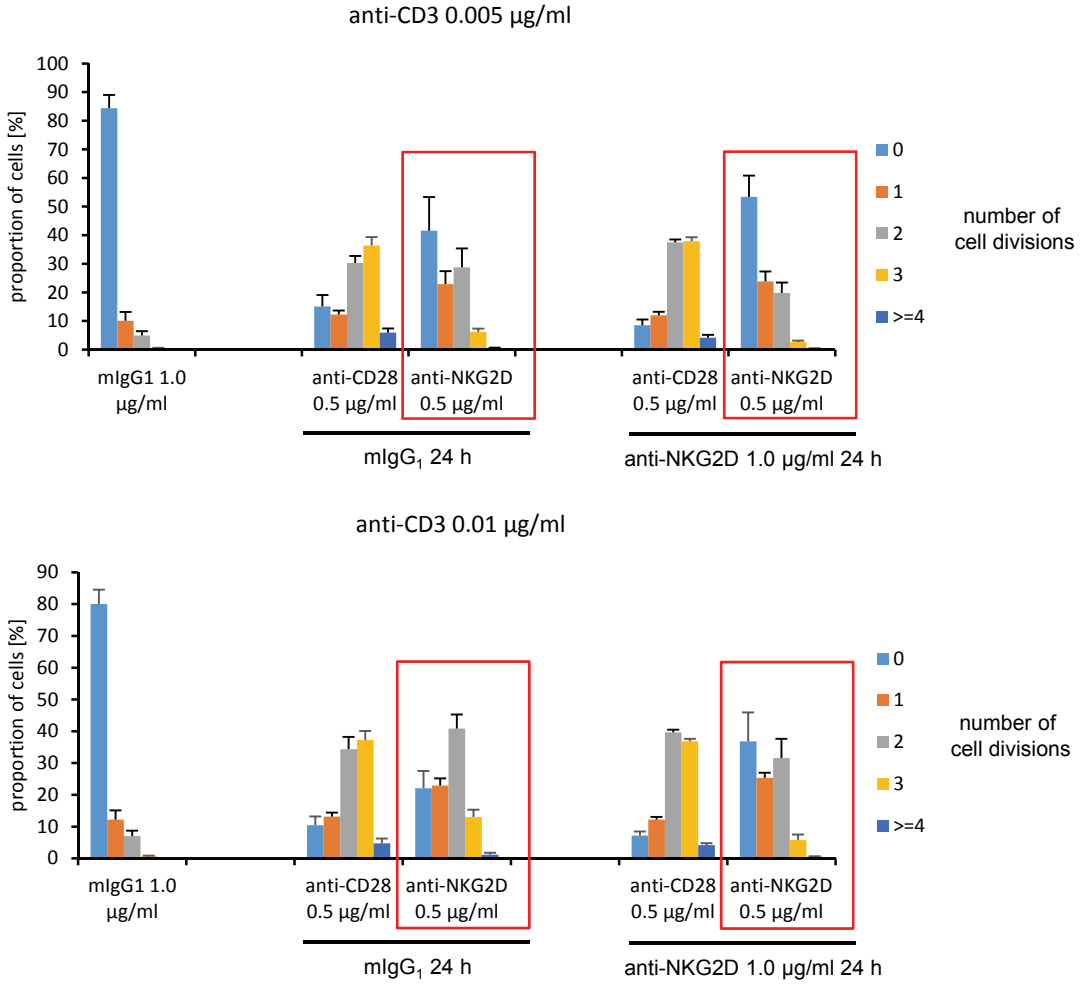

Appendix Figure S15

A

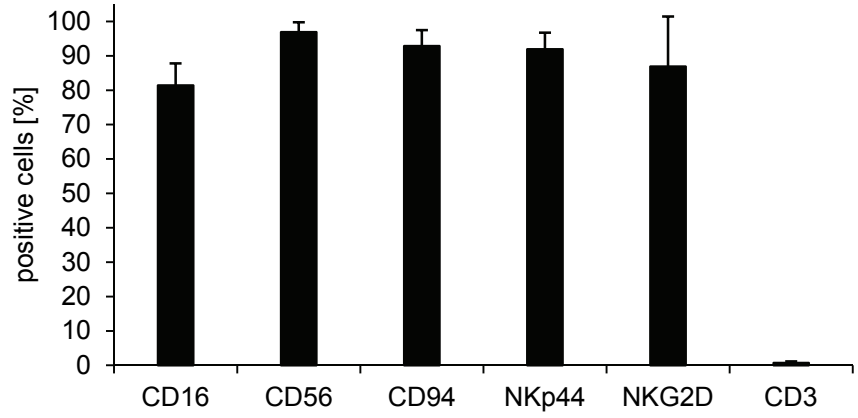

B

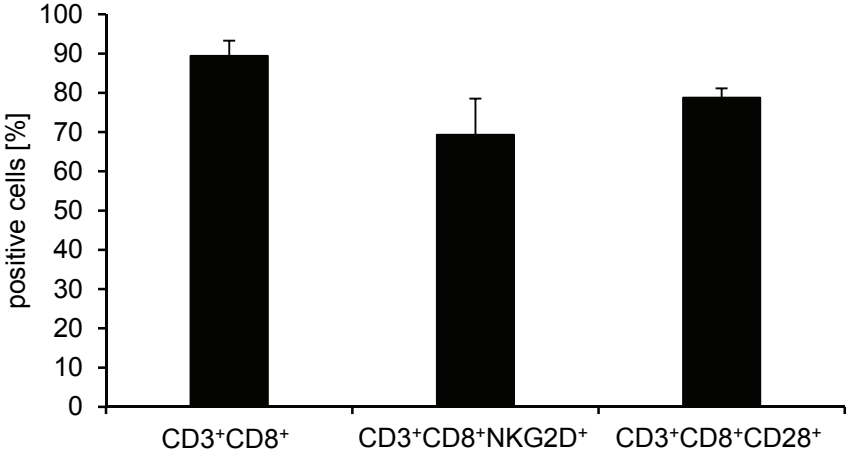

Appendix Table S1. Analysis of MICA shedding from L-MICA-129Met and L-MICA-129Val cells

cell type	**n**[1]	**MICA [MFI] mean ± SEM**	**sMICA [pg/10^6 cells] mean ± SEM**
Ltk^-	3	0.8 ± 0.0	0.0 ± 0.0
L-con	3	0.5 ± 0.2	0.0 ± 0.0
L-MICA-129Met	12	83.6 ± 16.9	0.0 ± 0.0
L-MICA-129Val	12	136.1 ± 17.1	0.0 ± 0.0
melanomas	4	13.0 ± 4.6	14.2 ± 8.3
melanomas + SAHA[2]	4	48.4 ± 18.4	79.2 ± 12.7

[1] For the control cells (Ltk^- and L-con) 3 replicates cultured independently at different time point were analyzed, for L-MICA-129Met and L-MICA-129Met 12 independent clones were used, and for melanomas, which served as positive controls, 4 different melanoma cell lines (Sk-Mel-29, Juso, Parl, and Mel Ho) were tested.

[2] The melanoma cell lines were treated with 10 µM suberoylanilide hydroxyamic acid (SAHA, Qbiogene-Alexis, Grünberg, Germany) for 20 h before analysis to increase MICA expression as described previously (Elsner L, Flügge PF, Lozano J, Muppala V, Eiz-Vesper B, Demiroglu SY, Malzahn D, Herrmann T, Brunner E, Bickeböller H, Multhoff G, Walter L, Dressel R (2010) The endogenous danger signals HSP70 and MICA cooperate in the activation of cytotoxic effector functions of NK cells. *J Cell Mol Med* 14: 992-1002).

Appendix Table S2. Antibodies used in the study

Antigen	Isotype	Clone	Label	Supplier
CD3	mouse IgG_{2a}	MEM 57	FITC	ImmunoTools, Friesoythe, Germany
CD3	mouse IgG_{2a}	HIT3a	PE	BioLegend, Fell, Germany
CD3	mouse IgG_1	UCHT1 (LEAF)	-	BioLegend, Fell, Germany
CD8	mouse IgG_1	HIT8a	PE/Cy5	BioLegend, Fell, Germany
CD14	mouse IgG_{2a}	Tük4	PE	Caltag Laboratories, Hamburg, Germany
CD16	mouse IgG_1	3G8	PE/Cy5	BioLegend, Fell, Germany
CD19	mouse IgG_1	HIB19	PE	BioLegend, Fell, Germany
CD28	mouse IgG_1	CD28.2	PE	BioLegend, Fell, Germany
CD28	mouse IgG_1	CD28.2 (LEAF)	-	BioLegend, Fell, Germany
CD56	mouse IgG_1	HCD56	FITC	BioLegend, Fell, Germany
CD56	mouse IgG_1	HCD56	PE	BioLegend, Fell, Germany
CD94	mouse IgG_1	HP-3D9	FITC	Becton Dickinson, Heidelberg, Germany
CD107a (LAMP-1)	mouse IgG_1	H4A3	FITC	BioLegend, Fell, Germany
CD314 (NKG2D)	mouse IgG_1	149810	PE	R&D Systems, Wiesbaden, Germany
CD314 (NKG2D)	mouse IgG_1	149810	-	R&D Systems, Wiesbaden, Germany
CD335 (NKp46)	mouse IgG_1	9E2	PE	BioLegend, Fell, Germany
CD336 (NKp44)	mouse IgG_1	P44-8	APC	BioLegend, Fell, Germany
CD337 (NKp30)	mouse IgG_1	P30-15	PE	BioLegend, Fell, Germany
γδTCR	mouse IgG_{2a}	B1	PE	BioLegend, Fell, Germany
β-actin	mouse IgG_1	AC-15	-	Sigma-Aldrich, Taufkirchen, Germany
IFNγ	mouse IgG_1	4S.B3	PE	BioLegend, Fell, Germany
MICA	mouse IgG_1	AMO1	-	Bamomab, Gräfelfing , Germany
MICA	goat IgG	polyclonal (BAF1300)	Biotin	R&D Systems, Wiesbaden, Germany

Ovalbumin (OVA)	mouse IgG_1	OVA-14	-	Sigma-Aldrich, Taufkirchen, Germany
phospho-Tyr	mouse IgG_{2b}	4G10	-	Merck Millipore, Darmstadt, Germany
phospho-SRC family (Tyr419)	rabbit IgG	polyclonal (#2101)	-	Cell Signaling Technology, Danvers, MA, USA
mouse IgG	goat IgG	polyclonal (115-005-003)	-	Jackson Laboratories, via Dianova, Hamburg, Germany
mouse IgG	goat IgG F(ab')2 fragment	polyclonal (115-006-062)	-	Jackson Laboratories, via Dianova, Hamburg, Germany
mouse IgG	goat IgG	polyclonal (155-095-062)	FITC	Jackson Laboratories, via Dianova, Hamburg, Germany
mouse IgG	goat IgG	polyclonal (115-035-003)	HRP	Jackson Laboratories, via Dianova, Hamburg, Germany
human IgG	goat IgG	polyclonal (109-095-098)	FITC	Jackson Laboratories, via Dianova, Hamburg, Germany
rabbit IgG	goat IgG	polyclonal (#31430)	HRP	Thermo Fisher Scientific, Bonn, Germany

The following abbreviations are used: APC allophycocyanin; Cy5, Cyanine 5; FITC, fluorescein isothiocyanate; HPR, horseradish peroxidase; LEAF, low endotoxin azide-free; PE, phycoerythrin. The phospho-SRC family (Tyr419) is also known as Tyr416 when following the original nomenclature from chicken.

The MICA-129 dimorphism affects NKG2D signaling and outcome of hematopoietic stem cell transplantation

Antje Isernhagen, Dörthe Malzahn, Elena Viktorova, Leslie Elsner, Sebastian Monecke, Frederike von Bonin, Markus Kilisch, Janne Marieke Wermuth, Neele Walther, Yesilda Balavarca, Christiane Stahl-Hennig, Michael Engelke, Lutz Walter, Heike Bickeböller, Dieter Kube, Gerald Wulf, & Ralf Dressel

Corresponding author: Ralf Dressel, University Medical Center G^ttingen

Review timeline:

Submission date:	14 March 2015
Editorial Decision:	21 April 2015
Revision received:	20 July 2015
Editorial Decision:	11 September 2015
Revision received:	15 September 2015
Accepted:	17 September 2015

Transaction Report:

(Note: With the exception of the correction of typographical or spelling errors that could be a source of ambiguity, letters and reports are not edited. The original formatting of letters and referee reports may not be reflected in this compilation.)

Editor: Céline Carret

1st Editorial Decision 21 April 2015

Thank you for the submission of your manuscript to EMBO Molecular Medicine. We have now heard back from the three referees whom we asked to evaluate your manuscript.

You will see below that all three referees are rather enthusiastic about your article, although referees 1 and 2 do have suggestions to further improve conclusiveness and strengthen the study.

Should you be able to address these criticisms in full, we would be happy to consider a revised manuscript.

Please note that it is EMBO Molecular Medicine policy to allow only a single round of revision and that, as acceptance or rejection of the manuscript will depend on another round of review, your responses should be as complete as possible.

EMBO Molecular Medicine has a "scooping protection" policy, whereby similar findings that are published by others during review or revision are not a criterion for rejection. Should you decide to submit a revised version, I do ask that you get in touch after three months if you have not completed it, to update us on the status.

Please also contact us as soon as possible if similar work is published elsewhere. If other work is published we may not be able to extend the revision period beyond three months.

I look forward to receiving your revised manuscript.

***** Reviewer's comments *****

Referee #1 (Comments on Novelty/Model System):

These findings are extremely interesting, especially when looking at the correlation of the survival curves with MICA-129 dimorphisms. The findings suggest that analysis for MICA-129met may have diagnostic potential for predicting survivability from aGVHD following HSC transplantation.

Referee #1 (Remarks):

In the manuscript entitled "The MICA-129 dimorphism affects NKG2D signaling and outcome of hematopoietic stem cell transplantation," the authors present correlative data that seem to show better survival outcomes in patients that show the presence of the MICA-129met versus MIVA-129val following HSC transplantation. The data are interesting and may have great translational implications in predicting the potential susceptibility of these patients to aGVHD.

Major points.

1) In Figure 3, did the authors assess what the effect of the src inhibitor had on IFN-gamma secretion by NK cells and effect on specific lysis (as in Figure 4C)? Did they also assess potential cellualr toxicity of the src inhibitor on NK cells?

2) The authors should perform an ELISPOT assay to determine the number of NK cells secreting IFN-gamma in the presence of MICA-129met versus MICA-129val. This would be more informative than looking at overall IFN-gamma secretion and analysis by ELISA. Also, description of Figure 4D is missing in the Figure Legend.

3) In Figures 6B and 7C, the authors should include the untreated, CFSE cells to show what the starting labeled levels on non-proliferating cells looked like. In addition, the authors should include % proliferation and not MFI levels.

4) In Figure 7A, the authors should include the flow cytometric data showing CD3, CD8, and NKG2D co-staining.

Referee #2 (Comments on Novelty/Model System):

The technical quality is in principle high but unfortunately, the most relevant NK cell subsets were not addressed separately but, instead, given as results of total NK cell with respect to cytotoxicity, IFN-g production and NKG2D down regulation. Since this important information is available by CD56, CD16 and CD94 staining, it should be possible to re-evaluate the data according to the CD56dm and CD56bright NK cell subsets. The relevance for this MICA polymorphism in Stem cell transplantation is novel. However, due to the complexity of stem cell transplantation with repect to conditioning, underlying disease etc., it is unlikely that a single polymorphism in the MICA gene is alone causing the observed effects in Figure 1. Therefore, MICA genotyping is certainly of scientific interest but the clinical relevance should be evaluated in light of both the complexity in stem cell transplantation and in NK cell regulation.

Referee #2 (Remarks):

The manuscript by Isernhagen et al. addresses the influence of a single polymorphism at amino acid 129 in the NKG2D-ligand, MICA, i.e. MICA-129Met vs. MICA-129Val on outcome after hematopoietic stem cell transplantation and on NK cell function like degranulation, and IFN-g

secretion.
The authors can nicely demonstrate that this MICA-polymorphism has clinical impact on survival, acute, chronic GVHD and relapse with the MICA-129Met allele increasing overall survival despite of an increased risk for aGVHD. In contrast, ATG-treatment of MICA-129Val carriers was associated with their increased survival. Functionally, this MICA polymorphism could be associated with enhanced binding, induction of cytotoxicity and IFN-g secretion of the MICA-129Met allele. With respect to T cell co-stimulation, this allele also induced faster T cell stimulation.
Although the association of this MICA-polymorphism with survival after stem cell transplantation, NK cell activation and T cell co-stimulation is interesting and relevant, there are some aspects that could be addressed more specifically in order to define the NK cell effect more precisely.
Major comments:
1. In general, isolated NK cells were pre-activated 4 days with IL-2 before testing them for CD107a degranulation, induction of cytotoxicity, and IFN-g secretion. However, cytokine stimulation with IL-2 for 4 days generally enhances NK cell activation at all levels. Therefore, the influence of these two alleles in transfected L cells as target cells should be demonstrated with freshly isolated NK cells - et least exemplarily.
2. Throughout the manuscript, activity of all NK cells is shown without looking at specific NK cell subsets. Since the two major subsets of peripheral NK cells, i.e. CD56dimCD16+ and CD56bright CD16- NK cells have been shown to differ also functionally, these two subsets should be nalayzed also separately. Since in the methods section, several NK cell markers such as CD16, CD94, NKp30, NKp44 and NKp46 are mentioned as part of the phenotyping FACS panel, it should be possible at least distinguish between these two subsets. In case of the known disappearance of the CD56brightCD16- NK subsets during the 4 day-culture period with IL-2, the results would apply for the CD56dimCD16+ NK cell subset which could then nicely be demonstrated. Therefore, FACS plots should be added to Figures 2showing CD107a vs. CD56 or CD16 staining or differential gating on the two major NK cell subsets.
3. The CD94 receptor in combination with the inhibitory NKG2A or the activating NKG2C receptor represents an important functional NK cell marker due to its binding to HLA-E. Therefore, it should be demonstrated whether activation with the two MICA alleles has also an impact on CD94 expression following stimulation.

Minor comments:
With respect to cytokines, only IFN-g was analyzed. If these data are available, other effector cytokines like TNF-a, IL-10 or IL-13 should also be included into the manuscript even there were no significant differences between the two MICA alleles.

Referee #3 (Comments on Novelty/Model System):

This is an important translational study which really provides new information because the association of MICA variants (Val/Val or Met/Met) with cGVHD and /or aGVHD after HSCT have been known for some time but the mechanisms had not at all been elucidated.
The data represent a major advance in the knowledge of how NK cell function can be modified by NKG2D interaction with different MICA alleles as both regulation of NKG2D mediated activation signals and regulation of NKG2D expression at the plasma membrane are demonstrated. The relatiionship betwwen expression density and function of NKG2D and MICA is revealed.
The technical quality of the paper is very high.
The experiments have been carefully planned and the data reported in this paper strongly support the conclusions of the paper.

Referee #3 (Remarks):

The paper provides novel information about the regulation of MICA function in relation to the polymorphism of this molecule.
The data represent a major advance in the knowledge of how NK cell function can be modified by NKG2D interaction with different MICA alleles as both regulation of NKG2D mediated activation

signals and regulation of NKG2D expression at the plasma membrane are demonstrated.

Minor points
In the Discussion, the authors mention the expression of MICA by non-professional antigen presenting cells which activate alloreactive CD8+ T cells. Some discussion of the cell types implicated (endothelial ? epithelial ? tumoral ?) would be informative and particularly in the context of GVHD.

The potential for ATG to target cell types, other than T lymphocytes, should be mentionned as non-T lymphocytes may also be implicated in the results seen in patients receiving ATG.

The title of Figure 4 should be reconsidered

1st Revision - authors' response 20 July 2015

Response to the reviewer's comments

We would like to thank the reviewers for their overall encouraging comments for our study and their most valuable criticisms. In addition to addressing the comments of the reviewers, we have included in the revised version of the manuscript in Figure 1 the panels G and H to better illustrate the therapeutic effect of anti-thymocyte globulin in the homozygous carriers of the MICA-129Val genotype in our cohort. Please find below the reviewer's comments and our answers (in italics).

***** Reviewer's comments *****

Referee #1 (Comments on Novelty/Model System):

These findings are extremely interesting, especially when looking at the correlation of the survival curves with MICA-129 dimorphisms. The findings suggest that analysis for MICA-129met may have diagnostic potential for predicting survivability from aGVHD following HSC transplantation.

Referee #1 (Remarks):

In the manuscript entitled "The MICA-129 dimorphism affects NKG2D signaling and outcome of hematopoietic stem cell transplantation," the authors present correlative data that seem to show better survival outcomes in patients that show the presence of the MICA-129met versus MIVA-129val following HSC transplantation. The data are interesting and may have great translational implications in predicting the potential susceptibility of these patients to aGVHD.

Major points.

1) In Figure 3, did the authors assess what the effect of the src inhibitor had on IFN-gamma secretion by NK cells and effect on specific lysis (as in Figure 4C)? Did they also assess potential cellular toxicity of the src inhibitor on NK cells?

Answer:

We also determined the effect of the SRC kinase inhibitor PP2 on target cell lysis by NK cells (Appendix Figure S5A) and the release of IFNγ and TNFα (Appendix Figure S5B). In addition to

NK cell degranulation, also these effector functions, which can be triggered by NKG2D, were completely inhibited. Moreover, we assessed the potential cellular toxicity of PP2 (25 µM for 4 h) by Annexin V/propidium iodide staining (Appendix Figure S5C, D) and found no increase of apoptotic NK cells at least within 4 h, the time period used for these experiments.

2) The authors should perform an ELISPOT assay to determine the number of NK cells secreting IFN-gamma in the presence of MICA-129met versus MICA-129val. This would be more informative than looking at overall IFN-gamma secretion and analysis by ELISA. Also, description of Figure 4D is missing in the Figure Legend.

Answer:

We completely agree that information on the proportion of NK cells producing IFNγ is important. Since the reviewer #2 requested information on the NK cell subpopulations, which produce IFNγ in response to NKG2D engagement, we performed intracellular flow cytometry instead of ELISPOT assays to be able to address both questions. We could show that mainly $CD56^{bright}CD16^{-}$ and to a lesser extent $CD56^{bright}CD16^{+}$ NK cells secrete IFNγ in response to NKG2D engagement (Figure EV3). The proportion of NK cells reacting by IFNγ expression upon stimulation by MICA-129Met-Fc and MICA-129Val-Fc proteins is shown in Figure EV3B. At the used (relatively low) concentrations more $CD56^{bright}CD16^{-}$ NK cells produced IFNγ in response to the MICA-129Met-Fc than the MICA-129Val-Fc protein (P=0.0025; ANOVA). In co-culture experiments with L cells expressing the MICA-129 variants, the percentage of IFNγ-expressing NK cells increased with expression intensity of the MICA-129Val isoform (Figure 4A, Appendix Figure S7A, B). It did not increase for NK cells exposed to the L-MICA-129Met clones (Figure 4A). On $CD56^{bright}CD16^{+}$ NK cells, the proportion of $IFN\gamma^{+}$ cells even decreased with increased MICA expression intensity (Appendix Figure S7A). A description of Figure 4D (now Figure 4B) is provided.

3) In Figures 6B and 7C, the authors should include the untreated, CFSE cells to show what the starting labeled levels on non-proliferating cells looked like. In addition, the authors should include % proliferation and not MFI levels.

Answer:

In these figures (still Figure 6B and 7C) the untreated CFSE stained cells are now included. We also added the percentage of proliferating cells. A detailed analysis of the number of cell divisions is provided in the Appendix Figure S14.

4) In Figure 7A, the authors should include the flow cytometric data showing CD3, CD8, and NKG2D co-staining.

Answer:

The CD3, CD8, and NKG2D co-staining is now shown in Figure EV5.

Referee #2 (Comments on Novelty/Model System):

The technical quality is in principle high but unfortunately, the most relevant NK cell subsets were not addressed separately but instead, given as results of total NK cell with respect to cytotoxicity, IFN-g production and NKG2D down regulation. Since this important information is available by CD56, CD16 and CD94 staining, it should be possible to re-evaluate the data according to the CD56dm and CD56bright NK cell subsets. The relevance for this MICA polymorphism in Stem cell transplantation is novel. However, due to the complexity of stem cell transplantation with respect to conditioning, underlying disease etc., it is unlikely that a single polymorphism in the MICA gene is

alone causing the observed effects in Figure 1. Therefore, MICA genotyping is certainly of scientific interest but the clinical relevance should be evaluated in light of both the complexity in stem cell transplantation and in NK cell regulation.

Referee #2 (Remarks):

The manuscript by Isernhagen et al. addresses the influence of a single polymorphism at amino acid 129 in the NKG2D-ligand, MICA, i.e. MICA-129Met vs. MICA-129Val on outcome after hematopoietic stem cell transplantation and on NK cell function like degranulation, and IFN-g secretion.

The authors can nicely demonstrate that this MICA-polymorphism has clinical impact on survival, acute, chronic GVHD and relapse with the MICA-129Met allele increasing overall survival despite of an increased risk for aGVHD. In contrast, ATG-treatment of MICA-129Val carriers was associated with their increased survival. Functionally, this MICA polymorphism could be associated with enhanced binding, induction of cytotoxicity and IFN-g secretion of the MICA-129Met allele. With respect to T cell co-stimulation, this allele also induced faster T cell stimulation.

Although the association of this MICA-polymorphism with survival after stem cell transplantation, NK cell activation and T cell co-stimulation is interesting and relevant, there are some aspects that could be addressed more specifically in order to define the NK cell effect more precisely.

Major comments:

1. In general, isolated NK cells were pre-activated 4 days with IL-2 before testing them for CD107a degranulation, induction of cytotoxicity, and IFN-g secretion. However, cytokine stimulation with IL-2 for 4 days generally enhances NK cell activation at all levels. Therefore, the influence of these two alleles in transfected L cells as target cells should be demonstrated with freshly isolated NK cells - at least exemplarily.

Answer:

Engagement of NKG2D alone is known not to be sufficient to induce the release of cytotoxic granules from resting NK cells (Bryceson et al, 2009). We have now included data (see page 8) showing that resting NK cells indeed failed to kill L-MICA-129Met and L-MICA-129Val cells in contrast to K562 cells (Appendix Figure S4A, B). Moreover, no degranulation (CD107a expression) or IFNγ release was elicited (Appendix Figure S4C, D). Exposure to MICA-expressing targets also failed to induce the release of TNFα, IL-10, and IL-13 from NK cells at least within the first 4 h of co-culture (Appendix Figure S4E). However, we have shown previously that NK cells can readily kill MICA-expressing L cells after being stimulated for 4 days with a low dose of IL-2 (Elsner et al, 2010). Therefore, we used IL-2-stimulated NK cells in the subsequent experiments. This allowed us to elicit NK cell effector functions by engagement of NKG2D only. A comparison of freshly isolated and IL-2-stimulated (100 U/ml for 4 days) NK cells with respect to NKG2D expression is now displayed in Figure EV1.

2. Throughout the manuscript, activity of all NK cells is shown without looking at specific NK cell subsets. Since the two major subsets of peripheral NK cells, i.e. CD56dimCD16+ and CD56bright CD16- NK cells have been shown to differ also functionally, these two subsets should be analyzed also separately. Since in the methods section, several NK cell markers such as CD16, CD94, NKp30, NKp44 and NKp46 are mentioned as part of the phenotyping FACS panel, it should be possible at least distinguish between these two subsets. In case of the known disappearance of the CD56brightCD16- NK subsets during the 4 day-culture period with IL-2, the results would apply for the CD56dimCD16+ NK cell subset which could then nicely be demonstrated. Therefore, FACS plots should be added to Figures 2showing CD107a vs. CD56 or CD16 staining or differential gating on the two major NK cell subsets.

Answer:

We agree with the reviewer that the differentiation of NK cell subpopulations with respect to their functional capabilities is very important. We have now differentiated $CD56^{dim}CD16^{+}$ and $CD56^{bright}CD16^{-}$ NK cells and the intermediate $CD56^{bright}CD16^{+}$ NK cell population. This was possible for the MACS purified IL-2-stimulated NK cells at day 4 although the borders between the populations were sometimes less clear than on freshly isolated NK cells. On IL-2-stimulated PBMC (i.e. LAK cells, which had been used before for some experiments) we could not clearly identify a $CD56^{bright}$ population that was sufficient in numbers for a reanalysis of data. However, we performed new experiments and analyzed the NKG2D expression, which was similar on the three NK cell populations (Figure EV1), degranulation, which was strongest in $CD56^{dim}CD16^{+}$ NK cells (Figure EV2), IFNγ expression, which was strongest in $CD56^{bright}CD16^{-}$ NK cells (Figure EV3), and NKG2D-downregulation, which occurred similarly on all three NK cell populations in response mainly to the MICA-129Met variant (Figure EV4). The $CD56^{bright}CD16^{+}$ NK cells had an intermediate phenotype with respect to degranulation and IFNγ production.

3. The CD94 receptor in combination with the inhibitory NKG2A or the activating NKG2C receptor represents an important functional NK cell marker due to its binding to HLA-E. Therefore, it should be demonstrated whether activation with the two MICA alleles has also an impact on CD94 expression following stimulation.

Answer:

We had included CD94 as control for NKG2D in co-culture experiments with L-MICA-129Met and L-MICA-129Val clones (now Appendix Figure S9). These experiments demonstrated that CD94 expression was not altered in response to engagement of NKG2D by the two MICA isoforms on L cells.

Minor comments:

With respect to cytokines, only IFN-g was analyzed. If these data are available, other effector cytokines like TNF-a, IL-10 or IL-13 should also be included into the manuscript even there were no significant differences between the two MICA alleles.

Answer:

We have included now a data set showing that also TNFα production was stimulated after engagement of NKG2D by the two MICA-129 isoforms (Appendix Figure S8). We found a similar difference of the MICA-129 variants to induce production of TNFα as for IFNγ. IL-10 production was not elicited (at least within 4 h) and IL-13 production even appeared to decrease upon engagement of NKG2D by both MICA-129 variants.

Referee #3 (Comments on Novelty/Model System):

This is an important translational study, which really provides new information because the association of MICA variants (Val/Val or Met/Met) with cGVHD and /or aGVHD after HSCT have been known for some time but the mechanisms had not at all been elucidated.

The data represent a major advance in the knowledge of how NK cell function can be modified by NKG2D interaction with different MICA alleles as both regulation of NKG2D mediated activation signals and regulation of NKG2D expression at the plasma membrane are demonstrated. The relatiionship betwwen expression density and function of NKG2D and MICA is revealed.

The technical quality of the paper is very high.

The experiments have been carefully planned and the data reported in this paper strongly support the conclusions of the paper.

Referee #3 (Remarks):

The paper provides novel information about the regulation of MICA function in relation to the polymorphism of this molecule.

The data represent a major advance in the knowledge of how NK cell function can be modified by NKG2D interaction with different MICA alleles as both regulation of NKG2D mediated activation signals and regulation of NKG2D expression at the plasma membrane are demonstrated.

Minor points

In the Discussion, the authors mention the expression of MICA by non-professional antigen presenting cells, which activate allo-reactive CD8+ T cells. Some discussion of the cell types implicated (endothelial? epithelial? tumoral?) would be informative and particularly in the context of GVHD.

Answer:

We thank the reviewer for this suggestion and we have now briefly discussed this issue (see page 17).

The potential for ATG to target cell types, other than T lymphocytes, should be mentioned as non-T lymphocytes may also be implicated in the results seen in patients receiving ATG.

Answer:

We agree with the reviewer and have mentioned now that ATG can affect other immune cell populations beside T cells (see page 19).

The title of Figure 4 should be reconsidered

Answer:

The title of Figure 4 has been modified.

2nd Editorial Decision 11 September 2015

Thank you for the submission of your revised manuscript to EMBO Molecular Medicine. We have now received the enclosed reports from the referees that were asked to re-assess it. As you will see the reviewers are now supportive and I am pleased to inform you that we will be able to accept your manuscript pending some final editorial amendments.

***** Reviewer's comments *****

Referee #1 (Comments on Novelty/Model System):

From the initial review, I found the findings extremely interesting and novel - using MICA-129met as a diagnostic tool for predicting survivability from aGVHD following HSC transplantation.

Referee #1 (Remarks):

The authors responded adequately and in detail to my initial comments and questions.

Referee #2 (Comments on Novelty/Model System):

The in vitro studies support the hypothesis of a functional relevance of the MICA polymorphism for NK cell function

Referee #2 (Remarks):

With the response to the reviewer's comments and the data privided by the Appendix, the authors have answered all comments and questions properly.

